MANIFESTATIONS OF QUANTUM MECHANICS IN OPEN SYSTEMS: FROM OPTO-MECHANICS TO DYNAMICAL CASIMIR EFFECT

GIOVANNI VACANTI

NATIONAL UNIVERSITY OF SINGAPORE

2013

MANIFESTATIONS OF QUANTUM MECHANICS IN OPEN SYSTEMS: FROM OPTO-MECHANICS TO DYNAMICAL CASIMIR EFFECT

GIOVANNI VACANTI

(Master in physics, Universitá degli studi di Palermo, Palermo, Italy)

A THESIS SUBMITTED

FOR THE DEGREE OF DOCTOR OF PHILOSOPHY

CENTRE FOR QUANTUM TECHNOLOGIES

NATIONAL UNIVERSITY OF SINGAPORE

2013

Declaration

I hereby declare that this thesis is my original work and it has been written by me in its entirety. I have duly acknowledged all the sources of information which have been used in the thesis.

This thesis has also not been submitted for any degree in any university previously.

Giovanni Vacanti

August 2, 2013

To my father

Acknowledgements

A number of people have contributed, in different ways, to the realization of this thesis, and my sincere gratitude goes to them.

First of all, I want to thank Vlatko, for his guidance and his friendship, and for the freedom and the trust he gave me in conducting my research. Working with him has been a real pleasure.

I would like to thank all my collaborators, without whom this thesis probably would have never been written: the "Sicilian connection", Massimo, Mauro and Saro, and the non-sicilian folks, Myungshik, Nicolas and Stefano, for their fundamental contributions to the research projects this thesis is based on, and above all for their friendship.

My gratitude also goes to my good friends Agata, Alex, Kavan and Paul for slowly proofreading my thesis and for the valuable and insightful feedback they provided. Thanks a lot, guys.

Finally, for no reason at all, I want to thank my friend Calogero.

Abstract

The aim of this thesis is to study the behaviour of different types of open systems in various scenarios. The first part of the thesis deals with the generation and the detection of quantum effects in mesoscopic devices subjected to dissipative processes. We show that genuine quantum features such as non-locality and negative values of Wigner function can be observed even in presence of a strong interaction of the system with the environment. Moreover, we prove that, in some particular circumstances, the action of the environment is directly responsible for the generation of a geometric phase in the system. The second part of the thesis focuses on the study of critical systems subjected to an external time-dependent parameters' modulation. More specifically, we propose a scheme for the observation of dynamical Casimir effect (DCE) close to the super-radiant quantum phase transition in the Dicke model. We also show that in this context the emergence of DCE is linked to another phenomenon typically related to criticality, the Kibble-Zurek mechanism.

List of Publications

This thesis is based on the following publications:

- **G. Vacanti**, S. Pugnetti, N. Didier, M. Paternostro, G. M. Palma, R. Fazio and V. Vedral, "Photon production from the vacuum close to the superradiant transition: Linking the Dynamical Casimir Effect to the Kibble-Zurek Mechanism ", Physical Review Letters **108**, 093603 (2012)

- **G. Vacanti**, R. Fazio, M. S. Kim, G. M. Palma, M. Paternostro and V. Vedral, "Geometric phase kickback in a mesoscopic qubit-oscillator system ", Physical Review A **85**, 022129 (2012)

- **G. Vacanti**, S. Pugnetti, N. Didier, M. Paternostro, G. M. Palma, R. Fazio and V. Vedral, "When Casimir meets Kibble-Zurek ", Physica Scripta T 151, 014071 (2012) (proceeding of FQMT11)

- **G. Vacanti**, M. Paternostro, G. M. Palma, M. S. Kim and V. Vedral, " Non-classicality of optomechanical devices in experimentally realistic operating regimes", (Accepted for publication in Physical Review A)

Other publications not related to the content of this thesis:

- **G. Vacanti**, M. Paternostro, G. M. Palma and V. Vedral, "Optomechanical to mechanical entanglement transformation", New Journal of Physics **10**, 095014, (2008)

- **G. Vacanti** and A. Beige, "Cooling Atoms Into Entangled States", New Journal of Physics **11**, 083008, (2009)

- L. Chen, E. Chitanbar, K. Modi, and **G. Vacanti**, "Detecting multipartite classical states and their resemblances ", Physical Review A **83**, 020101, (2011)

Contents

List of Figures

Introduction

Ever since quantum mechanics was formulated, the fundamental nature of the theory itself has been subject of ardent debates. In this regard, many problems posed in the first years of quantum theory, such as the completeness problem [1] or the Schrödinger's cat paradox [2], have remained unsolved for a long time and they are still subject of speculations. Indeed, the famous statement by Richard Feynman "I think I can safely say that nobody understands quantum mechanics" [3] is probably still meaningful nowadays, although great progresses have been made in this direction in the last decades.

Such progresses in our understanding of the fundamental aspects of the theory have been triggered by continuos refinements of our ability to test quantum mechanics in different scenarios. The predictions of quantum mechanics have been experimentally verified over the last decades in a number of variegated situations. So far, the theory has always been successful in describing experimental observations at a microscopic level. However, in the quest to a complete comprehension of the quantum reign, many problems are yet to be solved. In this regard, pushing the theoretical and experimental investigations to the boundaries of the quantum world is probably one of the best ways to have a profound insight about the physical principles behind the theory. In particular, massive systems strongly

interacting with the environment are perfect candidates to pursue this line of research.

The study of such systems poses problems which are relevant from a purely theoretical prospective and from a technological and experimental point of view. Roughly speaking, it is believed that the rules of quantum mechanics apply only to very small isolated objects, while classical mechanics describes the behaviour of physical systems at a macroscopic level. However, thinking about reality as neatly divided in a microscopic and a macroscopic realms is quite misleading. Indeed, a gray region exists in which the transition between quantum and classical behaviours occurs. In this context, a very fundamental question arises naturally: how small and how isolated does a system have to be in order to show genuine quantum features?

Recent discoveries in this field have challenged the assumption that quantumness is an exclusive prerogative of microscopic and isolated systems. Indeed, it has been shown that complex extended objects comprising many elementary constituents and heavily interacting with the environment can in fact display important non-classical features. In general, quantum control under unfavorable conditions is an important milestone in the study of the quantum-to-classical transition. This line of research represents a major contribution to our understanding of the conditions enforcing quantum mechanical features in the state of a given system.

The topic has recently become the focus of an intense research activity, boosted by the ability to experimentally manipulate systems composed of subparts having diverse nature. We can now coherently control the interaction between radiation and Bose-Einstein condensates [4, 5] while mesoscopic superconducting devices compete with atoms and ions for the realization of cavity quantum electrody-

namics and in simple communication tasks based on quantum interference effects [6–8]. Equally remarkably, we have witnessed tremendous improvements in the cooling of purely mechanical systems such as oscillating cavity mirrors [9–18] and in their general experimental controllability [19–24]. The operative conditions and the intrinsic nature of the systems involved in these examples often deviate from the naive requirements for "quantumness": ultra-low temperatures, full addressability and ideal preparation of the system. On the theoretical side, a number of proposals focusing on superposition of macroscopic states of mechanical oscillators [25], light-oscillators entanglement [26–29] and oscillator-oscillator quantum correlations [30] gained considerable interest in the last years.

Following this line of thought, in this thesis we study a general model in which an harmonic oscillator is coupled with a two level system [31, 32]. In the spirit of the ideas illustrated above, such model can be considered as an example of a microscopic-macroscopic interaction, where the microscopic system (the qubit) is used to induce and detect quantum features in the state of the macroscopic one (the harmonic oscillator). Albeit relatively simple, the model gives rise to a variety of non-trivial effects, such as geometric phases generated by a cyclic displacement of the harmonic oscillator state in phase space, non-local correlations between the two subsystems and negative values of the oscillator's Wigner function.

The model we consider can be implemented in different physical systems, ranging from superconducting devices [33, 34] to ions traps [35]. Here, we focus in particular on opto-mechanical devices consisting of a single atom trapped in a cavity with movable mirrors, which constitute the macroscopic mechanical resonators. The resonators currently employed in these type of experiments are undoubtedly massive compared to usual quantum mechanical systems [15, 18, 22,

36–38], and as such they can be considered as genuine macroscopic objects. However, we would like to point out that our interest in macroscopic quantumness is not exclusively related to the mass and the size of a given object. In this regard, one of the most characteristic features of macroscopic systems is a strong interaction with the environment, which leads to dissipation and reduced purity of the state of the system. Such condition itself, independently of the size of the object considered, constitutes one of the main targets or our study.

In the journey to the frontiers of quantum mechanics, the investigation of macroscopic systems is not the only unexplored territory. In particular, open systems subjected to time-dependent external perturbations constitute another optimal playground to test the limits of quantum theory. This is particularly true in the case of critical systems. Close to a quantum phase transition there is an intimate relation between equilibrium and dynamical properties. The critical slowing down, characteristic of continuous phase transitions, suggests that the response to an external periodic drive may be highly non-trivial. Investigating this type of systems is intriguing for at least two reasons: the detection of the dynamical Casimir effect (DCE) [39–43] and the investigation of the Kibble-Zurek mechanism (KZM) [44–46].

As well as the widely known Casimir-Polder forces, DCE can be considered as a manifestation of the vacuum fluctuations. More specifically, DCE refers to the amplification of the zero-point fluctuations due to a time modulation of the boundary conditions of the problem. Such modulation results in a generation of excitations from vacuum (for example photons in the case of an electromagnetic field). Although a number of interesting proposals directed toward the observation of this phenomenon have been put forth in the last decades [47–50], DCE has been

experimentally verified only recently [51].

On the other hand, KZM provides a simple and accurate description of the dynamics of a continuous phase transition. First formulated in a cosmological context to describe the expansion of the early universe by Kibble [44], and later employed to explain the formation of topological defects in ^{4}He by Zurek [45], KZM represents one of the characteristic phenomena encountered in critical systems. Fundamentally, KZM originates in the unavoidable departure from adiabaticity experienced by a system when it is brought close enough to its critical point. The general mathematical framework provided by KZM is surprisingly versatile and it can be applied to a variety of situations, ranging from continuous phase transition at cosmological scale [44] to avoided crossing in two level quantum systems [52].

In this thesis, we pursue the intriguing task of studying a genuine manifestation of quantum mechanics such as DCE in the context of critical systems [53,54]. In particular, we consider a periodic modulation of the Hamiltonian parameters close to the so called *superradiant phase transition* in the Dicke model [55–57]. The aim of our study consists of proposing a way to lower the otherwise prohibitive experimental requirements needed for the observation of DCE in optical systems by exploiting the peculiarities of quantum phase transitions. Specifically, due to the characteristic reduction of the energy gap between the ground state and the first excited state in the proximity of the critical point, the frequency at which the Hamiltonian parameters need to be modulated in order to achieve DCE can be considerably lowered by bringing the system close to criticality.

Moreover, our study reveals an intriguing connection between the DCE and the KZM. We show that, when the system is brought close to the quantum phase transition, the photon production arising from DCE can be interpreted as a mani-

festation of KZM. The connection between DCE and KZM can be tracked down to their common fundamental cause, the inability of the system to adiabatically follow the changes in the control parameters when criticality is approached. In this regard, our analysis provides a novel, general interpretation of the processes involved in the dynamics of a continuous quantum phase transition.

This thesis comprises four chapters. In Chapter 2, we briefly introduce the fundamental concepts and the mathematical tools used throughout this thesis. In the first part of the chapter, we give a definition of geometric phases for pure states and for mixed states. In the second part, we describe the physical principle at the core of opto-mechanics, the *radiation pressure force*, and we introduce the mathematical tools used to characterize quantumness in opto-mechanical devices. In the third part, we give a brief overview of two fundamental phenomena which play an important role in the context of this thesis, the Dynamical Casimir effect (DCE) and the Kibble-Zurek Mechanism (KZM).

In chapter 3, we introduce so called *reverse Von Neumann measurement model*, in which a two level system is coupled with a quantum harmonic oscillator. Using the two level system as a probe, we show how it is possible to detect a geometric phase picked up by the harmonic oscillator during a cyclic evolution. We also show that the phase can still be observed in presence of interactions between the oscillator and the environment. Indeed, in some particular condition, the dissipative component in the oscillator's dynamics is responsible for the generation of the geometric phase.

In chapter 4, we analyze optomechanical setups in which a three level atom is effectively coupled with the movable mirrors of a cavity. Such effective coupling results in a conditional displacement of the mirrors subjected to the internal state

of the atom. Our study is focused on non-classical features of the atom-mirrors system, including atom-mirrors entanglement, non-locality and negative values of the mirrors' Wigner function. Such quantum behaviors are tested in a realistic regime, i.e. the mirrors are in equilibrium with a thermal bath at finite temperature and they undergo dissipative dynamics. We perform our analysis for two different setups: in the first setup we assume that only one of the cavity's mirrors is able to move. In the second setup, we treat the case in which both mirrors can oscillate around their equilibrium positions.

In Chapter 5, we address the second topic treated in this thesis, the connection between the Dynamical Casimir effect (DCE) and the Kibble-Zurek mechanism (KZM). We propose a scheme where N two level atoms are able to collectively interact with the electromagnetic field inside an optical cavity, realizing the so called *Dicke model*. We exploit the fundamental characteristics of the quantum phase transition existing in such model in order to simplify the experimental observation of DCE in the optical range. Moreover, we show how the generation of photons arising from DCE can be linked to KZM, a phenomenon typically related to criticality.

Chapter 2

Tools and Concepts

In this chapter, we give a general overview of the key concepts and tools used in this thesis. The chapter is intended as a propaedeutic introduction for the subjects treated in the rest of the thesis. In Section 2.1, we introduce a general definition of geometric phase and its connection with the idea of gauge transformations and gauge invariance, both for pure and for mixed states. In Section 2.2, we give a short overview on opto-mechanical systems, describing the basic working mechanism of such devices, the radiation pressure force, and focusing on the theoretical tools generally used to analyze their properties. Finally, the aim of Section 2.3 is to give a general picture of two important subjects of this thesis, the dynamical Casimir effect and the Kibble-Zurek mechanism, emphasizing the aspects of these two phenomena which are relevant for our arguments.

2.1 Geometric Phases

First proposed by Berry in the context of cyclic adiabatic evolution of quantum systems [58] and then generalized by Anandan and Aharonov for general non-adiabatic unitary evolution [59], the concept of geometric phase is regarded as one of the fundamental features of quantum mechanics since then. Although this concept is well defined for pure states undergoing cyclic and non-cyclic unitary evolution, many physicists have been challenged by the problem of defining geometric phases for mixed states. In this section, we start from an intuitive picture of the so called *quantum kinematic approach to geometric phases* [60, 61] to arrive to an *interferometric definition* of geometric phases, an operational approach proposed in [62].

2.1.1 Gauge invariance: an intuitive picture

Geometric phases are strongly related to the existence of gauge invariants in quantum theory. Gauge invariance is one of the key concepts in modern physics, and it plays a fundamental role in quantum field theory, classical electrodynamics and quantum mechanics in general. In order to emphasize the fundamental importance of this concept, let us introduce it starting from the very basic building blocks of quantum mechanics.

In quantum theory [63,64], the state of a physical system is described in terms of normalized vectors living in a N-dimensional complex vector space $\mathcal{H}$ called Hilbert space. In the widely adopted Dirac notation, a vector in $\mathcal{H}$ is written as $|\psi\rangle$, while the scalar product between two vectors $|\psi\rangle$ and $|\phi\rangle$ is denoted by $\langle\psi|\phi\rangle$. Within this notation, the normalization condition is then given by $\langle\psi|\psi\rangle = 1$. The

vector $|\psi\rangle$ contains information about the outcomes of a measurement performed on the system. However, these outcomes can be only predicted in a probabilistic way.

According to quantum theory, observable quantities are represented by Hermitian operators acting on the Hilbert space $\mathcal{H}$. When an observable $\mathcal{A}$ is measured, the only possible outcomes of the measurement are the eigenvalues $\{a_k\}$ of $\mathcal{A}$, and the probability of obtaining the outcome a_k is given by $P_k = |\langle\varphi_k|\psi\rangle|^2$, where $|\varphi_k\rangle$ is the eigenvector of $\mathcal{A}$ associated with the eigenvalue a_k (for the sake of simplicity, here we are only considering the case in which $\mathcal{A}$ has a discrete non-degenerate spectrum). This means that the predictions about the outcomes of a measurement are *intrinsically* probabilistic, and the probabilities P_k are indeed the only experimentally accessible quantities.

A consequence of this observation is that, if we consider two vectors $|\psi\rangle$ and $|\psi'\rangle$ such that the probabilities $P_k = |\langle\varphi_k|\psi\rangle|^2$ and $P'_k = |\langle\varphi_k|\psi'\rangle|^2$ are the same for any possible observable, then the two vectors describe, *at the most fundamental level*, the same physical state. This characteristic of quantum states can be seen by considering the two vectors $|\psi\rangle$ and $|\psi'\rangle = e^{i\alpha}|\psi\rangle$. It is straightforward to see that the probabilities P_k are the same for the two vectors no matter what observable is measured, and we have to conclude that they represent the same physical state. The operation of adding a phase factor to a vector in Hilbert space is called *phase transformation* and it can be seen as a particular type of *gauge transformation*.

We can now put the first postulate given above in a more correct form: physical states are represented by normalized vector in Hilbert space defined *up to an overall phase factor*. In terms of gauge theory, adding an overall phase factor will

change the gauge in which the system is described, although this operation does not change the outcomes of any possible measurement.

Let us now rephrase the concept of gauge transformations in a more mathematical way. A phase transformation is a map $\mathcal{G} : \mathcal{H} \to \mathcal{H}$ acting on the Hilbert space $\mathcal{H}$ defined as

$$\mathcal{G}_\alpha|\psi\rangle = e^{i\alpha}|\psi\rangle. \tag{2.1}$$

The transformations $\mathcal{G}_\alpha$ can be regarded as symmetry transformations in the group $U(1)$, so we will also refer to them as $U(1)$ transformations. Given the group $U(1)$, we can define the set of equivalence classes under $U(1)$ transformations for each vector $|\psi\rangle \in \mathcal{H}$. This set is called the *projective Hilbert space* and it is denoted by $\mathcal{P}$, while its elements are called *rays*. The set $\mathcal{P}$ can be identified with the set of pure density matrices defined on the Hilbert space $\mathcal{H}$, i.e. the set of the $N \times N$ Hermitian matrices ρ such that $\mathrm{Tr}\{\rho\} = 1$ and $\rho = \rho^2$. For that reason, we will also call an element of $\mathcal{P}$ a *pure density matrix* corresponding to the vector $|\psi\rangle$ and we denote it as $\rho^\psi \equiv |\psi\rangle\langle\psi|$.

We are now in the position to introduce the map $\Pi : \mathcal{H} \to \mathcal{P}$, called a *projection*, transforming vectors into pure density matrices and defined as

$$\Pi|\psi\rangle = \rho^\psi. \tag{2.2}$$

The projection operation is a surjective mapping from $\mathcal{H}$ to $\mathcal{P}$. We also introduce the "inverse" relation $\mathcal{L}_\alpha : \mathcal{P} \to \mathcal{H}$, which is called a *lift* and maps pure density matrices back into vectors according to

$$\mathcal{L}_\alpha(\rho^\psi) = e^{i\alpha}|\psi\rangle, \quad \text{with} \quad \mathcal{L}_0(\rho^\psi) = |\psi\rangle. \tag{2.3}$$

There are infinitely many ways of choosing a lift $\mathcal{L}_\alpha$ corresponding to all possible real values of the parameter α. The lift operation introduces the overall phase factor $e^{i\alpha}$, which does not change the physical properties of the state. Such phase factor fixes the gauge in which the state is described.

In the light of this formalism, the discussion in the previous paragraphs can be now rephrased in the following terms: all of the physical accessible information about the (pure) state of a system is contained only in the pure density matrix ρ^ψ living in the projective Hilbert space $\mathcal{P}$, which is then the actual space where the physical properties of the system are encoded. However, the state of the system is mathematically described by a vector $|\psi\rangle$ living in $\mathcal{H}$, which is obtained by applying a lift $\mathcal{L}_\alpha$ to ρ^ψ. Choosing one particular lift is equivalent to choose the gauge in which the system is described. The choice of the gauge does not influence the experimental outcomes of a measurement, so changing the gauge will not have any observable consequences. Any choice for the gauge is legitimate, but all physical quantities are required to remain unchanged under gauge transformations, i.e. are required to be *gauge invariants*.

The general argument used in the discussion above is analog to the one used in classical electrodynamics. It is known that an electromagnetic field is described using an abstract vector potential $\mathbf{V}$ which is defined up to a term ∇f, with f a general scalar field. Choosing the function f is equivalent of choosing the gauge, while changing f defines a gauge transformation. However, the Maxwell equations describing the dynamics of the observable electromagnetic field arising from $\mathbf{V}$ do not depend on the choice of f, i.e. they are gauge invariant. Gauge transformations and gauge invariance play an important role also in other areas of physics. In particular, in quantum field theory, the so called *gauge theories* in-

vestigate gauge invariance under symmetry groups different from $U(1)$. However, this subject is far beyond the purposes of this introduction and it is not going to be treated here.

Let us conclude this section giving a simple example of gauge invariance, which gives the flavour of the practical implications of this concept. Let us consider the modulus of the scalar product between two (non-orthogonal) vectors $|\psi_0\rangle$ and $|\psi_1\rangle$, which is written as $|\langle\psi_0|\psi_1\rangle|$. After applying a phase transformation mapping $|\psi_0\rangle \to |\psi_0'\rangle$ and $|\psi_1\rangle \to |\psi_1'\rangle$, with $|\psi_0'\rangle = e^{i\alpha_0}|\psi_0\rangle$ and $|\psi_1'\rangle = e^{i\alpha_1}|\psi_1\rangle$, it is straightforward to see that $|\langle\psi_0'|\psi_1'\rangle| = |\langle\psi_0|\psi_1\rangle|$. The invariance of this quantity under $U(1)$ transformation is not surprising after all, since taking the modulus of the scalar product "washes out" all the phase factors. To find more interesting gauge invariant quantities, we need to consider combinations involving more then two vectors.

2.1.2 Geometric phase and Gauge invariants

In the previous section we have pointed out how the outcomes of any physical observations performed on a system are independent on the particular choice of the gauge. That means that any measurable quantity must be a gauge invariant, i.e. must depend only on the structure of the projective Hilbert space $\mathcal{P}$. In this section, we introduce geometric phase as a quantity with this properties using an operational approach, meaning that our definition of geometric phase is given in terms of the amount by which the interference fringes arising from an interferometric experiment are shifted due to the cyclic evolution of a generic quantum system.

Let us start by considering a quantum state whose initial state is given by the pure density matrix ρ_0^ψ, and let's suppose the state is subsequently transformed in ρ_1^ψ, ρ_2^ψ and back in ρ_0^ψ. We now want to apply a lift to the three pure density matrices to obtain three vectors in Hilbert space according to $\mathcal{L}_{\alpha_0}(\rho_0^\psi) = |\psi_0\rangle$, $\mathcal{L}_{\alpha_1}(\rho_1^\psi) = |\psi_1\rangle$ and $\mathcal{L}_{\alpha_2}(\rho_2^\psi) = |\psi_2\rangle$ (notice that here the phase factors are implicitly included in the definition of $|\psi_j\rangle$). This operation fixes the gauge in which the system is described. As pointed out in the previous section, any choice of gauge is legitimate, since such choice does not influence the physical properties of the system. We then choose the phases α_0, α_1 and α_2 such that $\arg\langle\psi_0|\psi_1\rangle = 0$ and $\arg\langle\psi_1|\psi_2\rangle = 0$. Under this gauge choice, the vectors $|\psi_0\rangle$ and $|\psi_1\rangle$ (as well as the vectors $|\psi_1\rangle$ and $|\psi_2\rangle$) are said to respect the condition of *distant parallelism* [65] and the state is said to be *parallel transported* from $|\psi_0\rangle$ to $|\psi_1\rangle$ and from $|\psi_1\rangle$ to $|\psi_2\rangle$.

It is important to notice that, even though it is possible to choose a gauge such that the parallel transport condition is always satisfied, i. e. $\arg\langle\psi_0|\psi_1\rangle = 0$ and $\arg\langle\psi_1|\psi_2\rangle = 0$, the first vector $|\psi_0\rangle$ and the last vector $|\psi_2\rangle$ might not respect the condition of distant parallelism, meaning that $\arg\langle\psi_0|\psi_2\rangle \neq 0$ in general. The non-transitive nature of parallel transport plays a fundamental role in the arising of geometric phases, as we will see shortly.

Keeping this in mind, let us consider a quantum system initially prepared in the pure density matrix ρ_0^ψ. We suppose that the system's evolution is given by a sequence of pure density matrices $\mathcal{S} \equiv \{\rho_0^\psi, \rho_1^\psi, \ldots \rho_n^\psi\}$. The sequence $\mathcal{S}$ defines a discrete cyclic path in the projective Hilbert space $\mathcal{P}$. This means that the state of the system is subsequently transformed along $\mathcal{S}$ and back to ρ_0^ψ, according to $\rho_0^\psi \rightarrow \rho_1^\psi \cdots \rightarrow \rho_n^\psi \rightarrow \rho_0^\psi$. Let us now apply a lift $\mathcal{L}_{\{\alpha_j\}}$

to the whole sequence $\mathcal{S}$. This operation fixes the gauge in which the evolution is described, generating a sequence of vectors in $\mathcal{H}$ (or a path in $\mathcal{H}$) given by $S \equiv \{\mathcal{L}_{\{\alpha_0\}}(\rho_0^\psi), \mathcal{L}_{\{\alpha_1\}}(\rho_1^\psi), \ldots, \mathcal{L}_{\{\alpha_n\}}(\rho_n^\psi)\}$. The question we would like to ask is wether it is possible to find a physical quantity which depends only on the *geometry* of the path $\mathcal{S}$ in the projective Hilbert space $\mathcal{P}$, meaning that it is determined only by the pure density matrices $\{\rho_j^\psi\}$ and by their order in the sequence. Obviously, this quantity is also required to be gauge invariant.

To answer this question, let us now choose a gauge such that the state of the system results parallel transported along the path S. Within this gauge choice, the path S in Hilbert space is given by $S \equiv \{|\psi_0\rangle, |\psi_1\rangle, \ldots, |\psi_n\rangle\}$, with the vectors $\{|\psi_j\rangle\}$ fulfilling the parallel transport condition $\arg\langle\psi_j|\psi_{j+1}\rangle = 0$, $\forall j \in \{0, 1, \ldots, n-1\}$. Once the gauge is chosen, we are in the position of considering the interference experiment sketched in Figure 2.1: after going through the first beam splitter, the initial state of the system $|\psi_0\rangle$ evolves independently in the two arms of the interferometer. While a simple phase shifting is applied in the upper arm, the system undergoes the cyclic evolution defined by the path S in the lower arm. The two system are recombined by the second beam splitter, and interference fringes are generated at the interferometer output. An explicit calculation shows that the interference fringes will result shifted, respect to the phase reference given by χ, by an amount corresponding to

$$\theta_g(\mathcal{S}) = \arg \Delta(\psi_0, \ldots, \psi_n), \tag{2.4}$$

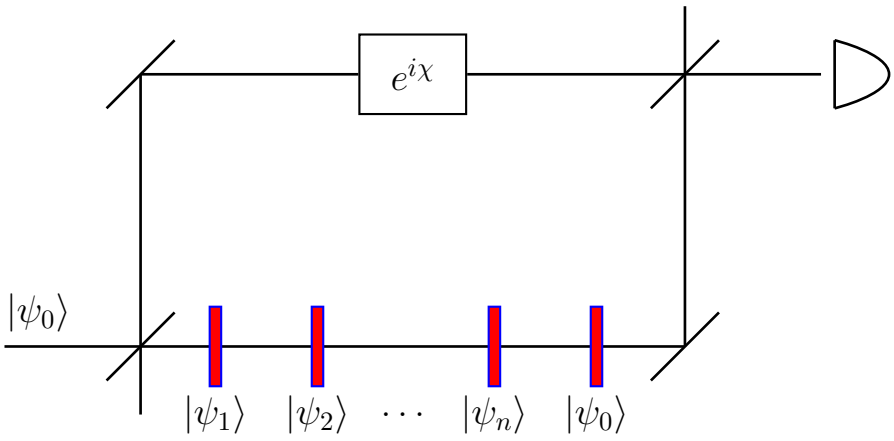

Figure 2.1: Schematic representation of an interference experiment in which a state $|\psi_0\rangle$ undergoes a cyclic evolution in the lower arm of a Mach-Zender interferometer. The geometric phase acquired in the process can be detected by looking at the shifting in the interference pattern generated in the output of the interferometer.

where the complex quantity $\Delta(\psi_0, \ldots, \psi_n)$ is given by

$$\Delta(\psi_0, \ldots, \psi_n) = \langle\psi_n|\psi_0\rangle \prod_{j=0}^{n-1} \langle\psi_j|\psi_{j+1}\rangle. \tag{2.5}$$

It can be easily checked that the quantity $\Delta(\psi_0, \ldots, \psi_n)$ is invariant under gauge transformations. This quantity, which is called *Bargmann invariant* [60, 66, 67], thus depends only on the path $\mathcal{S}$ in the projective Hilbert space $\mathcal{P}$ and it is independent on the choice of the gauge. As a consequence of the invariance of $\Delta(\psi_0, \ldots, \psi_n)$, the phase $\theta_g(\mathcal{S})$ is also a physical observable quantity which depends only on the geometric properties of the path $\mathcal{S}$ followed during the cyclic evolution, and as such we will call it the geometric phase associated with $\mathcal{S}$.

The discussion above can be generalized to the case in which the system evolves along a continuous curve in the projective Hilbert space. In this scenario,

a continuous curve in $\mathcal{P}$ is defined as $\mathcal{C} \equiv \{\rho^{\psi}(s)\}$. The situation is analogous to the one treated above, with the difference that the discrete index j has been substituted by the continuous real parameter $s \in [s_i, s_f]$. We can now apply a lift to the whole curve $\mathcal{C}$ to obtain a curve $C \equiv \{\mathcal{L}_{\alpha_s}(\rho^{\psi}(s))\}$ formed by vectors in $\mathcal{H}$.

The passage between the discrete and the continuous case can be implemented by dividing the interval $[s_i, s_f]$ into n smaller intervals $[s_j, s_{j+1}]$ such that

$$\begin{aligned} & s_j < s_{j+1}, \quad \forall j \\ & |s_{j+1} - s_j| = \epsilon, \quad \forall j \\ & s_0 = s_i, \quad s_n = s_f. \end{aligned} \tag{2.6}$$

Making use of this subdivision, we can consider the same interference experiment described above where the discrete path in $\mathcal{H}$ followed during the evolution is defined by the sequence $\{|\psi(s_0)\rangle, |\psi(s_1)\rangle \ldots |\psi(s_n)\rangle\}$. According to Equation (2.4), the interference fringes in the interferometer's output are then shifted by $\arg \Delta_{\epsilon}(\psi(s_0), \psi(s_1), \ldots, \psi(s_n))$. To obtain the geometric phase for the continuous curve $\mathcal{C}$, it is sufficient to take the limit of this expression, i.e.

$$\theta_g(\mathcal{C}) = \lim_{\epsilon \to 0} \arg \Delta_{\epsilon}(\psi(s_0), \psi(s_1), \ldots, \psi(s_n)). \tag{2.7}$$

A detailed calculation shows that the limit in Equation (2.7) exists and is given by [61]

$$\theta_g(\mathcal{C}) = \arg\langle\psi(s_i)|\psi(s_f)\rangle + i \int_{s_i}^{s_f} ds \langle\psi(s)|\frac{\partial}{\partial s}|\psi(s)\rangle. \tag{2.8}$$

The quantity $\theta_g(\mathcal{C})$ is the geometric phase associated with the curve $\mathcal{C}$. Opera-

tionally, it can be defined as the amount by which the interference fringes arising from an interferometric experiment are shifted due to the cyclic evolution of the system along a continuous closed curve $\mathcal{C}$.

Some additional remarks are due regarding the form of Equation (2.8). The geometric phase $\theta_g(\mathcal{C})$ is written as the sum of two terms, each of which can be interpreted as an independent contribution to the total gauge independent quantity $\theta_g(\mathcal{C})$. The first term on the RHS of Equation (2.8), given by

$$\theta_{\rm tot} = \arg\langle\psi(s_i)|\psi(s_f)\rangle, \tag{2.9}$$

can be regarded as the *total* phase difference between the initial state $|\psi_i\rangle$ and the final state $|\psi_f\rangle$ in the curve C. On the other hand, the second term

$$\theta_{\rm d} = i\int_{s_i}^{s_f} ds\langle\psi(s)|\frac{\partial}{\partial s}|\psi(s)\rangle \tag{2.10}$$

represents the *dynamical* contribution to the geometric phase arising from the evolution along C. It is important to stress that these two terms, if considered *individually*, are not independent on the choice of the gauge. Only the sum of them is gauge invariant, and as such represents a physical property of the system which can be observed through an interference experiment. The form of Equation (2.8) shows that the formalism presented above is equivalent to the original Berry-Aharonov-Anandan proposals [58, 59], and it is indeed the most general way to define geometric phases in the context of pure states undergoing a unitary evolution.

We would like to stress one more time that $\theta_g(\mathcal{S})$ represents the amount by

which the interference fringes are shifted due to the cyclic evolution $\mathcal{S}$ of the system in the lower arm of the interferometer. Indeed, an interference experiment where the shifting of the fringes with respect to a fixed reference is observed represents the only way to measure a phase picked up by a given system [65], and in this sense in can be regarded as an *operational* definition of geometric phase. This idea is particularly useful in our discussion, since it allows us to extend the definition of geometric phase to the case of mixed states (see Section 2.1.3).

2.1.3 Geometric phases for mixed states

In the previous section we have treated the problem of defining geometric phases for pure states undergoing a cyclic unitary evolution, considering an operational definition of geometric phase in terms of the amount by which the fringes arising from an interference experiment are shifted. This approach is useful since it can be generalized to the case of cyclic evolution of *mixed* states.

Following [62], let us consider an interference experiment in which a quantum system undergoes an unitary transformation U in the lower arm of an interferometer while only a fixed phase shift $e^{i\chi}$ is applied in the upper arm. The situation is analogous to the one considered in the previous section, with the difference that here the initial state of the system is not a pure state but a general density matrix ρ_0. Differently from the case of a pure density matrix, ρ_0 can not be associated with a vector in Hilbert space. In general, a density matrix can be written as an incoherent sum of pure states according to $\rho_0 = \sum_k w_k |\psi_k\rangle\langle\psi_k|$.

Let us now consider the effect of the unitary transformation applied to ρ_0 on the output intensity of the interferometer. Considering that the action of U is given

by $\rho_1 = U\rho_0 U^\dagger$, the intensity I at the interferometer output can be calculated and it turns out to be [62]

$$I = \frac{1}{2}\big(1 + |\mathrm{Tr}\{U\rho_0\}| \cos[\chi - \arg \mathrm{Tr}\{U\rho_0\}]\big). \tag{2.11}$$

It is clear from Equation (2.11) that the unitary transformation applied to the initial state ρ_0 in the lower arm of the interferometer results in a shifting of the interference fringes in the output by an amount corresponding to $\theta = \arg \mathrm{Tr}\{U\rho_0\}$. Moreover, the *visibility* of the fringes ν, defined as $\nu = (I_{\max} - I_{\min})/(I_{\max} + I_{\min})$, is reduced by a factor $|\mathrm{Tr}\{U\rho_0\}|$.

Recalling the decomposition of the density matrix ρ_0 as an incoherent sum of pure density matrix given above, the quantities θ and ν can be regarded as *average* values over the probability distribution w_k. Indeed, for a pure state $|\psi_k\rangle$, Equation (2.11) reduces to

$$I_k = \frac{1}{2}\big(1 + \nu_k \cos[\chi - \theta_k]\big), \tag{2.12}$$

where $\nu_k = |\langle\psi_k|U|\psi_k\rangle|$ and $\theta_k = \arg\langle\psi_k|U|\psi_k\rangle$. Taking the average over the probability distribution w_k we obtain

$$I = \frac{1}{2}\sum_k w_k I_k = \frac{1}{2}\big(1 + \sum_k w_k \nu_k \cos[\chi - \theta_k]\big). \tag{2.13}$$

This equation can be recast into the form $I = (1/2)(1 + \nu\cos[\chi - \theta])$ observing

that

$$\begin{aligned} \theta &= \arg \sum_k w_k \nu_k e^{i\theta_k} = \arg \mathrm{Tr}\{U\rho_0\}, \\ \nu &= \left| \sum_k w_k \nu_k e^{i\theta_k} \right| = |\mathrm{Tr}\{U\rho_0\}|. \end{aligned} \tag{2.14}$$

It is important and crucial to point out that, within this operational definition, the shifting in the interference pattern due to the cyclic evolution *defines* the geometric phase θ acquired by the system.

Let us reconsider the argument above in the context of a unitary time evolution described by the time-dependent operator $U(t)$. As done in the case of pure states, we assume that the parallel transport condition is always satisfied during the evolution. For the mixed state case, the parallel transport condition can be stated as $\mathrm{Tr}[\rho(t)\dot{U}(t)U^\dagger(t)] = 0$. Moreover, a more stringent condition is required to be fulfilled. Together with the parallel transport condition for the density matrix $\rho(t)$, we also require that the instantaneous eigenstates $|\varphi_k(t)\rangle$ of $\rho(t)$ fulfill the condition $\langle\varphi_k(t)|\dot{U}(t)U^\dagger(t)|\varphi_k(t)\rangle = 0$. These two conditions define the parallel transport in the case of a non-degenarate density matrix. Considering a curve in the density matrices space defined by the unitary operator $U(t)$ whose end points are ρ_0 and $\rho(T)$, the two conditions above ensure that the dynamical contribution to the total phase picked up along the curve is identically zero. For that reason, following the argument put forth above, we can associate a geometric phase $\theta_g = \theta = \arg \mathrm{Tr}\{U(T)\rho_0\}$ to this curve.

2.2 Opto-mechanical devices

The study of opto-mechanics devices have received a huge boost in the recent years triggered by the constant advances in engineering high finesse optical cavities and mechanical resonators at a microscopic level. In this section, we give a general overview on this topic, both from an experimental and a theoretical point of view. In Section 2.2.1, we give a brief overview of the fundamental mechanism these devices are based on, the radiation pressure force, and we describe some of the recent experimental achievements in the field. In Section 2.2.2, we analyze the mathematical tools we will use in the rest of this thesis to witness quantum behaviors in such devices.

2.2.1 Radiation pressure

Radiation pressure is a phenomenon first observed at the beginning of the last centuries [68,69]. The idea that light is able to "push" a surface made of conducting material is due to Maxwell himself, who predicted the existence of such an effect starting from his famous equations governing the dynamics of a classical electromagnetic field. In a quantum context, radiation pressure can be intuitively understood in terms of photons transferring their momentum to a surface.

Modern opto-mechanical devices are based on the radiation pressure effect. An opto-mechanical device is constituted by a Fabry-Perot cavity where one or both end mirrors are able to oscillate around their equilibrium positions. The oscillating mirror is treated as a quantum harmonic oscillator described by the annihilation and creation bosonic operators b and $b^\dagger$, with the canonical momentum and position operators p and q given by $p = i(b^\dagger - b)/\sqrt{2}$ and $q = (b^\dagger + b)/\sqrt{2}$. On

the other hand, the field inside the cavity is described by the photonic operators $a^\dagger$ and a, with the photons number operator n given by $n = a^\dagger a$. The moving mirror and the field inside the cavity interact through the radiation pressure Hamiltonian, given by

$$H_{\text{rp}} = \chi a^\dagger a(b^\dagger + b), \tag{2.15}$$

where χ is a coupling constant given by $\chi = (\omega/L)\sqrt{\hbar/2m\omega_m}$, with ω the fundamental mode of the cavity, L the cavity length, m the mass of the mirror and ω_m its frequency [1] [70]. The Hamiltonian H_{rp} is valid only under the adiabatic approximation for the motion of the mirror, i.e. under the condition $\omega \gg \omega_m$. This condition is usually widely satisfied when optical cavities and mechanical cantilevers are considered. The adiabatic condition ensures that no photons are scattered by the mirror in other modes of the cavity, so that the cavity field can be considered as monochromatic for practical purposes.

The Hamiltonian in Equation (2.15) clearly shows how the radiation pressure interaction affects the position of the oscillator. To see that, let us consider the time evolution operator $U(t) = \exp(-iH_{\text{tot}}t)$ corresponding to the total Hamiltonian of the system, i. e.

$$H_{\text{tot}} = \omega a^\dagger a + \omega_m b^\dagger b + H_{\text{rp}}. \tag{2.16}$$

Using Baker-Campbell-Hausdorf expansion, it can be shown that the time evolution operator assumes the form [71]

$$U(t) = e^{-i\omega a^\dagger a t} e^{i\tilde{\chi}^2 (a^\dagger a)^2 \Lambda(t)} D_m[\zeta(t)\tilde{\chi} a^\dagger a] e^{-i\omega_m b_s^\dagger b_s}, \tag{2.17}$$

[1] Notice that, although we have set $\hbar \equiv 1$ in equation (2.15), $\hbar$ appears in the definition of χ, which has the correct units of s^{-1}.

with $\tilde{\chi} = \chi/\omega_m$, $\Lambda(t) = \omega_m t - \sin(\omega_m t)$, $\zeta(t) = 1 - e^{-i\omega_m t}$ and $D_m[\ldots]$ is the displacement operator for the mirror. Equation (2.17) clearly shows that the oscillator is displaced in phase space by an amount proportional to the number of photons present in the cavity due to the radiation pressure effect.

The time evolution operator arising from radiation pressure gives rise to a variety of interesting phenomena which have been subject of extensive studies. In this thesis, we will consider a different Hamiltonian model which can be directly derived from Equation (2.15) under some particular conditions (see Chapter 3 and Chapter 4).

2.2.2 Quantum witnesses

In the context of opto-mechanics, it is unrealistic to assume a pure unitary evolution of the mechanical resonators. Factors like mechanical damping and thermal fluctuations heavily influence the dynamics of the system, giving rise to non-trivial dissipative evolutions. The question we want to ask is whether such massive systems strongly interacting with the environment can still display important non-classical features. In particular, we consider entanglement between various subparts of the system, violations of Bell inequalities and negative values of the Wigner function as signatures of non-classicality. Such features are widely regarded as characteristic manifestations of quantum mechanics.

Opto-mechanical systems are better described using the continuous variables formalism. Quantifying the amount of entanglement in a general continuous variable mixed state is not a trivial task. Indeed, a precise quantification of entanglement is possible only for a certain class of states called *Gaussian states* [72],

i.e. those states whose Wigner function is Gaussian. The non-linearity of the radiation pressure Hamiltonian leads to field-mirror states that are in general non-Gaussian throughout the evolution of the whole system. Although it is possible to make some approximations which lead to a linearized effective interaction Hamiltonian [29, 73–75], in this thesis we are interested in the effects arising from the non-linear nature of the interaction (see Chapter 4). For these reasons, we are going to introduce mathematical tools that are suitable for the detection of entanglement in non-Gaussian states. Due to the lack of necessary and sufficient separability criteria for such states, in general entanglement can only be witnessed by making use of *entanglement witnesses,* which rely on existing necessary (but not sufficient) separability conditions for non-Gaussian states.

The first entanglement witness we introduce is based on the Peres-Horodecki separability criterion [76, 77]. In general, a density matrix ρ describing the state of a bipartite quantum system formed by the two parts A and B can be written as $\rho = \sum \rho_{jk}^{\mu\nu} |j\rangle_A\langle k| \otimes |\mu\rangle_B\langle\nu|$, where $\{|j\rangle_A\}$ and $\{|\mu\rangle_A\}$ are complete orthonormal basis for the subsystems A and B, respectively. The density matrix ρ is said to be separable if and only if it can be written in the form $\rho = \sum_k w_k \rho_k^A \otimes \rho_k^B$, where ρ_k^A (ρ_k^B) are generic density matrices referring to the system A (B) alone and w_k are real coefficients fulfilling the condition $\sum_k w_k = 1$.

According to the Peres-Horodecki criterion, a density matrix is separable only if none of the eigenvalues of its partial transpose with respect to A (or, equivalently, to B) is negative, being the partial transposition operation with respect to A defined as $\rho^{T_A} \equiv \sum \rho_{jk}^{\mu\nu} |k\rangle_A\langle j| \otimes |\mu\rangle_B\langle\nu|$. The implication can be simply proven, since for a separable density matrix the partial transpose reduces to $\rho^{T_A} = \sum_k w_k (\rho_k^A)^T \otimes \rho_k^B$, which is a non-negative density matrix. Based on

Peres-Horodecki criterion, it is possible to define an entanglement witness, called *logarithmic negativity* [78], that quantifies the negativity of the partial transposed density matrix. The logarithmic negativity E is defined as $E(\rho) = \log(||\rho^{T_A}||)$, where $||.||$ denotes the trace norm of an operator. For a density matrix, the trace norm is defined as $||\rho|| = \mathrm{Tr}|\rho|$.

The quantity E provides a quantification of the amount of entanglement in the cases in which the Peres-Horodecki criterion is also a sufficient condition for separability. These includes the case in which A and B are two-dimensional systems and the case in which one of the systems is two-dimensional and the other three-dimensional [77]. In the context of continuous variable entanglement, the criterion has been proven a sufficient separability condition for Gaussian states [79,80]. For non-Gaussian states, logarithmic negativity can be seen only as an entanglement witness, meaning that a non-zero value of E still implies the non-separability of the state, although it is possible that $E = 0$ for a non-separable state.

Another way to witness non-classicality in a mixed state consists of making use of violations of Bell inequalities. According to Bell theorem [81,82], the predictions of quantum mechanics can not be reproduced by a local hidden variable theory. More precisely, assuming that the outcomes of quantum measurements are determined by some local hidden variable probability distribution necessarily leads to some limitation in the amount of correlations two parties A (Alice) and B (Bob) can share. Considering certain quantum states, these limitations can be overcome, meaning that no local hidden variable theory can explain this type of quantum correlations. In order to clarify this concept, we now briefly outline the proof of Bell theorem.

Let us consider the scenario in which Alice and Bob share a quantum state. Al-

ice (Bob) perform some measurement A (B) whose outcomes are given by a (b). The joint probability of a certain pair of outcomes $\{a, b\}$ given the measurements $\{A, B\}$ is given by $P(ab|AB)$. We assume that such outcomes are determined by the choice of the measurements A and B and by some hidden variable λ, such that the joint probability distribution is now given by $P(ab|AB, \lambda)$. We now assume the hidden variable λ can influence the outcomes of a given measurement only locally. This assumption can be formalized by assuming that the joint probability $P(ab|AB, \lambda)$ can be factorized into local probability distributions for Alice and Bob, according to $P(ab|AB, \lambda) = P(a|A, \lambda)P(b|B, \lambda)$. Within this assumption, and supposing that the probability distribution $\rho(\lambda)$ of λ is unknown (in this sense the variable is "hidden"), the observable joint probability distribution can be written as

$$P(ab|AB) = \int d\lambda P(a|A, \lambda)P(b|B, \lambda)\rho(\lambda). \tag{2.18}$$

Equation (2.18) constitutes the crucial assumption in the derivation of Bell's theorem.

The existence of a local hidden variable theory imposes a boundary on the amount of correlations that Alice and Bob can share. Let us now consider the scenario in which Alice performs two measurements A and A' whose outcome are $a = \pm 1$ and $a' = \pm 1$ and Bob also performs two measures B and B' whose outcome are $b = \pm 1$ and $b' = \pm 1$. The correlations shared by Alice an Bob can be quantified by the correlation function $C(A, B)$, which is defined as the expectation value of A and B, i.e. $C(A, B) = \sum_{a,b} abP(ab|AB)$. Actually, by performing two measurements each, Alice and Bob can construct four different correlation functions $C(A, B)$, $C(A, B')$, $C(A', B)$ and $C(A', B')$. It is proven [82,83] that,

under the assumption of locality, the inequality

$$|C(A,B) + C(A,B') + C(A',B) - C(A',B')| \leq 2 \tag{2.19}$$

is always satisfied for any possible choice of A, A' and A, B'. This means that the assumption of local realism contained in Equation (2.18), i.e. the assumption that the outcomes of a measurement are determined by the local hidden variable λ with probability distribution $\rho(\lambda)$, necessarily imposes an upper bound to the quantity in Equation (2.19).

Quantum states that allow the violation of this bound, such as pure entangled states, can not be described by any local hidden variable theory. Non-locality can be regarded as a strong signature of non-classicality. Indeed, it has been shown [84] that entanglement is a necessary condition for violations of Bell inequalities, which can be thus considered a reliable entanglement witnesses. In this regard, it is important to point out that, in the context of this thesis, we do not attempt to propose an experimental test of Bell inequalities. We will only consider Bell inequalities (in particular CHSH inequality) as a theoretical tool to witness entanglement in non-Gaussian states.

Together with entanglement and non locality, negative values of the Wigner function associated with a density matrix can be regarded as a strong signature of non classicality. The Wigner function is a quasi-probability distribution describing the state of the system in phase space [85]. Given the density matrix ρ, the associated Wigner function $W(q,p)$ is defined as

$$W(q,p) = (1/\pi) \int_{-\infty}^{\infty} dy \langle q - y|\rho|q + y\rangle e^{2ipy}. \tag{2.20}$$

An equivalent definition of the Wigner function can be given in terms of the Fourier transform of the Weyl characteristic function $\chi(\nu)$ as (see also Equation (4.12) in Chapter 4) [72]

$$W(\mu) = \pi \int d^2\nu (e^{\mu\nu^* - \mu^*\nu})\chi(\nu), \tag{2.21}$$

where $\mu = q + ip$ and $\chi(\nu) = \mathrm{Tr}[D(\nu)\rho]$. Here $D(\nu) = \exp(\nu a^\dagger - \nu^* a)$ is the displacement operator for the mode a. For certain classes of states, the Wigner function associated with their density matrix is non-negative for all values of μ. In this case, $W(\mu)$ can be interpreted as the quantum analog to the classical Liouville density probability distribution. However, quantum states may exhibit negative values of the Wigner function. In this case, the quantum-to-classical analogy can not be put forth any longer, since the Liouville density probability distribution must be, by definition, non-negative. In this sense, negative values of the Wigner function can be seen as a genuine witness of non-classicality.

2.3 Dynamical Casimir effect and Kibble-Zurek Mechanism

A distinctive feature of the quantum theory of the electromagnetic field, and of quantum field theory in general, consists of the existence of vacuum fluctuations, also called zero-point fluctuations, which have no correspondence in the classical world. Such vacuum fluctuations are able to produce measurable effects such as the Casimir-Polder force between two neutral surfaces brought close enough to each other [86]. Another intriguing manifestation of zero-point fluctuation is the

photons' production from vacuum induced by time-dependent boundary conditions, an effect known as Dynamical Casimir effect (DCE) [39–43].

The challenge of finding an experimental evidence of DCE has been an open problem until very recently [51], given the highly demanding operating regimes at which this effect becomes observable. In this thesis (see chapter 5), we address the problem of bringing the observation of DCE close to experimentally achievable conditions making use of the peculiar behaviour of a system brought close to a quantum phase transition. Moreover, we will also show that DCE can be linked to another fundamental effect typically encountered in critical systems, the Kibble-Zurek mechanism (KZM) [44–46]. The purpose of this section is to give a brief overview of DCE and KZM, focusing on the aspects of these two phenomena which are particularly relevant for our discussion.

2.3.1 Dynamical Casimir effect: a brief overview

The fundamental connection between DCE and vacuum fluctuations relies on the fact that the number operator N is not a conserved quantity when the boundary condition of the problem are time-dependent. This concept can be understood better by analyzing a simple example. Following Moore [39], we consider a system formed by a 1-dimensional cavity where the two end mirrors can move along arbitrary (time-like) trajectories given by the functions $x = q_1(t)$ and $x = q_2(t)$. To obtain a quantum description of such system, we first address the problem from a classical point of view. In a second stage, we describe the field's quantization procedure, showing how the quantum nature of the vacuum state gives rise to DCE.

We thus start by considering a (classical) electromagnetic field inside the cavity and we assume that the electric component of the field is polarized along the z direction. The field can be then described by a vector potential $\vec{A} = \{A_x = 0, A_y = 0, A_z = A\}$, which generates the electric and the magnetic fields given by $\vec{E} = \{0, 0, -\partial_t A\}$ and $\vec{B} = \{0, -\partial_x A, 0\}$. According to Maxwell's theory, the vector potential is required to fulfill Maxwell's equation in free space,

$$\partial_t^2 A = \partial_x^2 A, \tag{2.22}$$

with boundary conditions determined by the position of the mirrors. For the fixed mirrors problem, the boundary conditions need to ensure the continuity of the electric field, which requires $\vec{E} = 0$ at the mirrors' surface. Here we are interested in the case in which the two mirrors are moving. In this situation, the natural generalization of the continuity principle imposes that the electric field vanishes at the mirrors' surface *in the Lorenz frame where the mirrors are at rest*. This requirement is satisfied when the conditions $A(q_1(t), t) = A(q_2(t), t) = 0$ are imposed on the vector potential. The classical problem is then completely defined by Equation (2.22) and by the boundary conditions given above.

We now consider the space $\mathcal{S}$ whose elements are all the solutions $f(x, t)$ of Equation (2.22) for which: (i) f is a real function satisfying the boundary conditions; (ii) f and $\partial_t f$ are square-integrable over x for any fixed time t. Given the space $\mathcal{S}$, the product between two elements f_1 and f_2 is defined as

$$(f_1|f_2) = \int_{q_1(t)}^{q_2(t)} dx (f_2 \partial_t f_1 - f_1 \partial_t f_2). \tag{2.23}$$

The form given in Equation (2.23) is antisymmetric (i.e. $(f_1|f_2) = -(f_2|f_1)$), non-degenerate (i.e. if $(f_1|f_2) = 0$ for all f_2, then $f_1 = 0$) and totally isotropic (i.e. $(f|f) = 0$ for all f). The space $\mathcal{S}$ has thus the structure of a symplectic vector space. As a final step in the construction of our classical theory, we define a canonical basis in the space $\mathcal{S}$ formed by the normal modes $\{A_n(x,t), B_n(x,t)\}$ (with $n = 1, 2, \ldots, \infty$) such that $(A_n|A_m) = 0$, $(B_n|B_m) = 0$ and $(A_n|B_m) = \delta_{n,m}$. The existence of a canonical basis in $\mathcal{S}$ (which can be explicitly constructed, as explained in [39]) implies that every f can be written as a linear combination of the normal modes $\{A_n(x,t), B_n(x,t)\}$. Since the space of the solutions has the structure of a vector space, we will denote an element in $\mathcal{S}$ as $|f)$. Within this notation, a vector $|f)$ can be written as $|f) = \sum_n \xi_n|A_n) + z_n|B_n)$, where $\xi_n = -(B_n|f)$ and $z_n = (A_n|f)$.

We are now in the position to construct a quantum theory of the field. In order to do so, we will follow [87]. First, we define a map $\Re : \mathcal{S} \to \mathcal{B}$, where $\mathcal{B}$ is the space of Hermitian operators defined over the Hilbert space $\mathcal{H}$ of physical states of the electromagnetic field (notice that the actual structure of the Hilbert space $\mathcal{H}$ is not known yet, and it will emerge later from the definition of the field operators). The map $\Re$, which associates solutions f of the classical problem with quantum mechanical operators, is chosen such that

$$[\Re(f_1), \Re(f_2)] = -i(f_1|f_2). \tag{2.24}$$

Considering the action of $\Re$ on the canonical basis $\{A_n, B_n\}$, we define the operators $p_n = \Re(A_n)$ and $q_n = \Re(B_n)$. It follows from Equation (2.24) and from the properties of A_n and B_n that p_n and q_n obey the commutation relations

$[p_n, p_m] = 0$, $[q_n, q_m] = 0$ and $[q_n, p_m] = -i\delta_{n,m}$. This means that they can be regarded as the canonical operators for each mode of the electromagnetic field in our quantum theory.

Given the position and momentum operators, it is now possible to define the relevant quantities in the discussion about DCE, i.e. the creation and annihilation operators (which also define the physical Hilbert space $\mathcal{H}$), the number operator and the field operator. The creation and annihilation operators for each mode can be defined in the usual way as $a_n = (q_n + ip_n)/\sqrt{2}$ and $a_n^\dagger = (q_n - ip_n)/\sqrt{2}$. Given a_n and $a_n^\dagger$, it is straightforward to define the number operator as $N = \sum_n a_n^\dagger a_n$. On the other hand, the field operator of our theory $\phi(x,t)$ can be defined in terms of the canonical operators as $\phi(x,t) = \sum_n B_n(x,t)p_n - A_n(x,t)q_n$. The definition of the number operator N in our quantum theory plays a fundamental role in the context of DCE.

To clarify this point, let us consider the relations between N and the field operator $\phi(x,t)$. Exploiting the definition of $\phi(x,t)$, the number operator can be written as

$$\begin{aligned} N =& \frac{1}{2}\sum_n (q_n - ip_n)(q_n + ip_n) = \\ =& -\frac{1}{2}\sum_n (\phi|B_n)(B_n|\phi) + (\phi|A_n)(A_n|\phi) + i(\phi|\phi) = \\ & -\frac{1}{2}\sum_n (\phi|J|\phi) + i(\phi|\phi), \end{aligned} \tag{2.25}$$

where we have introduced the quantity $J = \sum_n |B_n)(B_n| + |A_n)(A_n|$. In the language of functions, J corresponds to the anticommutator function, which is

given by

$$D(x,t;x',t') = \sum_n B_n(x,t)B_n(x',t') + A_n(x,t)A_n(x',t'). \tag{2.26}$$

It is important to notice that the anticommutator function is the expectation value of the field operator anticommutator in the vacuum state, i.e. $D(x,t;x',t') = \langle 0|\phi(x,t)\phi(x',t') + \phi(x',t')\phi(x,t)|0\rangle$. That means that the nature of the vacuum state is directly connected to the definition of the number operator N.

The properties of the anticommutator function in Equation (2.26) are crucial in the arising of DCE. To see that, let us first discuss the situation in which the two mirrors are fixed. In this case, the result of the field quantization is known, and the basis A_n and B_n (which define the anticommutator function and the number operator) can be chosen in a natural way (see [39] for more details). The result is that the anticommutator function is *invariant under time translations*. This invariance results on the fact that the number operator (and, consequently, the vacuum state) does not depend on time. If the cavity field is initially unpopulated, it will remain as such.

On the contrary, in the case of time dependent boundary conditions, it is in general not possible to find a set of normal modes $A_n(x,t)$ and $B_n(x,t)$ such that the anticommutator function is invariant under time translations. This means that the vacuum state at some time t will not have the properties of the vacuum at some later time t', with a finite number of photons generated in the cavity. We would like to point out that also in the classical theory it is not possible to find a set of normal modes for which the anticommutator function is time-translationally invariant. However, this results in generation of radiation only when the quantum

nature of the field is taken into account. Indeed, a crucial role in the process is played by the existence of the number operator N, which does not have a counterpart in the classical formalism.

2.3.2 Experimental observation of dynamical Casimir effect

Observing DCE has been a very elusive task until very recently, when Wilson *et. al.* [51] provided the first experimental demonstration of this phenomenon. In [51], the boundary conditions of a transmission line are sinusoidally modulated in time at frequencies ≈ 11GHz by applying a magnetic field through the loop of a superconducting quantum interference device (SQUID) placed at the end of the line. Using this technique, observable radiation is generated through a DCE-like mechanism, providing the first evidence of DCE in the microwaves regime. However, observing DCE in systems where the typical frequencies are in the optical range might be very demanding, due to the very high modulation rates at which the photons production becomes observable.

Let us consider, for example, a cavity where one of the mirrors moves around its stationary position x_0, while the other one is fixed. The stationary position of the moving mirror determines the stationary fundamental frequency of the cavity ω_0. In principle, DCE can arise from any modulation of the mirror's position with non-uniform acceleration. However, the probability of generating photons is negligible for practical purposes when the motion of the cavity's mirrors is slow compared to the normal mode stationary frequency ω_0. Indeed, in such a situation the field adiabatically follows the changes in the boundary conditions, and the initial vacuum state can be considered as such for all times t with good approx-

imation. On the contrary, in a situation where the changing rate in the mirror's position is comparable with the field fundamental frequency, the number of photons generated through DCE increases considerably.

Recently, various setups have been proposed to overcome the technological barriers still precluding the observation of DCE in systems with very high characteristic frequencies. In the following, we will briefly review a proposal where the interaction between the electromagnetic field and a two level atom is analyzed in the context of DCE [49,50]. The study of such system constitutes the starting point for the achievement of the results presented in Chapter 5.

Let us thus consider a system in which a two level atom is placed inside a cavity with fixed mirrors. The atom is able to interact with the field inside the cavity through the usual dipole-dipole interaction. The total Hamiltonian of the atom-cavity system is then given by

$$H = \omega_a a^\dagger a + \omega_b \sigma_z + g(\sigma_+ + \sigma_-)(a^\dagger + a), \tag{2.27}$$

where $a^\dagger$, a are the bosonic operators for the field inside the cavity, $\{\sigma_z, \sigma_+, \sigma_-\}$ are the pseudo-spin angular momentum components describing the atom, ω_a is the fundamental frequency of the cavity, ω_b is the energy splitting between the two atomic levels and g is the atom-field interaction constant. We assume that at the initial time t_0 the cavity field is in its vacuum state and the atom is in its ground state, so no field or atomic excitations are initially present.

We now notice that the action of changing the mirrors' position modifies the length of the cavity and consequently its fundamental frequency. This action is thus equivalent to introducing a time dependence in the Hamiltonian's parameter

ω_a. Such a parametric modulation is then expected to result in DCE [47]. Moreover, it is sufficient to consider an appropriate Heisenberg representation in order to switch from an Hamiltonian in which ω_a is a function of time to an Hamiltonian in which ω_b or g are time-dependent and ω_a is constant. For that reason, DCE can arise from the modulation of any parameter appearing in the Hamiltonian (2.27).

This observation is important from a practical perspective, since the possibility of choosing which parameter is modulated in time may results in a significative advantage from an experimental point of view. For example, in some situations modulating the coupling constant g is easier than changing the cavity mirrors' position [56], while in other setups considering a time-dependent atomic splitting ω_b might be the most advantageous choice. However, the choice of the time dependent parameter does not influence the frequency range at which DCE is observable. The case in which ω_b is modulated sinusoidally is analyzed in [49]. It is shown how the photons' production from vacuum becomes non-negligible only when the modulation frequency η is on the same order of the cavity's fundamental frequency ω_a (in particular, the calculations show that DCE arises when $\eta \approx 2\omega_a$). This means that, for an optical cavity, changing the time-dependent parameter does not change the modulation frequency, which is still in the optical range. On the contrary, in Chapter 5 we will present a scheme where the modulation frequency η required by DCE can be lowered significantly by exploiting the properties of a critical system close to a quantum phase transition.

2.3.3 Kibble-Zurek mechanism: the basic idea

We are now going to introduce the other fundamental phenomenon studied in Chapter (5), the KZM [44,45]. The main idea behind KZM is intimately related to the concept of phase transition. A phase transition is typically characterized by a change in the properties of the ground state of the system after crossing the critical point. The critical point is defined by a certain critical value of a characteristic parameter of the system (for example the temperature T). Above the critical point, the ground state of the system usually possesses some symmetry properties, while below the critical point such symmetries are broken. Such symmetries are characterized by a so called *order parameter*, which assumes a finite value in the broken symmetry phase while is zero in the symmetric phase. For example, the total magnetization of a ferromagnetic material can be regarded as the order parameter for the so called ferromagnetic phase transition: while the ferromagnetic domains are randomly oriented above a certain temperature, resulting in a spacial symmetric ground state for which the total magnetization averages to zero, such domains tend to spontaneously align toward a specific direction below the critical point, breaking the initial symmetry and inducing a finite total magnetization.

When dealing with the dynamics of a phase transition, the concept of adiabaticity plays a fundamental role. Indeed, when a system is driven across a continuous phase transition, the energy gap between the ground state and the first excited state goes to zero. Since the inverse of this gap defines the typical time scale of the system reaction, approaching the critical point results in the so call *critical slowing down*. This means that when the system is brought close to criticality, there is always a point in which its state is not able to adiabatically follow

the changes in the control parameter any longer. This fundamental aspect of critical systems is described by KZM.

Indeed, although KZM was originally formulated to explain the formation of galaxy in the expansion of the early universe [44] and the arising of topological defects in condensed matter systems [45], its essence relies on the description of the departure from adiabaticity close to the critical point, which is a general concept applicable to a variety of situations. In this thesis, we will only focus on this aspect of KZM, which basically consists on approximating the dynamics of a system close to the critical point as a sequence of adiabatic and impulsive evolutions.

Let us now consider the main idea behind KZM in more details. We start by introducing the quantity $\mathcal{T}(t)$. In general, when a control parameter $g(t)$ is varied in time and a critical value g_c exists at which the system undergoes a phase transition, $\mathcal{T}(t)$ can be regarded as a measure of the distance between $g(t)$ and g_c. For example, in the context of a temperature-driven phase transition, $\mathcal{T}(t)$ is called the relative temperature and is defined as $\mathcal{T}(t) = (T(t) - T_c)/T_c$, where T_c is the critical temperature. Notice that $\mathcal{T}(t)$ is defined such that it is positive above the phase transition, zero at the critical point and negative below the phase transition. In the context of KZM, it is also important to consider the rate at which $\mathcal{T}(t)$ changes, which constitutes a measure of the rapidity at which criticality is approached.

In this regard, we are interested in comparing the typical time scale of the changes in $\mathcal{T}(t)$, which is given by $\mathcal{T}(t)/\dot{\mathcal{T}}(t)$, with the typical reaction time of the system, which in general is a time-dependent parameter $\tau(t)$. According to KZM, the evolution of the system is adiabatic as long as $\mathcal{T}(t)/\dot{\mathcal{T}}(t)$ is long

compared to the system reaction time. On the contrary, when the critical point is approached and the changes on the control parameter are too fast with respect to $\tau(t)$, the system enters the impulsive regime. In order to rephrase this concept in a more quantitative way, let us consider the equation

$$\frac{\mathcal{T}(t)}{\dot{\mathcal{T}}(t)} = \tau(t). \tag{2.28}$$

The solutions of Equation (2.28) define the so called *freeze out* points, i.e. the points at which the transitions between the adiabatic and the impulsive regimes occur. During the time intervals in which $\mathcal{T}(t)/\dot{\mathcal{T}}(t) > \tau(t)$, the dynamics are governed by the adiabatic approximation, meaning that the state of the system adiabatically follows the changes in the control parameter. On the contrary, when $\mathcal{T}(t)/\dot{\mathcal{T}}(t) < \tau(t)$ the impulsive regime takes place, where the state of the system does not change anymore (i.e. it *freezes*) due to the inability of the system to follow the fast changes of the control parameter.

We would like to stress that, although in some case a simple relation between the reaction time $\tau(t)$ and the relative temperature $\mathcal{T}(t)$ can be established (see examples in Section 2.3.4), the existence of such relations is not a necessary condition for the validity of Equation (2.28). Indeed, the description of the system's dynamics as a sequence of adiabatic and impulsive evolutions is a general framework provided by KZM and as such it can be applied to a variety of situations. This framework is usually applied to the dynamics of a phase transition process, but it can also be used in the case of avoided crossing (like in the Landau-Zener model, see Section 2.3.4) or even when the phase transition does not occur at all, providing that the system is brought close enough to the critical point. The study

of this latter situation is one of the main result presented in this thesis and will be treated extensively in Chapter 5.

2.3.4 Kibble-Zurek mechanism in action

In order to further clarify the discussion in the previous section, here we briefly analyze two examples in which KZM is applied. The first example we consider is the case treated in the original paper by Zurek [45], where formation of defects in 2D superfluid ^{4}He is studied. The second example we present is the case treated in [52], where the Landau-Zener model [88,89] is studied in the light of KZM.

In ^{4}He, a critical temperature T_c exists at which the system passes from the normal phase to the so called superfluid phase. In the normal phase, the value of the order parameter averages to zero. In the superfluid phase, a mosaic of domains are formed for which the order parameter assumes a finite value. The size of such domains is determined by the correlation length $\xi(t)$, which can be thought as the typical distance at which the values of the order parameter become uncorrelated. The other relevant quantity in our discussion is of course the reaction time of the system $\tau(t)$, which determines the typical time scale at which the system reacts to external changes. In the following, we will show how the correlation length $\xi(t)$ in the superfluid phase can be estimated using KZM.

Let us assume that the evolution starts at the initial time $t_i \to -\infty$ with the initial temperature $T_i > T_c$, i.e. with the system in the normal phase. The system is then cooled down to a temperature $T_f < T_c$, in such a way that the critical point is crossed at $t = 0$. The dynamics of the phase transition can be characterized by the relative temperature $\mathcal{T}(t) = (T(t) - T_c)/T_c$. Near the critical point, a linear

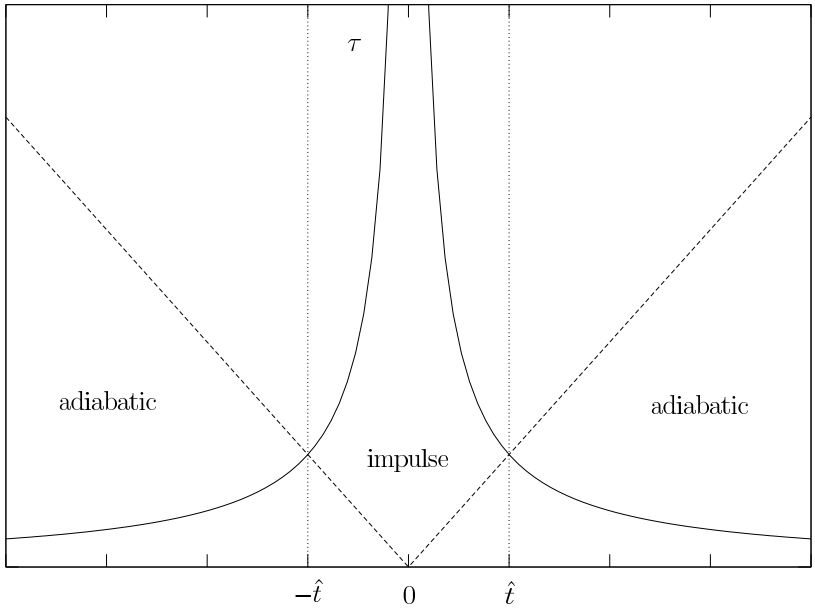

Figure 2.2: Schematic representation of the adiabatic-impulsive-adiabatic regimes transition in KZ theory applied to the superfluid phase transition in ^{4}He. (figure taken from [90]).

time dependence for $\mathcal{T}(t)$ is assumed. Denoting the rate of the linear quench by $1/\tau_Q$, the relative temperature is then written as

$$\mathcal{T}(t) = -t/\tau_Q. \tag{2.29}$$

In the proximity of the critical point, the correlation length $\xi(t)$ and the reaction time $\tau(t)$ are related to the relative temperature $\mathcal{T}(t)$ through an exponential law. In general, such dependences can be written as $\xi(t) \propto |\mathcal{T}(t)|^{-\nu}$ and $\tau(t) \propto |\mathcal{T}(t)|^{-\nu z}$, where the exponents ν and z are called *critical exponents*. For ^{4}He, a mean field theory treatment of the problem gives

$$\xi(t) = \frac{\xi_0}{\sqrt{|\mathcal{T}(t)|}}; \qquad \tau(t) = \frac{\tau_0}{|\mathcal{T}(t)|}, \tag{2.30}$$

with ξ_0 and τ_0 constants. The divergence of these two quantities at the critical point (i.e. when $|\mathcal{T}(t)| \to 0$) results in the critical slowing down of the system.

For a linear quench of the relative temperature $\mathcal{T}(t)$, Equation (2.28) assumes the form

$$t = \tau(t) \tag{2.31}$$

and admits the two solutions $t = \pm\hat{t} = \pm\sqrt{\tau_Q \tau_0}$. The two *freeze-out* points $-\hat{t}$ and $\hat{t}$ determine the transitions between the adiabatic and the impulsive regimes (see Figure 2.2): for the time interval $t \in [t_i, -\hat{t}]$, i.e. when $\mathcal{T}(t)/\dot{\mathcal{T}}(t) > \tau(t)$, the adiabatic regime takes place. During this period, the system is able to respond fast enough to the quench of the control parameter, and its state can adiabatically follow the changes in the relative temperature $\mathcal{T}(t)$. In the period $t \in [-\hat{t}, \hat{t}]$, during which the critical point is crossed and $\mathcal{T}(t)/\dot{\mathcal{T}}(t) < \tau(t)$, the critical slowing down does not allow the system to readjust quickly enough to the parameter's changes. The system enters the impulsive regime, where its state is frozen during the whole time interval. After the phase transition, adiabaticity is restored at time $t = \hat{t}$, and the state can follow again the parameter's changes.

The final correlation length of the domains in the superfluid phase is given by $\xi(\hat{t})$. Considering that the system freezes at $-\hat{t}$, this can be calculated using Equations (2.29) and (2.30) as

$$\xi(\hat{t}) = \xi(-\hat{t}) = \frac{\xi_0}{\sqrt{|\mathcal{T}(-\hat{t})|}} = \xi_0 \sqrt[4]{\frac{\tau_Q}{\tau_0}}. \tag{2.32}$$

Although the main approximation employed by KZM (i.e. the assumption that the state of the system completely freezes for a period of time) might appear as

an oversimplified description of the system's dynamics at first look, experimental observations have shown that the prediction given in Equation (2.32) is indeed very accurate. In the following, we will see how KZM provides a good description of the system's evolution also in a quantum mechanical context.

Let us now pass to analyze the idea proposed by Damski [52], where KZM is applied to the Landau-Zener model. As mentioned in the previous section, the framework provided by Kibble-Zurek theory can be applied to various scenarios. The key ingredient behind KZM is the departure from adiabaticity, a condition which is not exclusively encountered in the case of a continuous phase transition. Also in the situation of a system going through a so called *avoided crossing*, like in the case of Landau-Zener theory, KZM provides an accurate description of the system's evolution.

Let us thus consider a two-level system whose evolution is driven by a the time-dependent Landau-Zener Hamiltonian $H_{\mathrm{LZ}}(t)$ given by

$$H_{\mathrm{LZ}}(t) = \frac{1}{2}\begin{pmatrix} \Lambda \cdot t & \Omega_0 \\ \Omega_0 & -\Lambda \cdot t \end{pmatrix}, \tag{2.33}$$

where Λ and Ω_0 are constant parameters and the Hamiltonian is written in the basis of time independent states $\{|0\rangle, |1\rangle\}$. The time-dependent instantaneous eigenvectors of $H_{\mathrm{LZ}}(t)$ can be written as

$$\begin{aligned} |G(t)\rangle &= -\sin\left(\theta(t)/2\right)|0\rangle + \cos\left(\theta(t)/2\right)|1\rangle, \\ |E(t)\rangle &= \cos\left(\theta(t)/2\right)|0\rangle + \sin\left(\theta(t)/2\right)|1\rangle, \end{aligned} \tag{2.34}$$

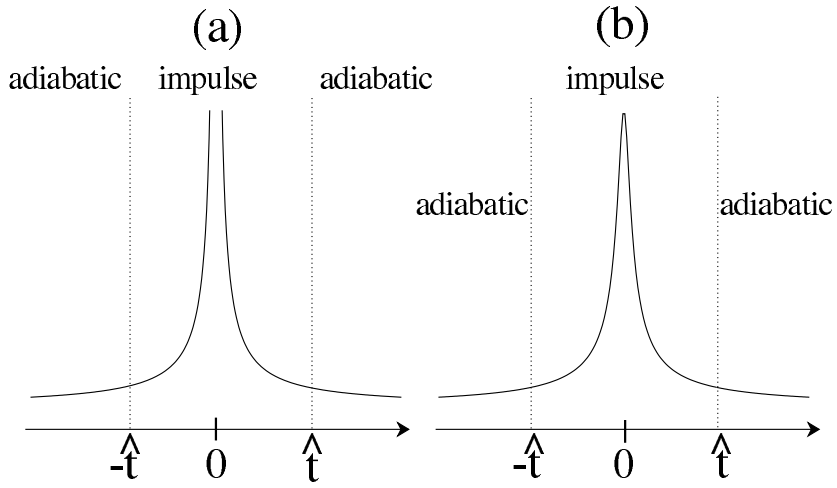

Figure 2.3: Schematic representation of KZM in Landau-Zener theory. (a) Reaction time of the system in KZM for a continuous phase transition. (b) Reaction time of the system in Landau-Zener model. (figure taken from [52]).

where

$$\begin{aligned} \cos\left(\theta(t)/2\right) &= \frac{\mathcal{T}(t)}{\sqrt{1+\mathcal{T}^2(t)}}, \\ \sin\left(\theta(t)/2\right) &= \frac{1}{\sqrt{1+\mathcal{T}^2(t)}}, \\ \mathcal{T}(t) &= \frac{\Lambda \cdot t}{\Omega_0}. \end{aligned} \tag{2.35}$$

Here, the parameter $\mathcal{T}(t)$ plays the role of the relative temperature. In terms of $\mathcal{T}(t)$, the energy gap between the ground state $|G(t)\rangle$ and the excited state $|E(t)\rangle$ can be written as $\epsilon(t) = |\Omega_0|\sqrt{1+\mathcal{T}^2(t)}$. As expected, the relative temperature assumes the value $\mathcal{T}(t) = 0$ when the Landau-Zener avoided crossing is reached and the energy gap $\epsilon(t)$ assumes its minimal value.

In the context of KZM, we are interested in the case in which the system is in its ground state $|G(t_i)\rangle$ at the initial time $t_i < 0$. The generation of excitations can be then characterized by the probability P_f of finding the system in the excited

state $|E(t_f)\rangle$ at final time $t_f > 0$, i.e. after the Landau-Zener point is crossed. The probability P_f is given by $P_f = |\langle E(t_f)|\psi(t_f)\rangle|^2$, where $|\psi(t_f)\rangle$ is the final state of the system. The problem is then reduced to finding the state of the system at the final time $|\psi(t_f)\rangle$. In order to solve the dynamics of the system, we use the KZM framework, i.e. we consider the dynamics of the system as a sequence of adiabatic and impulsive evolutions.

To solve Kibble-Zurek Equation and find the freeze-out point, we need to define the time scale of the linear quench and the characteristic response time of the system. The typical time scale of the linear quench is given by the constant $\tau_Q = \Omega_0/\Lambda$. On the other hand, the characteristic response time $\tau(t)$ is given by the inverse of the energy gap between the ground and the first excited state of the system. Defining the constant $\tau_0 = 1/\Omega_0$, we have

$$\tau(t) = \frac{\tau_0}{\sqrt{1+\mathcal{T}^2(t)}}, \qquad \mathcal{T}(t) = \frac{t}{\tau_Q}. \tag{2.36}$$

The freeze-out points can be found as the solution of the modified Kibble-Zurek Equation given by

$$\alpha t = \tau(t). \tag{2.37}$$

Adding the factor α is advantageous for solving the equation, although it does not change the main principle behind KZM. Solving equation (2.37) and employing the KZM paradigm, the probability P_f of finding the system in the excited state at time t_f can be calculated to be

$$P_f = e^{-\alpha\frac{\tau_Q}{\tau_0}} + \mathcal{O}(3), \tag{2.38}$$

which is the known result for the Landau-Zener model up to a third order correction if we chose $\alpha = \pi/2$.

Chapter 3

Environmental induced geometric phase

In this chapter, we focus on the study of the generation and the detection of a geometric phase [58, 59] in a harmonic oscillator. In the spirit of previous works [91,92], we reconsider the *Von Neumann measurement scheme*, which models the measurement process as a coupling between a large measurement apparatus, used as a probe, and the microscopic system on which the measurement is performed, under a "*reverse*" prospective, using the microscopic system (a qubit) to measure the geometric phase attached to the macroscopic one (a harmonic oscillator).

The chapter is organized as follow: In Section 3.1, we will introduce the Hamiltonian model under study, we will derive the unitary evolution operator and we will show how a non-dissipative evolution is able to attach a geometric phase to the state of the harmonic oscillator. In Section 3.2, we will extend our analysis to the case of a system undergoing a non-unitary evolution, showing that not only

the geometric phase survive to dissipative processes, but in some cases it is indeed *induced* by such incoherent dynamics.

3.1 Description of the model

Let us start by considering a general Hamiltonian model for the interaction between a qubit and a harmonic oscillator. We will discuss the presentation of a physical scenario suited for the implementation of such model in the conclusive section of this chapter. We thus take a two-level system with logical states $\{|0\rangle, |1\rangle\}$ (which we dub as the *control qubit*) coupled with a harmonic oscillator through the interaction Hamiltonian

$$H = \eta|0\rangle\langle 0| \otimes (b^{\dagger}e^{-i\phi} + be^{i\phi}), \tag{3.1}$$

where b and $b^{\dagger}$ are the annihilation and creation operators for the oscillator, η is the coupling constant and ϕ is a phase that can be externally adjusted to change the direction of the harmonic oscillator canonical operator in phase space. For example, for $\phi = 0$, the qubit would be coupled with the position operator of the harmonic oscillator, while for $\phi = (\pi/2)$ it would be coupled with the momentum operator. As mention above, the Hamiltonian in Equation (3.1) can be regarded as an example of the Von Neumann measurement scheme, in which a microscopic system represented by the qubit is coupled with a macroscopic system represented by the harmonic oscillator. Here, the model presents an extra parameter, the externally adjustable phase ϕ, which allow the state of the system to "move" in various directions in phase space and which plays a very important

role in our analysis. As long as η and ϕ are constant in time, the unitary operator describing the conditional time evolution of the system is

$$U_\phi(t) = |1\rangle\langle 1| \otimes \mathcal{I} + |0\rangle\langle 0| \otimes D[\zeta], \tag{3.2}$$

where $D[\zeta] = e^{\zeta b^\dagger - \zeta^* b}$, with $\zeta = -i\int_0^t \eta e^{-i\phi}$, is a displacement operator acting on the oscillator. Equation (3.2) describes a spin state-dependent displacement of the oscillator, which remains unperturbed if the control qubit is in $|1\rangle$ and is displaced by ζ if the control qubit is in $|0\rangle$. The importance of the role played by ϕ in the process of creating geometric phases becomes evident when this parameter is assumed to be time-dependent. Indeed, by changing in time ϕ we can drag the state of the harmonic oscillator along a nontrivial path in phase space. In particular, when ϕ is changed along a closed loop a purely geometric phase can be associated with the corresponding closed curve generated in the harmonic oscillator phase space. Following References [35, 93], we assume that the value of ϕ is changed in n time steps δt such that $t = n\delta t$, $\delta\zeta_i = \dot{\zeta}_i \delta t$, and $U(t) = \prod_{i=1}^n D(\delta\zeta_i)$. Recalling that $D(\alpha)D(\beta) = \exp\{i\mathrm{Im}(\alpha\beta^*)\}D(\alpha+\beta)$, we have

$$U(t) = \exp\left[i\mathrm{Im}\sum_{k=2}^{n}\delta\zeta_k\sum_{l=1}^{k-1}\delta\zeta_l^*\right] D\left(\sum_{i=1}^{n}\delta\zeta_i\right). \tag{3.3}$$

In the continuous limit we take $\sum_{i=1}^n \delta\zeta_i \to \zeta$, $\sum_{k=2}^n \delta\zeta_k \sum_{l=1}^{k-1}\delta\zeta_l^* \to \int \zeta^* d\zeta$ and assume that ϕ is changed along a closed loop in a time τ such that $\zeta(\tau)=\zeta(0)$. Making use of Stokes' theorem, $\mathrm{Im}\left(\oint \zeta^* d\zeta\right) = \oint x dy - y dx = \int_\sigma dx dy = A$, where we have taken $\zeta = x + iy$. We thus find $U(\tau)=e^{iA}D(0)$ with A the area enclosed by the cyclic path in parameter space. The same result, *i.e.* an overall

phase θ_{tot} equal to A for an arbitrary closed loop, is obtained using Anandan's rule

$$\theta_{\text{tot}}=\theta_D + \theta_G \tag{3.4}$$

where the dynamical phase θ_D and the the geometric one θ_G are given by

$$\begin{aligned}\theta_D&=-\int_0^\tau \langle\psi(t)|H(t)|\psi(t)\rangle dt,\\ \theta_G&=i\int_0^\tau \langle\psi(t)|\partial_t|\psi(t)\rangle dt.\end{aligned} \tag{3.5}$$

with τ, τ_0 the initial and final time of the evolution [59] .

3.1.1 Unitary evolution geometric phase

Let us now suppose that the system can be initialized in the state $|\psi(0)\rangle = |+\rangle|\alpha\rangle$, where $|+\rangle = (1/\sqrt{2})(|0\rangle + |1\rangle)$ is the state of the control qubit and $|\alpha\rangle$ is a coherent state of the oscillator. We then change $\phi(t)$ along a closed path spanned in a time τ. The joint state of the qubit and oscillator at time τ will be

$$|\psi(\tau)\rangle = (1/\sqrt{2})(|1\rangle + e^{-iA}|0\rangle) \otimes |\alpha\rangle. \tag{3.6}$$

It should be remarked that Equation (3.6) is exact and arises simply from the conditional oscillator evolution induced by its coupling to the two-level system as described in Equation (3.1). To better understand such a result, we discuss an illustrative example where we consider a rectangular path implemented by a stepwise change of ϕ: its value is set to zero for an interval of length T and then changed to $\phi_n = n\pi/2$ at time $t = nT$ with $n = 1, 2, 3$. As shown above, the state

of the qubit acquires a phase $\theta = A = \eta^2 T^2$ equal to the area enclosed by the path [see Figure 3.1 **(a)**]. We now stress three important points. First: although in the above example the phase explicitly depends on T, it is invariant with respect to the parametrization of the path. Indeed, if the area enclosed by the path remains unchanged, even for an arbitrary dependence of $\zeta(t)$ on time we would obtain the same result $\theta = A$. Second: for a closed loop, θ does not depend on the amplitude α of the initial state of the harmonic oscillator. Third: the phase acquired by the harmonic oscillator is *kicked back* on the qubit state, which takes the role of a microscopic interferometer. As a final remark, it is important to stress that the geometric phase addressed here is a specific result of our interaction model and of the overall scheme that we have set up.

3.2 Thermal and non-unitary case

We now address the first two points that have been mentioned above. As shown by Equation (3.6), when the evolution of the system is purely unitary, the geometric phase picked up by the control qubit does not depend on the amplitude α of the oscillator's initial state. This leaves the value of θ unchanged even if the initial state of the oscillator is a highly mixed state. For example, we can consider the case in which the oscillator is initialized in a thermal state

$$\rho_V = \int d\alpha P(\alpha, 0, V) |\alpha\rangle\langle\alpha|, \tag{3.7}$$

where

$$P(\alpha, \alpha_0, V) = \frac{2}{\pi(V-1)} e^{-\frac{2|\alpha-\alpha_0|^2}{V-1}} \tag{3.8}$$

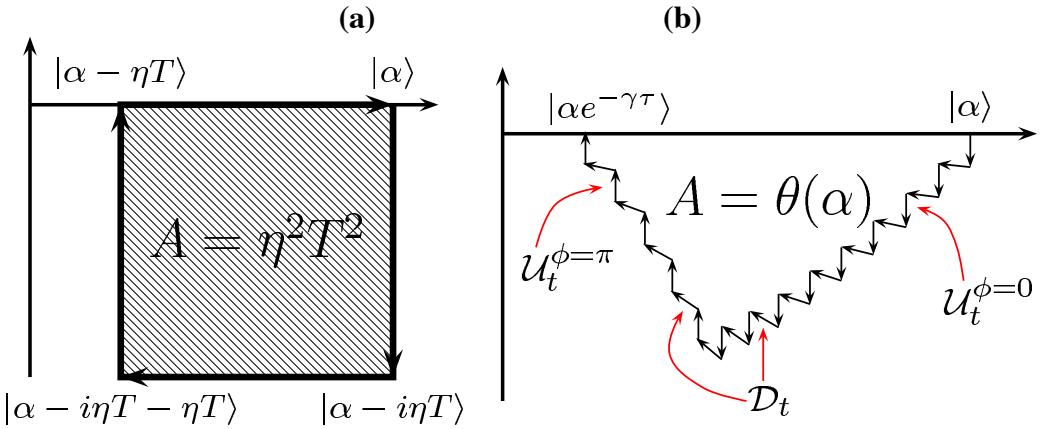

Figure 3.1: The oscillator's conditional dynamics pictured in phase space. In **(a)** the oscillator is displaced along a square whose area is proportional to the phase θ. In **(b)** the oscillator is displaced while undergoing a dissipative process. Here $\mathcal{U}_{\delta t}^{\phi}$ and $\mathcal{D}_{\delta t}$ are the superoperators describing the unitary and dissipative evolution of duration δt, respectively.

is the Gaussian thermal distribution centered at point α_0 in the phase space and having variance $V = (e^{\beta}+1)/(e^{\beta}-1)$, with $\beta = \hbar\omega_m/k_b\mathcal{T}$ (k_b is the Boltzmann constant and $\mathcal{T}$ is the temperature of the oscillator). By taking the initial state $\rho_0 = |+\rangle\langle+| \otimes \rho_V$, it is straightforward to see that a phase identical to the pure-state case is acquired by the qubit. In fact, the state at time τ reads $\rho(\tau) = |\varphi\rangle\langle\varphi| \otimes \rho_V$, where $|\varphi\rangle = (|1\rangle + e^{-i2\eta^2\tau^2}|0\rangle)/\sqrt{2}$. The invariance of θ in such a mixed-state scenario has also been confirmed using the framework for the evaluation of mixed-state geometric phases proposed in Reference [62]. This shows that ignorance on the initial preparation of the state of the harmonic oscillator does not affect the possibility to generate and detect a geometric phase.

3.2.1 Non-unitary dynamics in a zero-temperature bath

We now assess the potential effects that non-unitary dynamics may have on the occurrence of the geometric phase under scrutiny. On one hand, the consideration of an explicitly open dynamics will make our proposal closer to the reality of the potential experimental situations that will be addressed later on in this work. On the other hand, it is reasonable to expect significant deviations from the results found so far when we are far from unitarity. We thus consider the oscillator as affected by dissipation at rate γ with the control qubit still evolving unitarily, a situation that is formally described by the master equation

$$\dot{\rho} = -i[H, \rho] + \mathcal{L}\rho, \quad \text{with} \quad \mathcal{L}\rho = \frac{\gamma}{2}(b\rho b^{\dagger} - \{b^{\dagger}b, \rho\}), \tag{3.9}$$

where $\mathcal{L}$ formally describes the oscillator's damping in a bath at zero temperature. Although we do not refer to any explicit experimental configuration, at this stage, the analysis that we perform here adheres very well to the experimental observations on the open-system dynamics of mechanical systems availbale to date [110–114].

We start by discussing the case in which the initial state of the oscillator is a coherent state $|\alpha\rangle$. This scenario draws a particularly clear physical picture of the competition between the unitary displacement in phase space and the dissipative counter-action. In order to grasp this effectively, we divide the time-window of the evolution in small intervals, each of length δt. Inspired by the Suzuki-Trotter formula [94,95], the dynamics can then be approximated by alternatively applying the unitary evolution superoperator $\mathcal{U}_{\delta t}^{\phi}$ and the purely dissipative propagator $\mathcal{D}_{\delta t}$

defined as [96]

$$\mathcal{U}_{\delta t}^{\phi}\rho{=}U_{\phi}(\delta t)\rho U_{\phi}^{\dagger}(\delta t), \qquad \mathcal{D}_{\delta t}\rho{=}e^{\mathcal{L}\delta t}\rho. \tag{3.10}$$

After N iterations, we have the evolved state

$$\rho(N\delta t){=}\left(\mathcal{D}_{\delta t}\mathcal{U}_{\delta t}^{\phi}\right)^{N}\rho_0. \tag{3.11}$$

For the Hamiltonian consider here, the chosen approach is an excellent approximation of the exact dynamics of the system. Introducing the superoperator $\mathcal{H}\rho = -i[H,\rho]$, we write the formal solution of the open-system dynamics as $\rho(t) = e^{\mathcal{H}t+\mathcal{L}t}\rho_0$. Upon explicit calculation, it is straightforward to show that, as $\delta t \to 0$, $[\mathcal{D}_{\delta t}, \mathcal{U}_{\delta t}^{\phi}] = 0$ so that $\rho(N\delta t) \to \rho(t)$ in this limit. This approach is particularly useful in analyzing a damped harmonic oscillator. Indeed, the action of the dissipative superoperator $\mathcal{D}_t$ on the off-diagonal elements of a density matrix written in a coherent state basis is given by the dyadic expression [97,98]

$$\mathcal{D}_t|\lambda_1\rangle\langle\lambda_2| = \langle\lambda_2|\lambda_1\rangle^{1-\exp(-\gamma t)}|\lambda_1 e^{-\gamma t}\rangle\langle\lambda_2 e^{-\gamma t}|, \tag{3.12}$$

where $|\lambda_j\rangle$ $(j = 1, 2)$ are two coherent states. As we are interested in short-time intervals δt, we take $1 - \exp(-\gamma\delta t) \simeq \gamma\delta t$. Therefore, the action of $\mathcal{D}_{\delta t}$ on the state of our system results in the displacement of the harmonic oscillator and the exponential decrease of its initial amplitude α. Moreover, from Equation (3.12) we see that a phase factor is attached to the off-diagonal elements of the density matrix. Such features are useful to close the path across which the oscillator is displaced.

To better stress the role played by dissipation, we consider a different unitary

path in phase space with respect to the previous example. The path is such that the contribution to the geometric phase in the non-dissipative regime is zero. This allows us to clearly show how the dissipative process can induce a geometric phase on the system. Let us consider the case in which the phase ϕ is set to 0 for $t \in [t_0, t_0+T_1]$ and to π for $t \in [t_0+T_1, t_0+T_1+T_2]$. The state at the intermediate time $t_0 + T_1$ is given by $\rho(t_0 + T_1) = (\mathcal{D}_{\delta t}\mathcal{U}^0_{\delta t})^{N_1}\rho_0$, with $N_1\delta t = T_1$. Taking the limit $\delta t \to 0$, this turns out to be (see Appendix A.1 for a detailed calculation)

$$\begin{aligned}\rho(t_0 + T_1) =& \frac{1}{2}\left(|1, \alpha_1\rangle\langle 1, \alpha_1| + |0, \alpha_1 - i\beta_1\rangle\langle 0, \alpha_1 - i\beta_1|\right. \\ &\left. + e^{-i\theta_1(\alpha)}e^{-\Gamma_1}|0, \alpha_1 - i\beta_1\rangle\langle 1, \alpha_1| + h.c.\right),\end{aligned} \tag{3.13}$$

where

$$\begin{aligned}\theta_1(\alpha) &= \frac{\eta\alpha}{2\gamma}(1 - e^{-2\gamma T_1}), \\ \Gamma_1 &= \frac{\eta^2}{2\gamma^2}[\gamma T_1 + \frac{1}{2}(1 - e^{-2\gamma T_1}) - 2(1 - e^{-\gamma T_1})], \\ \beta_1 &= \frac{\eta}{\gamma}(1 - e^{-\gamma T_1}), \quad \alpha_1 = \alpha e^{-\gamma T_1}.\end{aligned} \tag{3.14}$$

Equation (3.13) shows that the state of the oscillator at time T_1 is conditionally displaced by a quantity $-i\beta_1$. We can now proceed to evauate the state of the system at time $t_0 + T_1 + T_2$ by setting $\phi{=}\pi$ and taking $\rho(t_0 + T_1 + T_2) = (\mathcal{D}_{\delta t}\mathcal{U}^{\pi}_{\delta t})^{N_2}\rho(t_0 + T_1)$, with $N_2\delta t = T_2$. This displaces the state of the oscillator by $i\beta_2$ in the opposite direction to what occurred at T_1. The time interval T_2 is chosen such that the oscillator displacement $-i\beta_1$ accumulated during T_1 is cancelled. This condition can be met by taking T_1 and T_2 such that $e^{-\gamma T_1}{=}2{-}e^{\gamma T_2}$.

By calling $\tilde{\tau} = T_1 + T_2$, the final state reads

$$\rho(t_0 + \tilde{\tau}) = \frac{1}{2}\left[\mathcal{I} + e^{-\Gamma}(e^{-i\theta(\alpha)}|0\rangle\langle 1| + h.c.)\right] \otimes |\alpha e^{-\gamma\tilde{\tau}}\rangle\langle\alpha e^{-\gamma\tilde{\tau}}|, \tag{3.15}$$

where

$$\theta(\alpha) = \eta\alpha\frac{1 - 2e^{-\gamma T_1} + e^{-2\gamma T_1}}{\gamma(2 - e^{-\gamma T_1})}, \quad \Gamma = \frac{\eta^2}{2\gamma^2}\tilde{\Gamma}(\gamma, T_1, T_2), \tag{3.16}$$

with $\tilde{\Gamma}(\gamma, T_1, T_2)$ a dimensionless function that behaves as γ^3 for $\gamma \to 0$, thus ensuring that $\Gamma \to 0$ as $\gamma \to 0$. The complete expression is given by

$$\begin{aligned}\tilde{\Gamma}(\gamma, T_1, T_2) = \gamma\tau + \frac{1}{4}(1 - e^{-\gamma T_1})^2(1 - e^{-2\gamma T_2}) + \frac{1}{2}(2 - e^{-2\gamma T_1} - e^{-2\gamma T_2}) - \\ - 2(2 - e^{-\gamma T_1} - e^{-\gamma T_2}) - (1 - e^{-\gamma T_1})[(1 - e^{-\gamma T_2}) - \frac{1}{2}(1 - e^{-2\gamma T_2})].\end{aligned} \tag{3.17}$$

Truncating the expansion of the exponential function to the second order in $\gamma T_j \ll 1$, the only non-null terms are those $\propto \gamma^3$. On the other hand, the phase $\theta(\alpha)$ goes to zero when $\gamma \to 0$, as expected from our choice of the path in the dissipative case.

It is easily seen that the phase $\theta(\alpha)$ gained by the oscillator in this process is equal to the area $\mathcal{A}$ enclosed by the displacement path in parameter space, as shown in Figure 3.1 **(b)**. The detectability of such phase depends on the function Γ, which determines the decoherence rate for the off-diagonal terms in $\rho(t_0 + \tilde{\tau})$. Indeed, in order to achieve a non-vanishing phase, we should ensure that $\Gamma \ll 1$. Remarkably, while $\theta(\alpha)$ depends on the amplitude of the initial coherent state, Γ does not. Surprisingly, by choosing $\eta/\gamma \ll 1$ (which embodies the weak-coupling condition between the oscillator and the control qubit), the requirement $\Gamma \ll 1$ is fulfilled. On the other hand, we can achieve any value of $\theta(\alpha)$ making an appropriated choice for the value of α, so as to compensate the conditions required

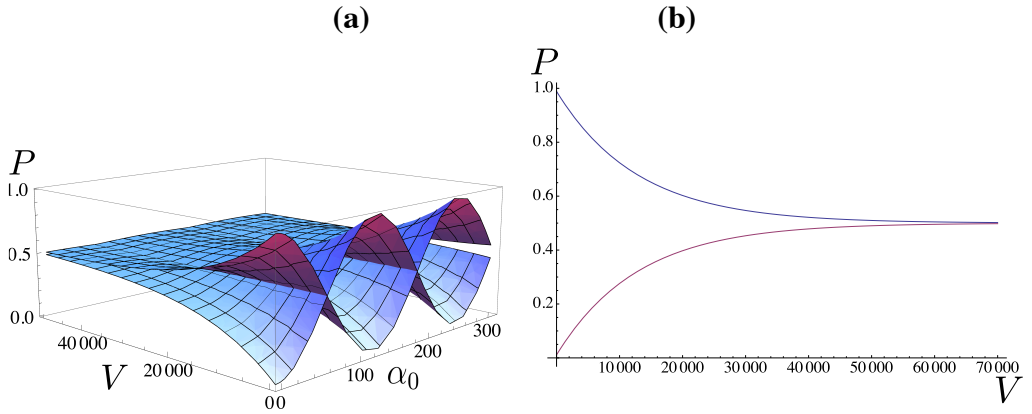

Figure 3.2: **(a)** Probabilities $\mathcal{P}_+$ and $\mathcal{P}_-$ against the displacement α_0 and the parameter V for $\eta/\gamma = 0.05$ and $\gamma T_1 = 20$. **(b)** Same probabilities against the temperature parameter V for and $\alpha_0 = 0$ and the same parameters as in panel **(a)** (notice that $V = (e^{\beta}+1)/(e^{\beta}-1)$, with $\beta{=}\hbar\omega_m/k_b\mathcal{T}$ and $\mathcal{T}$ the temperature of the oscillator).

for a negligible damping.

The approach described above can be applied so as to evaluate the effects, on the geometric phase, due to a thermal preparation of the state of the oscillator undergoing dissipative dynamics. We thus assume that the initial state of the oscillator is the displaced thermal state $\rho_V^{\alpha_0} = \int d\alpha P(\alpha, \alpha_0, V)|\alpha\rangle\langle\alpha|$. Following the lines sketched so far, we arrive at the evolved state

$$\rho_V^{\alpha_0}(t_0 + \tilde{\tau}) = \int d^2\alpha P(\alpha, \alpha_0, V)\rho(t_0 + \tilde{\tau}), \tag{3.18}$$

where $\rho(t_0{+}\tilde{\tau})$ is given by Equation (3.15). In light of the dependence of the phase θ on the amplitude α [as shown right after Equation (3.15)], the control qubit and the oscillator end up in a correlated state. This complicates the calculation of the overall geometric phase associated with $\rho_V^{\alpha_0}(t_0 + \tilde{\tau})$. Nevertheless, it is still possible to evaluate the geometric phase by adopting the framework developed

in Reference [62], which is based on the probability that a measurement over the state of the control qubit has outcomes $\{|+\rangle, |-\rangle\}$ (with $|\pm\rangle = (|0\rangle \pm |1\rangle)/\sqrt{2}$).

In order to understand this, let us first consider the state in Equation (3.15) and suppose to project the control qubit onto the $\{|\pm\rangle\}$ basis. The corresponding outcome probabilities are given by $\mathcal{P}_\pm = \langle \pm | \mathrm{Tr}_m\{\rho(t_0 + \tilde{\tau})\} | \pm \rangle$, where Tr_m denotes the partial trace over the oscillator's degrees of freedom. A straightforward calculation shows that $\mathcal{P}_\pm = [1 \pm v \cos\theta(\alpha)]/2$, where $v = e^{-\Gamma}$. This reminds us of the fringes of an interferometer whose visibility is v: the state of the composite qubit-oscillator system evolves along two branches (one associated to $|1\rangle$ and the other to $|0\rangle$) that can be seen as two arms of a Mach-Zehnder interferometer. The two components of the state of the system that have undergone the evolution ruled by H (and possibly the dissipative dynamics considered here) are then let interfere by projecting the qubit state onto the superposed basis. This analysis offers us an operative interpretation of $\theta(\alpha)$. In fact, by changing it, the probabilities $\mathcal{P}_\pm$ change, reaching the complete inversion when $\theta(\alpha) = \pi$. Therefore, $\theta(\alpha)$ can be seen as the inversion of the outcome probabilities $\mathcal{P}_\pm$. We can attach an analogous meaning to the phase associated with a mixed initial state. We thus now consider the state in Equation (3.18), which gives us $\mathcal{P}_\pm = (1 \pm |\Lambda| \cos[\tilde{\theta}])/2$ with $\tilde{\theta} = \arg(\Lambda)$ and

$$\Lambda = v \int d^2\alpha P(\alpha, \alpha_0, V) e^{i\theta(\alpha)}. \tag{3.19}$$

As in the case of a pure state, the phase $\tilde{\theta}$ is operatively defined through the inversion of the probabilities $\mathcal{P}_\pm$. Figure 3.2 **(a)** shows such quantities against the initial displacement α_0 and the temperature V. Although the visibility of the

fringes decreases with the increasing temperature, it is possible to see a population inversion even for high values of V. Another very interesting situation is the one in which the initial state is a non-displaced thermal state, i.e. the Gaussian distribution in Equation (3.18) is centered in $\zeta = 0$. The behavior of the outcome probabilities $\mathcal{P}_{\pm}$ against the thermal variance V is shown in Figure 3.2 **(b)**. A larger temperature results in an increase (decrease) of $\mathcal{P}_{-}$ ($\mathcal{P}_{+}$). The partial inversion of the probabilities is due to the average geometric phase $\tilde{\theta}(\alpha)$ picked up by the oscillator during the process.

3.2.2 Finite temperature bath

Such an analysis can be extended to the case of a non-zero temperature bath for which the dissipative part of the dynamics is accounted for by the Liouvillian

$$\mathcal{L}_T\rho = \frac{\gamma}{2}(\overline{n}+1)(b\rho b^{\dagger} - \{b^{\dagger}b, \rho\}) + \frac{\gamma}{2}\overline{n}(b^{\dagger}\rho b - \{bb^{\dagger}, \rho\}). \tag{3.20}$$

A dynamical approach fully analogous to the dyadic-based one used above can be adopted, following the lines of Reference [99]. In this case, the damping of a coherent state can be expressed in terms of displaced number states weighted by a thermal probability distribution determined by the actual value of $\overline{n}$. Yet, the geometric phase can still be tracked for moderate temperatures of up to 0.1mK, which marks the threshold above which thermal effects wash out the effect here at hand making the closure of a path in phase space basically impossible.

It should be notice that here we have treated the thermal nature of the initial state of the oscillator as an example of mixed state. Indeed, the same arguments put forth above are valid in the case of an initial state with an arbitrary $P(\alpha)$

function. By considering a thermal state, a clear and intuitive figure of merit of how mixed the initial state is can be given by the temperature parameter V. On the other hand, the thermal nature of the bath is treated independently. This approach is justified by our objective, i.e. the identification of the relevant conditions under which geometric phase can be still generated and observed in such a system.

3.3 Conclusive remarks

In summary, we have shown how to generate a geometric phase on a system in which a qubit is coupled to a harmonic oscillator. The phase can be detected using the qubit as an interferometer. We propose systems combining effective two-level devices to mechanical modes as potential scenarios for the implementation of our proposal [110–114]. In the nano-scale domain, Hamiltonian models of a form close to the one proposed here can be achieved by capacitively combining a nano-cantilever to a Cooper-pair box or growing a quantum dot on a nano-beam [33,34,36–38]. At the microscopic scale, on the other hand, the coupling in Equation (3.1) can be engineered by means of a three-level atom trapped within the volume of a pumped optomechanical cavity field and off-resonantly coupled to the latter (see Chapter 4 and [32]). Analogous configurations have been recently proposed [101] as valid alternative to consolidated schemes for the coupling between a mechanical mode and the vibrational degrees of freedom of a single atom, an ensemble of them or a levitating nanoparticle [101,104].

Under the presence of a dissipative environment and for a mixed thermal state of the oscillator, the geometric phase can still be observed under conditions over the coupling between the qubit and the oscillator that can be matched experi-

mentally [110–114]. For a nano-beam with fundamental frequency ~ 100MHz coupled to a superconducting qubit at a rate $\eta \sim 1$MHz and having a (realistic) decay rate of $\sim 1 - 10$MHz, which are values well within the validity of our approach, a temperature of 0.5K keeps the probabilities $\mathcal{P}_{\pm}$ at the visible level. By driving the mechanical mode with a two-tone signal [108], which is possible optically and electrically, thus covering both the micro- and nano-scale configurations. In the first scenario, one could consider, for instance, a single Cs atom coupled to a light mechanical resonator (masses are typically in the ng range) in both the end-mirror or membrane-in-the-middle arrangement [110–112], as recently considered for the problem of coupling the external degrees of freedom of an atom to the vibrations of a massive mechanical oscillator [101]. High-finesse cavities with small waists are currently employed in controllable optomechanical experiments (finesse$\sim 10^5$ with a waist of a few μm), thus guaranteeing a strong enough light-atom interaction that is suitable for the achievement of the effective Hamiltonian model proposed in Equation (3.1).

For the examples discussed here, all the experimental observations that are currently available are in full agreement with a Markovian description of the dynamics induced by the thermal background of phonons affecting the mechanical oscillator, thus making our study perfectly appropriate. Our proposal moves along the lines of an investigation assessing quantum effects in macroscopic systems. It enlarges the fan of indicators of quantumness at the meso-scale with a figure of merit, the geometric phase, that arises in virtue of the sole coherent qubit-oscillator interaction and survives against plainly adverse operating conditions.

Chapter 4

Non classicality of opto-mechanical devices

In this chapter, we prove how nonclassical behaviors can be induced in massive mesoscopic systems out of the reach of direct addressability. The indirect interaction of a mesoscopic system (the movable mirrors of an optical cavity) with a fully controllable microscopic system (a three level atom) enforces nonclassical mesoscopic states, robust against adverse operative conditions (such as temperature). Our study is performed in the micro-scale domain and involves two different optomechanical cavity-quantum electrodynamics settings. It proposes a scenario for the observation of induced nonclassicality that is truly mesoscopic (thus different from more extensively studied nano-scale setups [115–118]), well-controllable and, although close to experimental capabilities in the fields of optomechanics and light-matter interaction, yet unexplored.

In this chapter we are particularly interested in the analysis of two condidions: the thermal preparation of the oscillator's states and the interaction of the

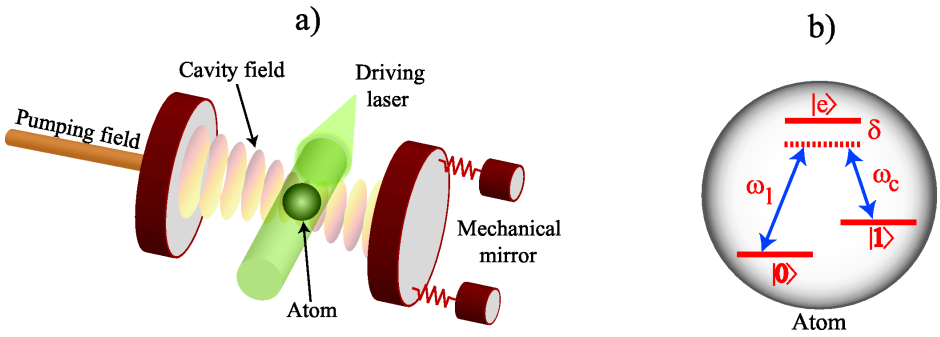

Figure 4.1: **(a)** Scheme of the system. **(b)** Energy levels of the atom driven by an off-resonant two-photon Raman transition.

oscillator with a thermal bath. We first analyze such conditions separately, considering the case of a an initial thermal preparation of the system followed by an unitary evolution and the case of an initial thermal state interacting with a zero-temperature bath. At the end, we consider also the most realistic scenario of a system in a thermal state undergoing a finite-temperature dissipative dynamics. This approach is justified by our objective, i.e. the identification of the relevant conditions under which quantum behaviours are observable.

The chapter is organized as follow: in Section 4.1, we will discuss a setup in which one mesoscopic object (a movable mirror at the end of an optical cavity) interacts with a microscopic system (a three level atom) through the radiation inside the cavity. In this context, we study the correlations between the two systems as well as the non-classical features induced on the state of the mirror. In Section 4.2, we will extend our analysis to a system where both cavity mirrors interact with the atom inside the cavity. This setup allow us to investigate the correlations between two truly mesoscopic systems, revealing how quantum effects can survive to adverse environmental conditions such as dissipation and thermalization.

4.1 Single Mirror

In this section, we consider an optomechanical system consisting of a cavity where the end mirror is able to oscillate around its equilibrium position under the action of radiation pressure force. A three level atom is placed inside the cavity and the system's parameters are chosen in such a way that an effective atom-mirror coupling is achieved. We will show how the state of the system reveals strong non-classical features like non-local correlations between the atom and the mirror and negative values of the Wigner function of the mirror alone even in presence of dissipative processes and at finite temperature.

4.1.1 Model

The system we consider involves a three-level atom in a Λ configuration, coupled to a single-mode optical cavity pumped by an laser field at frequency ω_p and with a movable mirror. The atom is driven by a second external field at frequency ω_i that enters the cavity radially (see Figure 4.1). We label with $\{|0\rangle, |1\rangle\}$ the states belonging to the fundamental atomic doublet and with $|e\rangle$ the excited state of the atom. The atomic transition $|0\rangle \leftrightarrow |e\rangle$ is guided, at rate Ω, by the external radial field at frequency ω_i . On the other hand, the transition $|1\rangle \leftrightarrow |e\rangle$ is coupled with the cavity field at frequency ω_c with coupling constant g. We call δ the detuning between each transition and the respective driving field, while $\Delta = \omega_c - \omega_p$ is the cavity-pump detuning. The movable mirror is modeled as a harmonic oscillator of frequency ω_m, coupled to the cavity field through radiation-pressure (see Chapter 2). We assume large single-photon Raman detuning and negligible decay rate γ_e from the atomic excited state, so that $\delta \gg \Omega, g \gg \gamma_e$ and an off-resonant two-

photon Raman transition is realized. Moving to an interaction picture defined by the operator $\hbar\omega_p a^\dagger a + \hbar\omega_i |e\rangle_a\langle e| + \hbar\omega_{10}|1\rangle_a\langle 1|$, the Hamiltonian of the overall system reads[1]

$$H_{\rm sys} = H_a + H_R + H_m + H_{cp} + H_{mc} + H_{cp}, \tag{4.1}$$

where

$$\begin{aligned}
H_{\rm a} &= \delta|e\rangle_a\langle e|, \\
H_{\rm R} &= \Omega(|e\rangle_a\langle 0| + |0\rangle_a\langle e|) + \\
&\quad + g(e^{i\Delta t}a^\dagger|1\rangle_a\langle e| + e^{-i\Delta t}a|e\rangle_a\langle 1|), \\
H_{\rm m} &= \omega_m b^\dagger b, \\
H_{\rm cp} &= -\Delta a^\dagger a, \\
H_{\rm mc} &= \chi a^\dagger a(b + b^\dagger).
\end{aligned} \tag{4.2}$$

Here, H_a is the atomic energy, H_R is the Raman coupling, H_m (H_c) is the mirror (cavity) free Hamiltonian and H_{mc} is the radiation-pressure term [70] (with coupling rate χ) with a ($a^\dagger$) the annihilation (creation) operator of the cavity field and b ($b^\dagger$) the corresponding operator of the mirror. Finally, H_{cp} is the cavity-pump interaction [72].

With the additional assumption of $\delta, \Delta \gg g, \Omega$, both the atomic excited state and the cavity field are virtually populated and they can be eliminated from the dynamics of the system. This leads to the effective interaction Hamiltonian $H_{\rm eff} = \eta|0\rangle_a\langle 0|(b^\dagger + b)$, where $\eta = 4\chi g^2\Omega^2/\delta^2\Delta^2$ (see Appendix B.1 for an explicit

[1] We have set $\hbar \equiv 1$.

derivation). The form of the effective coupling rate η shows that all the considered coupling mechanisms are necessary in order to achieve the atom-mirror coupling. Through the two-photon Raman transition, the virtual quanta resulting from the atom-cavity field interaction are transferred (by the bus embodied by the cavity field) to the mechanical system. As a consequence, the state of the latter experiences a displacement (in phase space) conditioned on the state of the effective two-level atomic system resulting from the elimination of the excited state. H_{eff} involves the position quadrature operator $q \propto b + b^\dagger$ of the movable mirror. It is worth to notice that, if the cavity is driven by a bichromatic pump with frequencies ω_p and $\omega_p + \omega_m$ and a relative phase ϕ, the effective coupling between the atom and the movable mirror can be made *flexible* in the sense that q is replaced by $be^{i\phi} + b^\dagger e^{-i\phi}$, making possible the displacement in any direction of the phase space of the movable mirror [31,35,73,93]. The final effective Hamiltonian of the system is then given by

$$H_{\text{eff}} = \eta|0\rangle_a\langle 0|(b^\dagger e^{-i\phi} + be^{i\phi}), \tag{4.3}$$

which represents the same model studied in Chapter 3.

4.1.2 Atom-Mirror Entanglement

Let us know focus on the quantification of microscopic-macroscopic correlations between the atom and the mirror. First, we assume that the initial state of the movable mirror is a coherent state $|\alpha\rangle_m$ with amplitude $\alpha \in \mathbb{C}$, while the atom is assumed intially in $|+\rangle_a = (|0\rangle + |1\rangle)_a/\sqrt{2}$. Under the action of the effective Hamiltonian in Equation (4.3), the initial state evolves into $|\psi(t)\rangle = U_t|+,\alpha\rangle_{am}$,

where

$$|\psi(t)\rangle = \frac{1}{\sqrt{2}}(|1,\alpha\rangle + e^{-i\Phi(t)}|0,\alpha - i\eta t e^{-i\phi}\rangle)_{am}, \tag{4.4}$$

with

$$\begin{aligned} &\Phi(t) = \eta t \mathrm{Re}[\alpha e^{i\phi}], \\ &U_t \equiv e^{-iH_{\mathrm{eff}}t} = |1\rangle_a\langle 1| \otimes \mathcal{I} + |0\rangle_a\langle 0| \otimes D(-i\eta t e^{i\phi}), \end{aligned} \tag{4.5}$$

where $D(\zeta) = e^{\zeta b^\dagger - \zeta^* b}$ is the one-mode displacement operator [72]. Equation (4.4) is, in general, an entangled state of a microscopic and a mesoscopic system: its Von Neumann entropy depends on the value of ηt only. Intuitively, the larger the phase-space distance between $|\alpha\rangle$ and $|\alpha - i\eta t\rangle$, the closer the evolved state to a balanced superposition of bipartite orthogonal states, thus maximizing the entanglement. To give a figure of merit, for $\eta t = 0.82$ the entropy is ~ 0.8, while for $\eta t > 1.7$ the entropy is > 0.996. Interestingly, the kind of control over the mirror state reminds of the "quantum switch" protocol for microwave cavities [119], although here it is achieved over a truly mesoscopic device.

Although impressive progresses have recently been accomplished in active and passive cooling of micro and nano-mechanical oscillators [18], in any experimental setting it is realistic to expect the mirror to be affected by thermal randomness due to their exposure to the driving field and/or to a phononic backgrounds in equilibrium at temperature T. This is particularly true for "slow" micro-mechanical systems, typically characterized by small frequencies ω_m. Exploiting the handiness of Equation (4.4), we write the initial state of the mirror in thermal equilib-

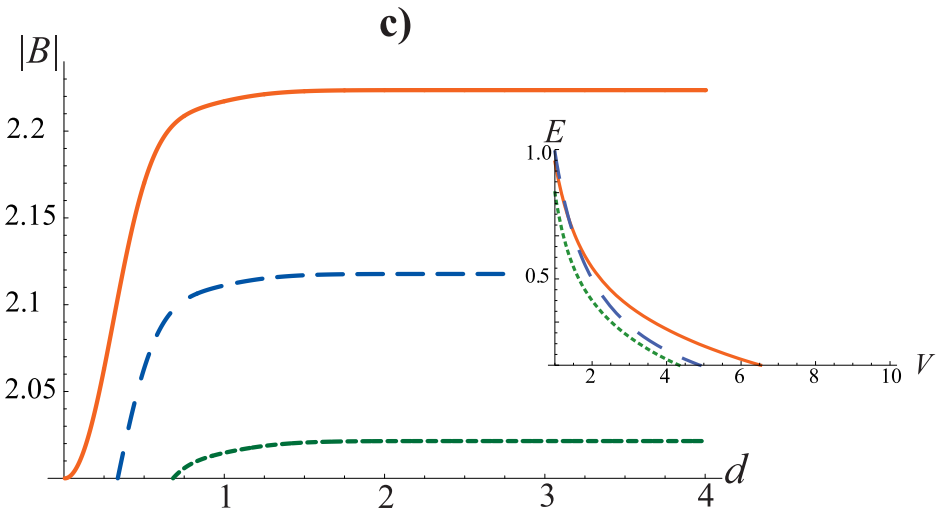

Figure 4.2: Maximum violation of the Bell-CHSH inequality against the displacement d. From top to bottom, the curves correspond to $V = 1, 3, 5$ with $\eta t = 2d$ and $\theta_1 \simeq 3\pi/2$ and are optimized with respect to θ. The inset shows, from top to bottom, the logarithmic negativity E against V for projected states with $p = 0, 1$ and 2, for $d = 2$.

rium at temperature T and displaced by d (due to the external pump) as

$$\varrho_{\rm m}^{\rm th} = \int d^2\alpha \mathcal{P}(\alpha, V)|\alpha\rangle_m\langle\alpha|, \tag{4.6}$$

with

$$\mathcal{P}(\alpha, V) = \frac{2e^{-\frac{2|\alpha-d|^2}{V-1}}}{\pi(V-1)}, \quad V = \coth(\omega_m/2k_bT), \tag{4.7}$$

and k_b the Boltzmann constant. Under U_t, the state $|+\rangle_a\langle+| \otimes \varrho_{\rm m}^{\rm th}$ evolves into

$$U_t|+\rangle_a\langle+|\varrho_{\rm m}^{\rm th}U_t^\dagger = \int d^2\alpha \mathcal{P}(\alpha)|\psi(t)\rangle\langle\psi(t)|, \tag{4.8}$$

which is in general mixed and reduces to the pure case of Equation (4.4) for $T = 0$. We proceed to show that the coupling mechanism embodied by our system

is characterized by interesting features, at the core of current experimental and theoretical interests. Let us consider the case of $\phi = \pi/2, V = 1$ (i.e. $T = 0$) and $\alpha \in \mathbb{R}$, which gives $|\psi(\tau)\rangle \propto |1, \alpha\rangle + |0, \alpha - \eta t\rangle$. This entangled state represents a mesoscopic instance of a pure Schrödinger-cat state. Interestingly, it has been discussed that a faithful implementation of the Schrödinger's cat paradox would use a mesoscopic subsystem initially prepared in a thermal state, rather than a pure one [23, 120, 121]. The state in Equation (4.8) is a significant example of such case. Unravelling the entanglement properties of this state is demanding due to the difficulty of finding an analytical tool for its undisputed revelation. In order to gain insight, here we propose to follow two paths.

The first relies on the nonlocality properties of this class of states, induced by the strong entanglement between the subsystems. Following References [122, 123], the microscopic part is projected along the direction $\vec{n} = (\sin\theta, 0, \cos\theta)$ of the single-qubit Bloch sphere while the mesoscopic one is probed by using the displaced parity observable $\Pi(\beta) = D^{\dagger}(\beta)(-1)^{b^{\dagger}b}D(\beta)$, where $D(\beta)$ is the displacement operator of amplitude $\beta = \beta_r + i\beta_i$. The correlation function for a joint measurement is thus

$$C(\beta, \theta) = \int d^2\alpha \mathcal{P}(\alpha, V) \langle\psi(t)| (\vec{n} \cdot \boldsymbol{\sigma}) \otimes \Pi(\beta) |\psi(t)\rangle , \tag{4.9}$$

and a Bell-Clauser-Horne-Shimony-Holt (Bell-CHSH) inequality is formulated as $|C(0, \theta_1) + C(0, \theta) + C(\beta, \theta_1) - C(\beta, \theta)| \leq 2$ [83]. Any state satisfying this constraint can be described by a local-realistic theory. Let us first discuss the pure

case of $V = 1$, which gives

$$C(\beta,\theta) = \frac{1}{2} e^{-2(d^2+\eta^2 t^2+|\beta|^2+\beta_r \eta t - 2\beta_r d)} \times \\ \times \left[\cos\theta (e^{4d\eta t - 2\eta t \beta_r} - e^{2\eta^2 t^2 + 2\eta t \beta_r}) + 2 e^{\eta t (2d + \frac{3}{2}\eta t)} \cos(2\eta t \beta_i) \sin\theta\right]. \tag{4.10}$$

At $\eta t = 0$, the microscopic and mesoscopic subsystems are uncorrelated and $C(\beta,\theta)$ can indeed be factorized. For a set value of d and a non-zero value of ηt, we observe violation of the Bell-CHSH inequality as illustrated in Figure 4.2. Moreover, there is a range of values of θ ($\sim \pi/2$) where, for $d \neq 0$, the local-realistic bound is violated, symmetrically with respect to $d = 0$. When the thermal character of the mesoscopic part is considered, the expression for the correlation function becomes cumbersome and we omit it. However, *the strong entanglement between microscopic and mesoscopic subsystems allows violation of Bell-CHSH inequality, to some extent, also in the mixed-state case*: the dotted curve in Figure 4.2, indeed, corresponds to $V \simeq 5$. Beyond this value, the inequality is no more violated.

The second path we follow uses the technique put forward in [124] and later reprised by Ferreira *et al.* in [26]. In this approach, state (4.8) is projected onto a bipartite bidimensional subspace spanned by the microscopic states $\{|0\rangle, |1\rangle\}_a$ and the phononic states $\{|p\rangle, |p+1\rangle\}_m$ ($p \in \mathbb{Z}$) for the mesoscopic one. The entanglement within Equation (4.8) cannot be increased by this projection, which is just a local operation. Thus, by quantifying the entanglement for fixed p, we provide a lower bound to the overall quantum correlations in the state of the system. As a measure for entanglement in each 2×2 subspace we use the *logarithmic*

negativity, which accounts for the degree of violation of the positivity of partial transposition criterion [76–78]. An example of the results achieved with this method is given in the inset of Figure 4.2, where we show the case of $d = 2$ and $p = 0, 1, 2$. Entanglement is found in each subspace with fixed p, up to values of $V \sim 5$, strengthening our findings about the resilience of nonclassical correlations set by the coupling being studied.

4.1.3 Non-classicality of the mirror

We now consider the effects of the microscopic-mesoscopic interaction over the state of the movable mirror. This is a hot topic in the current research of opto and electro-mechanical systems. The grounding of opto/electro-mechanical devices as potential candidates for research along the lines of fundamental physics and, in a visionary perspective, quantum information processing demands the design of protocols which enable to prepare a massive mechanical system in a nonclassical state. Various attempts have been performed in this direction, mainly at the nano-scale level, where a cantilever can be capacitively coupled to a superconducting two-level system [115–118]. Our proposal, on the other hand, is explicitly designed for a micro-scale optomechanical scenario, where truly *massive* mechanical systems are in order. Moreover, as remarked above, our coupling mechanism is indirect and based on the controllability of radiation-pressure.

Let us consider the case of $\phi = 0$. The optomechanical evolution encompassed by U_t alone is unable to give rise to any nonclassicality in the state of the mirror. This is easy to check simply by tracing out the state of the atom in Equation (4.4), which would leave us with a statistical mixture of two displaced mirror's

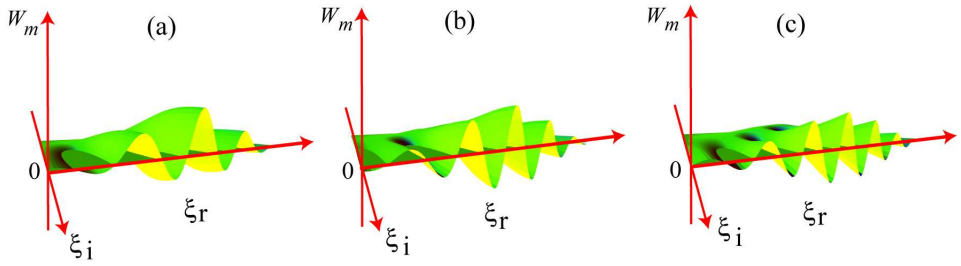

Figure 4.3: Wigner function of the conditional mirror state against $\xi_r = \mathrm{Re}(\xi)$ and $\xi_i = \mathrm{Im}(\xi)$, for $V = 3$ and $d = 0$. Panels **(a)**, **(b)**, **(c)** correspond to $\eta\tau = 2, 3, 4$ respectively.

states. On the other hand, a conditional process is able to project the coherence of a quantum mechanical superposition and simultaneously get rid of the atomic degree of freedom. In order to illustrate our claim, we consider an initial state of the system having the form $\rho(0)=|\varphi\rangle\langle\varphi|\otimes\rho_m(0)$ where $|\varphi\rangle=c_0|0\rangle+c_1|1\rangle$ is a pure state of the atom and $\rho_m(0)$ is an arbitrary state of the mechanical mode. We then project the atomic part of the evolved state $U_t\rho(0)U_t^\dagger$ onto $|\varphi\rangle\langle\varphi|$, thus post-selecting the mechanical state $\rho_m(t) = \langle\varphi|U_t|\varphi\rangle\rho_m(0)\langle\varphi|U_t^\dagger|\varphi\rangle$. Therefore, the state of the mirror undergoes an effective evolution driven by the operator

$$\langle\varphi|U_t|\varphi\rangle = |c_1|^2\mathcal{I} + |c_0|^2 D(-i\eta t), \tag{4.11}$$

with $\mathcal{I}$ the identity operator. In the remainder of this paper, we consider again the case where $|\varphi\rangle = |+\rangle \equiv (|0\rangle + |1\rangle)/\sqrt{2}$, which optimizes the performance of our scheme in terms of the degree of non-classicality enforced in the mechanical subsystem. For an initial coherent state of the mirror, i.e. $\rho_m(0) = |\alpha\rangle\langle\alpha|$, applying the conditional time evolution operator in Equation (4.11) leads to $|\mu_+\rangle_m = \mathcal{N}_+(|\alpha\rangle + e^{-i\Phi(t)}\,|\alpha - i\eta t\rangle)_m$, where $\mathcal{N}_+$ is the normalization factor. Depending on the value of ηt, such states exhibit coherences of quantum mechanical nature.

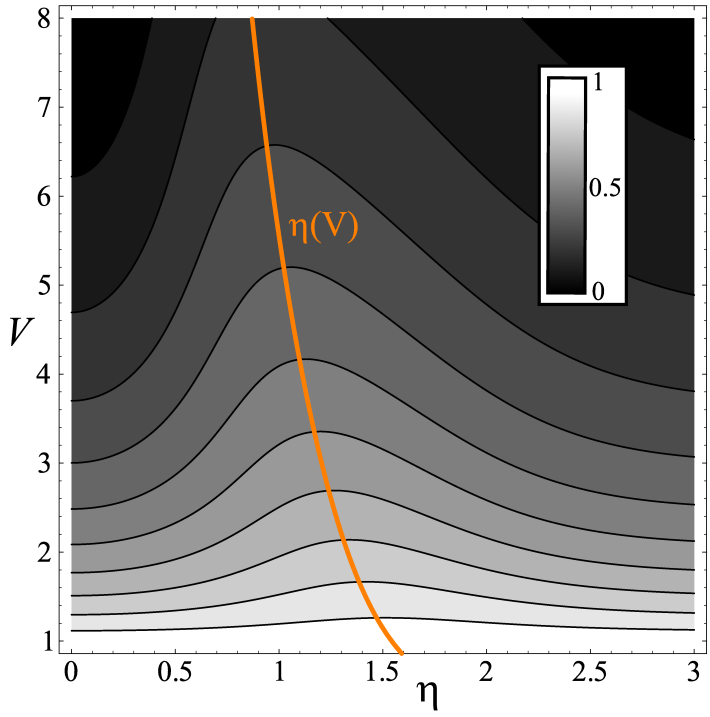

Figure 4.4: Density plot of fidelity against V and η. Darker regions correspond to smaller values of F_W. The function $\eta(V)$ at which F_W is maximum is fitted by $0.7e^{-0.3(V-1)} + 0.87$.

Obviously, the thermal convolution inherent in the preparation of mirror's state ϱ_m may *blur* such fixed-phase relation. In what follows we prove that this is not the case for a rather wide range of values of V.

Our esteem of nonclassicality would be the negativity in the Wigner function associated with the reduced mirror's state resulting from the measurement performed over the atomic part of the system. The Wigner function for a single bosonic mode is defined as

$$W(\mu) = \pi \int d^2\nu (e^{\mu\nu^* - \mu^*\nu}) \chi(\nu), \tag{4.12}$$

where $\mu \in \mathbb{C}$ and $\chi(\nu) = \mathrm{Tr}[D(\nu)\rho]$ is the Weyl characteristic function. An immedi-

ate figure of merit for non-classicality of $\rho(t)$ is given by the existence of negative values of the Wigner function. Considering an initial thermal state of the mirror and applying the conditional unitary evolution operator given in Equation (4.11), the Wigner function of the mirror after the post-selection process is

$$\begin{aligned} W_m(\mu) =& \mathcal{M}^{-1} e^{-\frac{2|\mu|^2+2\eta t\mu_i+\eta^2 t^2}{V}} \\ & \times[\cosh(\frac{\eta^2 t^2+2\eta t\mu_i}{V}) + e^{\frac{\eta^2 t^2}{2V}}\cos(2\eta t\mu_r)], \end{aligned} \tag{4.13}$$

with $\mathcal{M} = (1+e^{-\frac{V\eta^2}{2}})\pi V/2$. The behavior of $W_m(\mu)$ in the phase space is shown in Figure 4.3, where we clearly see the appearance of regions of negative values, witnessing nonclassicality of the corresponding state as induced by our microscopic-mesoscopic coupling. Interference fringes are created between two positive Gaussian peaks (not shown in the figure) corresponding to the position, in the phase space, of mutually displaced coherent states. This reminds of the Wigner function of a pure Schrödinger cat state although, as we see later, the analogy cannot be pushed. Remarkably, in contrast with the fragility of the nonlocality properties of the microscopic-mesoscopic state, $W_m(\mu)$ has a negative peak of -0.01 up to $V \sim 100$, which implies strong thermal nature of the mirror state. For a mechanical system embodying one of the mirrors of a cavity, $\omega_m/2\pi \sim 5$MHz is realistic. For $g\Omega/\delta\Delta \sim 0.1$, cavity-length ~ 0.3mm and a light mirror (mass $\sim$ 15ng), $\chi \sim 2.8$KHz, which corresponds to $\eta \sim 0.1$KHz. The elimination of $|e\rangle_a$ and the cavity field, whose damping rate is quenched by the off-resonant coupling, make the proposed dynamics quite feasible. For $V = 10$ (100), this corresponds to an effective temperature of 1mK (10mK), *i.e.* energies 10 (100) times larger than the ground-state energy of the mirror.

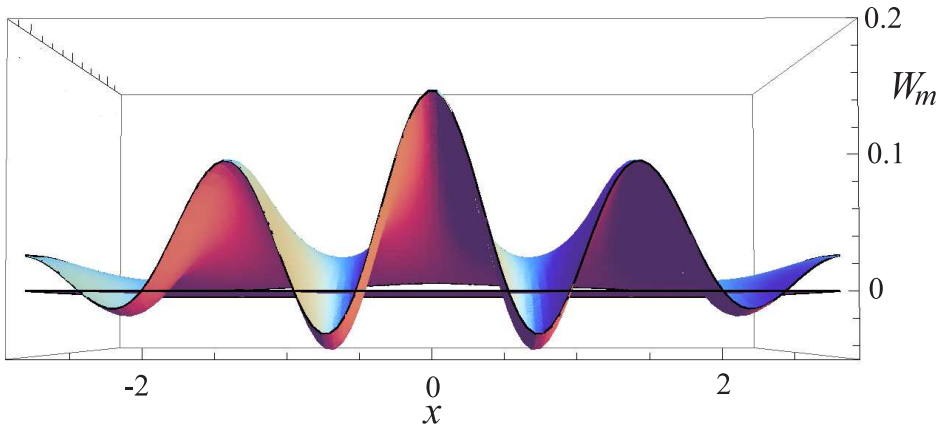

Figure 4.5: Wigner function of the mirror under dissipation after a projective measure on the atomic part of the system, for $\gamma \sim 0.1\eta$ and $V = 5$.

It is interesting to compare the mixed state resulting from the thermal convolution to a pure state in Equation (4.4) (with $\phi = 0$). As a measure of the closeness of two states, we use quantum fidelity between a mixed and a pure state written as the overlap between the corresponding Wigner functions $F_W = \pi \int d^2\mu W_P(\mu) W_M(\mu)$, where $W_P(\mu)$ ($W_M(\mu)$) is the Wigner function of the pure (mixed) state. F_W is shown in Figure 4.4 against $\eta\tau$ and V. While the thermal effect reduces the value of the fidelity as V grows, the behavior of F_W against ηt is, surprisingly, non-monotonic. At a given V, there is always a finite value of ηt associated with a maximum of F_W. Remarkably, the values of ηt maximizing F_W differ from those at which the Wigner function achieves its most negative value.

4.1.4 Finite temperature dissipative dynamics

So far, we have assumed a movable mirror of large mechanical quality factor. The progresses recently accomplished in fabrication processes guarantee very small mechanical dissipation rates. However, they are not yet negligible and their effect

should be considered in any proposal for quantumness in optomechanical devices. We thus include mechanical losses in our analysis, looking for their effects onto the nonclassicality induced in the movable mirror. We concentrate on the finite-temperature dissipative mechanism described by

$$\mathcal{L}^V(\rho) = \frac{\gamma}{2}\big[(2b\rho b^\dagger - \{b^\dagger b, \rho\}) + (V-1)[b\rho - \rho b, b^\dagger]\big], \tag{4.14}$$

which is the weak-damping limit of the Brownian-motion master equation [72]. The density matrix ρ describes the state of the atom-mirror system. The full master equation, including the unitary part $-i[H_e, \rho]$, is easily translated into a set of equations of motion for the mirror reduced density matrix obtained by considering the projections onto the relevant atomic states $\rho_{ij} = {}_a\langle i|\rho|j\rangle_a$ $(i, j = 0, 1)$. These can then be recast as Fokker-Planck equations for the Wigner functions W_{ij} of such mirror's state components [148]. These read

$$\partial_t \mathbf{W}(x, p, t) = \mathbf{M}\mathbf{W}(x, p, t) + \tilde{\mathcal{L}}_d \mathbf{W}(x, p, t), \tag{4.15}$$

where

$$\mathbf{W}(x,p,t) = \begin{pmatrix} W_{00}(x,p,t) \\ W_{01}(x,p,t) \\ W_{10}(x,p,t) \\ W_{11}(x,p,t) \end{pmatrix},$$

$$\mathbf{M} = \sqrt{2}\eta \begin{pmatrix} \partial_p & 0 & 0 & 0 \\ 0 & -\frac{ix+\partial_p}{2} & 0 & 0 \\ 0 & 0 & \frac{ix+\partial_p}{2} & 0 \\ 0 & 0 & 0 & 0 \end{pmatrix}, \tag{4.16}$$

$$\tilde{\mathcal{L}}_d = \Big[\frac{\gamma}{2}(x\partial_x + p\partial_p) + \frac{\gamma}{4}V(\partial_{p^2}^2 + \partial_{x^2}^2) + \gamma\Big]\mathcal{I}.$$

Here we have introduced the vector $\mathbf{W}(x,p,t)$, the diagonal operator $\mathbf{M}$ and the dissipative part of the Fokker-Planck equations $\tilde{\mathcal{L}}_d$ and we have used the quadrature variables $x = \sqrt{2}\text{Re}(\mu), p = \sqrt{2}\text{Im}(\mu)$. Each of these equations preserves the Gaussian nature of the corresponding Wigner's function component, whose time-evolved form is taken to be the ansatz

$$W_{ij}(x,p,t) \propto [\det(\mathbf{D}_{ij})]^{-1/2} e^{-\frac{1}{2}\mathbf{q}_{ij}^T \mathbf{D}_{ij}^{-1}\mathbf{q}_{ij} + i\Theta_{ij}(t)}, \tag{4.17}$$

with

$$\mathbf{q}_{ij} = \begin{pmatrix} x - \overline{x}_{ij} \\ p - \overline{p}_{ij} \end{pmatrix},$$
$$\mathbf{D}_{ij} = \begin{pmatrix} \sigma_{ij}^x & \sigma_{ij}^{xp} \\ \sigma_{ij}^{xp} & \sigma_{ij}^p \end{pmatrix} \tag{4.18}$$

parameterized by the time-dependent mean values $\overline{x}_{ij}, \overline{p}_{ij}$ and variances $\sigma_{ij}^{x,p,xp}$ of the variables x, p and xp. We have also introduced the time-dependent phases Θ_{ij}'s which account for the contributions from $\Phi(t)$ in Equation (4.4). The Wigner function of the mirror after a measure of the atomic part in the basis $\{||+\rangle, |-\rangle\}$ with outcome $|+\rangle$ is readily found to be $\sum_{i,j=0,1} W_{ij}(x,p,t)$ (apart from the normalization factor), which gives back the non-Gaussian character of the mirror's state. The negativity of the Wigner function can be studied for assigned values of γ and T and taking the time at which the ideal case would achieve the most negative value. The results are shown in Figure 4.5, where we see that nonclassicality is found even for quite a large ratio γ/η. Clearly, nonclassicality results from a subtle trade off between temperature and mechanical quality factor. Although small γ and T guarantee nonclassicality, such a behavior is still present at $\gamma/\eta \sim 0.1$ and for T well above the ground-state one.

4.2 Two Mirrors

In this section, we will consider a different setup, where both cavity mirrors are free to oscillate around their equilibrium positions and they are both interacting with a three level atom inside the cavity. Using this setup, we can study the correlations between the two mesoscopic systems and their quantum features. In this section, we will only focus on the conditional evolution of the two mirrors after a measurement of the atomic subsystem.

4.2.1 Hamiltonian and conditional unitary evolution

Let us consider the same Fabry-Perot cavity discussed in Section 4.1.1, pumped by a laser field at frequency ω_p and with a three-level Λ-type atom trapped within the mode-volume of the cavity field. The model is very similar to the one describing the single mirror case, with the difference that here the two mirrors of the cavity are both able to oscillate around their equilibrium positions and they are modeled as two harmonic oscillators with frequencies ω_1 and ω_2. By moving to an interaction picture respect to the same operator consider in the one-mirror scheme, the Hamiltonian of the system can be written in the same form as Equation (4.1), where only the terms involving the mirror's degrees of freedom are changed to take into account the addition of the second mirror. These terms read

$$\begin{aligned} H_{\rm m} &= \sum_{j=1}^{2} \omega_j b_j^\dagger b_j, \\ H_{\rm mc} &= a^\dagger a \sum_{j=1}^{2} (-1)^{j-1} \chi_j (b_j^\dagger + b_j). \end{aligned} \tag{4.19}$$

The bosonic operators $a^\dagger, a$ and $b_j^\dagger, b_j$ refer to the cavity field and the two mechanical mirrors, respectively. By assuming a large cavity quality factor and a small spontaneous emission rate from $|e\rangle$, in the limit of $(\Delta, \delta) \gg (\Omega, g)$ we can eliminate both the cavity field and the excited atomic level, thus arriving at the effective atom-mirrors Hamiltonian

$$H_{\rm eff} = |0\rangle\langle 0| \otimes \sum_{j=1}^{2} (-1)^{j-1} \eta_j (b_j^\dagger + b_j), \tag{4.20}$$

with $\eta_j = (\Omega^2 g^2/\delta^2\Delta^2)\chi_j$. The corresponding time-evolution operator reads

$$U_t = |1\rangle\langle 1| \otimes \mathcal{I} + |0\rangle\langle 0| \otimes D_1(-i\eta_1 t) \otimes D_2(i\eta_2 t), \tag{4.21}$$

where $D_j(\zeta) = \exp[\zeta b_j^\dagger - \zeta^* b_j]$ is the displacement operator for mode $j = 1, 2$ [72]. In analogy with the one-mirror case, the resulting dynamics of the mechanical systems is thus a conditional displacement controlled by the state of the atomic part: while nothing happens to the mechanical modes when the atom is prepared in $|1\rangle$, their state gets displaced in phase space where the atomic state is $|0\rangle$. In what follows we generalize the analysis performed in the previous section and we show how this mechanism, complemented with an appropriate post-selective step, results in non-classicality of the mechanical subsystem.

The generalization of the conditional time evolution operator given in Equation (4.11) to the two-mirrors case is straightforward. The new operator simply reads

$$\langle\varphi|U_t|\varphi\rangle = |c_1|^2\mathcal{I} + |c_0|^2 D_1(-i\eta_1 t)D_2(i\eta_2 t), \tag{4.22}$$

with $\mathcal{I}$ the identity operator. We consider again the case in which $|\varphi\rangle = |+\rangle$ and the initial state of the mirror is $\rho_m(0) = |\alpha_1, \alpha_2\rangle\langle\alpha_1, \alpha_2|$ where $|\alpha_j\rangle$ is a coherent state of mode j having amplitude $\alpha \in \mathbb{C}$. The state of the mirrors thus reads

$$|\psi_m(t)\rangle = (|\alpha_1, \alpha_2\rangle + e^{-i\Phi(t)}|\beta_1(t), \beta_2(t)\rangle)/\sqrt{2}, \tag{4.23}$$

where $\Phi(t) = \sum_{j=1}^{2}(-1)^{j-1}\eta_j \mathrm{Re}\{\alpha_j\}t$ and $\beta_j(t) = \alpha_j + (-1)^j i\eta_j t$ $(j=1,2)$. Equation (4.23) is an Entangled Coherent State (ECS) of modes 1 and 2 [126]. Its von Neumann entropy depends on a delicate trade off among the amplitudes $\alpha_j(t)$

and $\beta_j(t)$. ECSs play an important role in the context of continuous-variable (CV) quantum information processing as a valuable resource for communication and computation (the latter performed via teleportation-based gate operations) [127].

4.2.2 Mirror-Mirror correlations

The simple example analyzed in the previous section is instructive and, as we will see later, mathematically useful. However, as pointed out in Section 4.1.2, the interaction of the two oscillators with the thermal bath has to be taken into account, and it is realistic to assume a initial thermal state for the two mirros. The thermal state of a single bosonic mode is given by Equation (4.6). In the case of two modes, the initial mechanical state is $\rho_{\rm m}(0)=\varrho_1^{\rm th}\otimes\varrho_2^{\rm th}$, and it evolves under the action of $\langle+|U_t|+\rangle$ so as to give

$$\rho_m(t)=\int d^2\alpha_1 d^2\alpha_2 \mathcal{P}(\alpha_1,V)\mathcal{P}(\alpha_2,V)|\psi_m(t)\rangle\langle\psi_m(t)|. \tag{4.24}$$

We now show that, despite the thermal convolution at the basis of the definition of $\rho(t)$, the mechanical state of two mirrors can exhibit strong non-classical features even at non-zero temperature. We will focus on two different signatures of non-classicality: the negative values of the Wigner function associated with the state $\rho_m(t)$ and the non-local correlations between the two mirrors. The Wigner function of a two-modes system is defined as the straightforward generalization of Equation (4.12), i.e.

$$W(\mu_1,\mu_2)=\frac{1}{\pi^2}\int d^2\nu_1 d^2\nu_2\big(\prod_{j=1}^{2} e^{\mu_j\nu_j^*-\mu_j^*\nu_j}\big)\chi(\nu_1,\nu_2), \tag{4.25}$$

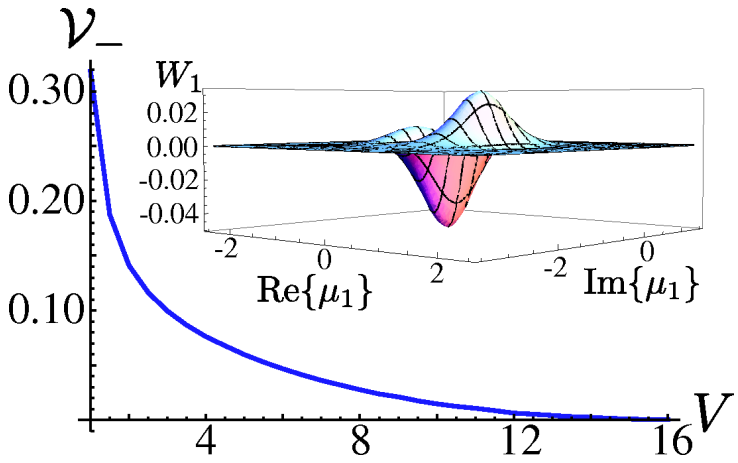

Figure 4.6: (Color online) Negative volume of $W(\mu_1, \mu_2)$ against V for $\eta t = 5$. Inset: Wigner function $W_1(\mu_1)$ at $\mu_2 = -(1+i)$, ηt=2 and T=0.

where $(\mu_j, \nu_j) \in \mathbb{C}$ and $\chi(\nu_1, \nu_2) = \mathrm{Tr}[D_1(\nu_1) D_2(\nu_2) \rho]$ is the two-modes Weyl characteristic function. Together with the study of Wigner function's negativity, we also investigate the quantum correlations between the two mirrors. To overcome the problem of inferring non-classical correlations in a mixed non-Gaussian state of a CV system, which is a very demanding task due to the lack of appropriate entanglement measures, we use the same approach taken in the previous section, which relies on the investigation of Bell inequality violations. This route is particularly viable in our case as we can take advantage of the dualism between density matrix and Wigner function for CV states. Here, one can formulate a Bell-Clauser-Horne-Shimony-Holt (Bell-CHSH) test using the two-mode Wigner function corresponding to $\rho_{\mathrm{m}}(t)$.

To begin with, one can study the behavior of the single-mirror Wigner functions calculated for a fixed point μ_0 in the other mirror phase space, i.e.

$$W_j(\mu_j) = W(\mu_j, \mu_i = \mu_0), \quad \text{with} \quad i \neq j = 1, 2. \tag{4.26}$$

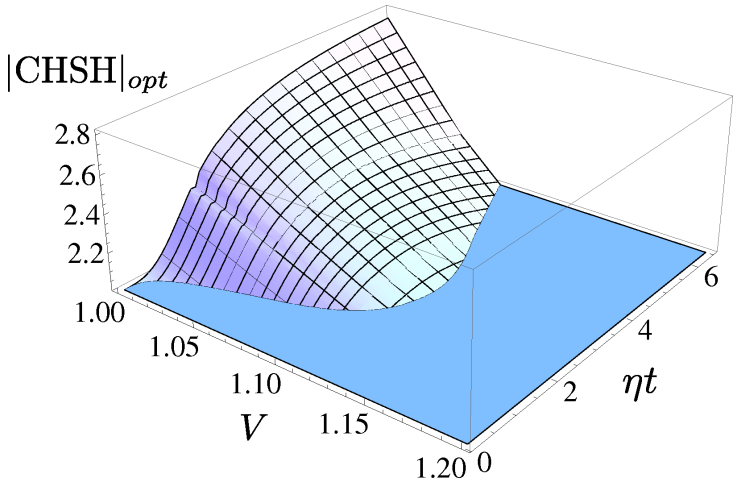

Figure 4.7: (Color online) Numerically optimized violation of the Bell-CHSH inequality for the two-mirror state against ηt and V.

It is seen from the inset of Figure 4.6 that, depending on the operating conditions of the system, $W_1(\mu_1)$ (equivalently $W_2(\mu_2)$) can be considerably negative, thereby proving its non-classical nature. This is remarkable, especially when compared to the case of a standard optomechanical setting where a mechanical mirror is coupled to the field of an optical resonator. There, in fact, it can be proven that the state of the mechanical subsystem is only *classically squeezed* and the device cannot be utilized in order to engineer non-classical states of the movable mirror [128]. Differently, using the mechanism we propose here, we have checked that the negative regions of $W_1(\mu_1)$ remain even at non-zero temperature. These considerations can be strengthened by extending them to the Wigner function of both the mechanical mirrors and studying the *negative volume*, which is defined as

$$\mathcal{V}_{-}=\int d^2\mu_1 d^2\mu_2[|W(\mu_1,\mu_2)|-W(\mu_1,\mu_2)]/2. \tag{4.27}$$

In Figure 4.6, $\mathcal{V}_{-}$ is plotted against V for $\eta t = 5$, revealing that non-classicality

persists up to $V\sim10$, *i.e.* well above zero temperature. We give an estimate of actual temperatures corresponding to such order of magnitude for V later on.

We now pass to the study of the Bell-CHSH inequality test [83] to infer non-classical correlations shared by the mechanical systems. For a two-mode bosonic system, the Bell-CHSH inequality can be re-cast in terms of the expectation values $\langle\Pi_1(\mu_1)\otimes\Pi_2(\mu_2)\rangle$, with $\Pi_i(\mu_j) = D_j(\mu_j)(-1)^{b_j^\dagger b_j}D_j^\dagger(\mu_j)$ [122]. The proportionality between displaced parity operators and the two-mode Wigner function is crucial as we have that $W(\mu_1,\mu_2) = (4/\pi^2)\langle\Pi_1(\mu_1)\otimes\Pi_2(\mu_2)\rangle$ and the CHSH function can thus be written as

$$\text{CHSH}=\frac{\pi^2}{4}[W(\mu_1,\mu_2)+W(\mu_1',\mu_2)+W(\mu_1,\mu_2')-W(\mu_1',\mu_2')]. \tag{4.28}$$

Any local realistic theory imposes the bound $|\text{CHSH}| \leq 2$. If the mechanical state is such that $|\text{CHSH}| > 2$, correlations of non-classical nature are necessarily shared by the two mirrors. In Figure 4.7 we show that, although hindered by the thermal nature of the mechanical modes, the two-mirror state violates the local realistic bound up to $V = 1.1$, which corresponds to a temperature $T \approx 0.1$mK (5μK) at $\omega_m/2\pi \sim 6$MHz (300KHz), a frequency easily achievable by current experimental setups [15, 22]. This shows that the mechanical state remains non-classically correlated even for thermal energies that are 10 times larger than the ground-state energy of each mirror. Quite expectedly, the CHSH inequality is increasingly violated in time at temperature $T = 0$, asymptotically reaching Tsirelson's bound.

The decreasing behavior of the CHSH function at $T>0$ can be explained by considering that, under such conditions, the coherences in the two-mirror state

are suppressed. In fact, let us consider the off-diagonal terms of $\rho_m(t)$ in the coherent-state basis. These are given by

$$\int d^2\alpha_1 d^2\alpha_2 P(\alpha_1, V) P(\alpha_2, V) e^{i\Phi(t)} |\alpha_1, \alpha_2\rangle\langle\beta_1(t), \beta_2(t)| \tag{4.29}$$

and its Hermitian conjugate. As a function of Re(α_j), the phase factor $e^{i\Phi(t)}$ oscillates at frequency $\eta_j t$. At T=0, $P(\alpha_j, 1)$ becomes a bidimensional Dirac delta-function $\delta^2(\alpha_j)$, which sets the phase factor to unity. At the same time, by increasing $\eta_j t$, the components of the ECS entering state $\rho_m(t)$ become increasingly orthogonal, which optimizes the violation of the CHSH inequality. Differently, at finite temperature $P(\alpha_j, V)$ has a non-null width within which the increasingly oscillating time-dependent phase factor is eventually averaged to zero. This occurs more rapidly as V grows.

4.2.3 Dissipative dynamics

We now proceed to include the mechanical damping of the two oscillator in our analysis on the same lines followed in Section 4.1.4. We consider the dynamics of the mirror-atom density matrix ρ as driven by the weak-damping limit of the standard Brownian-motion superoperator, whose generalization to the two mirrors system reads as

$$\mathcal{L}^V(\rho) = \sum_{j=1,2} \frac{\gamma}{2} (2b_j \rho b_j^\dagger - \{b_j^\dagger b_j, \rho\} + (V-1)[b_j \rho - \rho b_j, b_j^\dagger]). \tag{4.30}$$

From such master equation one can obtain with standard techniques four Fokker-Planck equations for the Wigner functions W_{ij} of the mechanical state compo-

nents associated the atomic operator $|i\rangle\langle j|$ $(i,j{=}0,1)$. The Fokker-Planck equations can be written in the same form given in Equation (4.15), and each equation is solved by using the Gaussian ansatz in Equation (4.17), which is worth to recall

$$W_{ij}(x,p,t)\propto[\det(\mathbf{D}_{ij})]^{-1/2}e^{-\frac{1}{2}\mathbf{q}_{ij}^{T}\mathbf{D}_{ij}^{-1}\mathbf{q}_{ij}+i\Theta_{ij}(t)}. \tag{4.31}$$

Here the vector $\mathbf{q}$ and the covariance matrix $\mathbf{D}_{ij}$ are the generalization of Equation (4.18) to the two modes case and they are given by

$$\begin{aligned}\mathbf{q}_{ij} &= \begin{pmatrix} x_1{-}\overline{x}_{1,ij} \\ p_1{-}\overline{p}_{1,ij} \\ x_2{-}\overline{x}_{2,ij} \\ p_2{-}\overline{p}_{2,ij}\end{pmatrix}, \\ \mathbf{D}_{ij} &= \begin{pmatrix} \sigma_{ij}^{x_1x_1} & \sigma_{ij}^{p_1x_1} & \sigma_{ij}^{x_2x_1} & \sigma_{ij}^{p_2x_1} \\ \sigma_{ij}^{x_1p_1} & \sigma_{ij}^{p_1p_1} & \sigma_{ij}^{x_2p_1} & \sigma_{ij}^{p_2p_1} \\ \sigma_{ij}^{x_1x_2} & \sigma_{ij}^{p_1x_2} & \sigma_{ij}^{x_2x_2} & \sigma_{ij}^{p_2x_2} \\ \sigma_{ij}^{x_1p_2} & \sigma_{ij}^{p_1p_2} & \sigma_{ij}^{x_2p_2} & \sigma_{ij}^{p_2p_2}\end{pmatrix}.\end{aligned} \tag{4.32}$$

As explained in the previous section, the sum of the four terms $\sum_{i,j=0,1}W_{ij}(x,p,\tau)$ gives the full non-Gaussian solution of the Fokker-Planck equations, and the negativity of the Wigner function can be use to witness non-classicality. Figure 4.8**(a)** reveals that $W(\mu_1,\mu_2)$ exhibits considerable regions of negativity also for $\gamma{\neq}0$. As expected, the negativity of the Wigner function increases when the coupling constant η becomes larger than the damping rate. In this situation is indeed possible to neglect the dissipation of the mirror and recover the purely unitary dynamics treated above. Interestingly, the Wigner function has still negative values

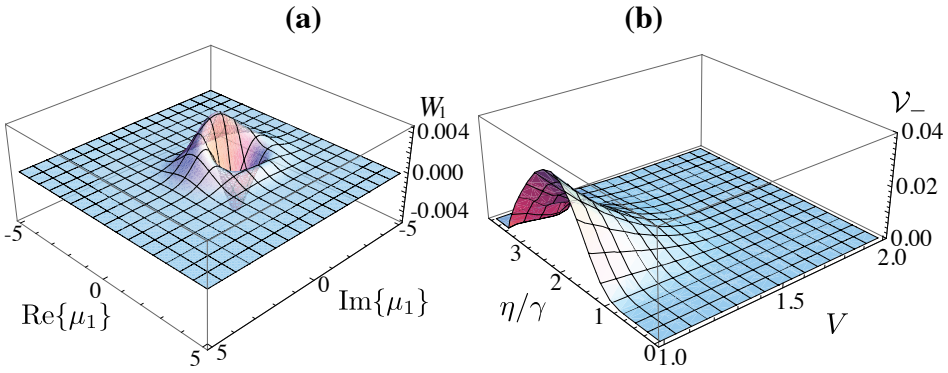

Figure 4.8: Wigner function for a mechanical system open to dissipation. **(a)** Wigner function of a single mirror for μ_2=1+i, η/γ=2, γt=V=1. **(b)** $\mathcal{V}_-$ against V and η/γ for $\gamma t = 1$ (we assume that all the relevant parameter are the same for both mirrors).

when $\eta \sim \gamma$, which means that in the dissipative regime the state of the two mirrors is non-classical. The decrease of $\mathcal{V}_-$ as $\eta/\gamma \gg 1$ shown in Figure 4.8**(b)** is simply due to our choice for the interaction time. By adjusting t, non-zero values of $\mathcal{V}_-$ are retrieved. The interplay between γ, η and t in setting non-classicality in the mechanical state can be best seen by studying non-locality. As shown in Figure 4.9, as η/γ increases for damped mechanical systems at zero-temperature, the interaction-time window has to be set so as to maximize the degree of violation of the CHSH inequality. As expected, the violation increases with the ratio between the coupling constant and the decay rate. However, large values of η/γ correspond to shorter time-windows for the violation to occur. This point can be understood solving explicitly the open-system dynamics corresponding to a low-temperature bath in an alternative way.

In order to do so, we follow the approach used in Chapter 3, which is worth to recall here. We divide the evolution time as t=$N\delta t$, with $\delta t/t \ll 1$ and approximate the dynamics of the total system as a sequence of the unitary dynamics ruled by

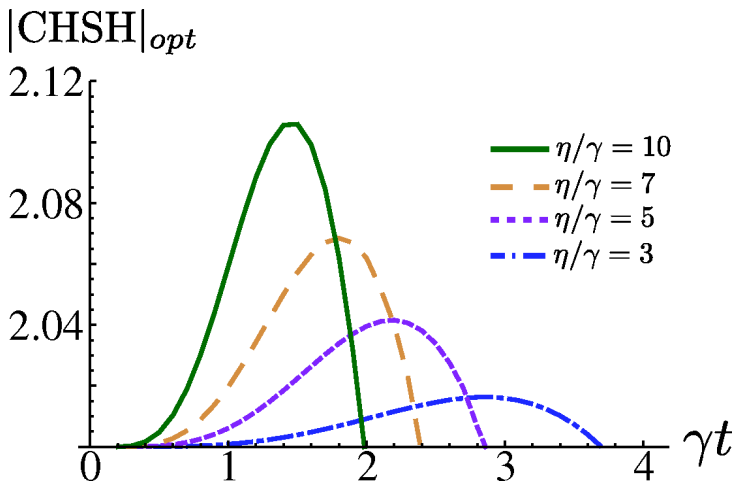

Figure 4.9: Violation of the CHSH inequality as a function of γt for four values of η/γ.

U_t and a purely dissipative one. After N steps, the evolved state reads

$$\rho(N\delta t)=\left(\mathcal{D}^1_{\delta t}\mathcal{D}^2_{\delta t}\mathcal{U}_{\delta t}\right)^N\rho(0), \tag{4.33}$$

where we have introduced the superoperators

$$\begin{aligned}\mathcal{D}^j_{\delta t}\rho&=e^{\mathcal{L}_j^{V=1}\delta t}\rho,\\ \mathcal{U}_{\delta t}\rho&=U_{\delta t}\rho U^\dagger_{\delta t},\end{aligned} \tag{4.34}$$

and where $\rho(0)=|+\rangle\langle+|\otimes|\alpha_1,\alpha_2\rangle\langle\alpha_1,\alpha_2|$ is the initial state. This approach is particularly useful in treating a damped harmonic oscillator. Indeed, the action of the dissipative superoperator $\mathcal{D}^j_{\delta t}$ on the diadic form $|\lambda\rangle\langle\sigma|$ (with $|\lambda\rangle$ and $|\sigma\rangle$ two coherent states) is given by [98]

$$\mathcal{D}^j_t|\lambda\rangle\langle\sigma| = \langle\sigma|\lambda\rangle^{\gamma\delta t}|\lambda e^{-\gamma\delta t}\rangle\langle\sigma e^{-\gamma\delta t}|. \tag{4.35}$$

In the limit $\delta t \to 0$, $N \to \infty$ (so as to keep $t = N\delta t$ finite), we get an accurate description of the dissipation-affected dynamics. Indeed, for the particular system considered here the superoperators $\mathcal{D}_{\delta t}$ and $\mathcal{U}_{\delta t}$ commute when $\delta t \to 0$ and this approach gives the exact dynamics of the system. After the projection on the atomic part of the system, the state of the two mirrors is

$$\begin{aligned}\rho_m(t) =& \frac{1}{2}\big[|\alpha_1(t),\alpha_2(t)\rangle\langle\alpha_1(t),\alpha_2(t)| + \\ &+ |\beta_1(t),\beta_2(t)\rangle\langle\beta_1(t),\beta_2(t)| + \\ &+ e^{-i\vartheta(t)-\Gamma(t)}|\beta_1(t),\beta_2(t)\rangle\langle\alpha_1(t),\alpha_2(t)| + \\ &+ e^{i\vartheta(t)-\Gamma(t)}|\alpha_1(t),\alpha_2(t)\rangle\langle\beta_1(t),\beta_2(t)|\big],\end{aligned} \tag{4.36}$$

where

$$\begin{aligned}&\alpha_j(t) = \alpha_j e^{-\gamma t}, \\ &\beta_j(t) = \alpha_j(t) + (-1)^{j-1} i\eta_j(1-e^{-\gamma t})/\gamma, \\ &\vartheta(t) = \frac{1}{2}\sum_{j=1,2}\frac{\eta_j}{\gamma}\alpha_j(1-e^{-2\gamma t}), \\ &\Gamma(t) = \frac{1}{2}\sum_{j=1,2}\frac{\eta_j^2}{\gamma^2}[\gamma t + \frac{1}{2}(1-e^{-2\gamma t}) - 2(1-e^{-\gamma t})].\end{aligned} \tag{4.37}$$

The analysis of the CHSH inequality using $\rho_m(t)$ leads to features consistent with the solutions gathered through the Fokker-Planck approach and reveals that the decoherence factor $\Gamma(t)$ grows with $(\eta/\gamma)^2$, thus tightening the time-window where violation of the local realistic boundary can be observed.

4.3 Conclusive remarks

Such possibilities for microscopically-induced control of a mesoscopic device will be treated in the next chapter and it will be the topic of further investigations. The second part of our study focus on the quantum correlations shared by two massive objects, bringing our analysis to the boundary between the quantum and the classical world. In such operating conditions, the dissipative part of the dynamics induced by damping processes in the mechanical oscillators plays an important role. It is thus clear that the achievement of the condition $\eta \sim \gamma$ is crucial in our scheme, and a comment about the possibility of reaching this regime is unavoidable. For state-of-the-art mechanical systems, typical values of γ are in the range of a few Hz. For mechanical modes having $\omega_m/(2\pi)$=300KHz and mass ~ 50ng placed to a cavity of 10mm length [129], a straightforward calculation shows that η can indeed be made comparable to γ, thus demonstrating the achievability of the conditions required by our proposal. It is remarkable that the state of the two mechanical systems exhibits non-classical features both for one and two mirrors, in contrast with a purely optomechanical coupling between a movable mirror and a cavity field [75].

Chapter 5

When Casimir meets Kibble-Zurek

When N two-level atoms interact collectively with a single mode of the electromagnetic field inside a cavity, thus realizing the so-called Dicke model [55], a critical value of the atom-photon coupling g_c exists at which the system undergoes a quantum phase transition, generally referred to as the *super-radiant transition*. In this Chapter, we prove that, close to the super-radiant transition, a DCE-like mechanism arises from the use of a time-dependent driving and results in a flux of photons generated from the vacuum fluctuations. DCE has been predicted to occur in QED settings involving a cavity with oscillating end mirror [47]. This scheme, however, appears to be technologically demanding given the prohibitively large frequency at which the mirrors should vibrate to produce a measurable flux of photons. Notwithstanding some interesting proposals [48–50] having the potential to ease the requirements for its observability, an experimental demonstration of DCE is still elusive in the optical domain. Recently, a DCE-like mechanism has been observed in an experiment performed using microwaves [51]. Our proposal pursues a different direction: we observe that, on approaching the Dicke super-

radiant phase transition, the frequencies at which the DCE-like effect becomes observable are lowered, thus narrowing the gap separating the experimental state-of-the-art from the observation of the effect.

Moreover, we unveil an intriguing connection between the occurrence of DCE through the mechanism we propose and the KZM. The latter predicts the formation of defects in a quantum many-body system dragged through a critical point [46, 133, 134] and is due to the inability of the system to remain in its ground state. The production of defects occurs regardless of how slowly the dragging is performed and the mechanism has been shown to be related to adiabatic quantum computation [135] and quantum annealing [136]. We are thus able to bridge two fundamental phenomena in out-of-equilibrium quantum systems with the goal of simplifying their observation. The recent demonstration of the Dicke super-radiant transition [56], which is the building block of our proposal, marks a promising starting point towards an experimental investigation along the lines of our work.

The Chapter is organized as follow: In Section 5.1 we will consider the case in which all the dissipative processes can be neglected and the system undergoes an unitary evolution. In Section 5.2 we will extend our analysis to the case in which the cavity experiences photons losses and we will show that a constant flux of photons is present in the output field of the cavity when the system's parameters are modulated in time. Finally, in Section 5.3 we will link the generation of photons arising from the DCE to the KZM, presenting qualitative and quantitative evidences of the connection between the two phenomena.

5.1 System's Hamiltonian and Unitary Evolution

We study a system consisting of N two level atoms placed inside a cavity in which the splitting between the ground and excited state of each atom can be modulated in time. In this Section, we first review some interesting properties of the system's Hamiltonian in absence of modulation [141] and then we address the case of a time dependent Hamiltonian, solving the unitary dynamics of the system.

5.1.1 Time-Independent Hamiltonian

Let us consider a system formed by N two-level atoms interacting with the fundamental mode of the field inside a cavity (see Figure 5.1). We assume that the splitting between the ground and the excited level of each atom can be externally modulated in time. The fundamental mode of the cavity is described using the annihilation and creation operators a and $a^\dagger$ and each two level atom is treated as a pseudo-spin with angular momentum components $\{\sigma_+^i, \sigma_-^i, \sigma_z^i\}$. Assuming that the atoms interact with the field in a collective way, the whole atomic cloud is described by the total angular momentum J with components $J_\pm = \sum_i \sigma_\pm^i$ and $J_z = \sum_i \sigma_z^i$. Within this notation and setting $\hbar = 1$, the Hamiltonian of the system in absence of modulation and in the dipole approximation reads as

$$H_0 = \omega_a a^\dagger a + \omega_b J_z + \frac{g}{\sqrt{2j}}(a^\dagger + a)(J_+ + J_-), \tag{5.1}$$

where ω_b is the static atomic splitting, which is assumed to be the same for every atom, ω_a is the fundamental frequency of the cavity and g is the atom-field coupling constant. Here j is the so called "cooperation number" in Dicke theory and

is an eigenvalue of J^2.

When the number of atoms N becomes large, Holstein-Primakoff representation of angular momentum [140] can be used to formally assimilate the atomic cloud to an harmonic oscillator. Using this representation, the components of the angular momentum J can be written in terms of bosonic annihilation and creation operators b, $b^\dagger$ as

$$\begin{aligned} J_+ &= b^\dagger \sqrt{2j\left(1 - \frac{b^\dagger b}{2j}\right)}, \\ J_- &= \sqrt{2j\left(1 - \frac{b^\dagger b}{2j}\right)} b, \\ J_z &= (b^\dagger b - j). \end{aligned} \tag{5.2}$$

Since the number of atoms is large and $j \gg 1$, a good approximation for the first two equations is given by $J_+ \approx \sqrt{2j} b^\dagger$, $J_- \approx \sqrt{2j} b$. Substituting these expressions in Equation (5.1) and neglecting the overall shifting term, the Hamiltonian becomes

$$H_0 = \sum_{k=a,b} \omega_k k^\dagger k + g(a^\dagger + a)(b^\dagger + b), \tag{5.3}$$

where $k = \{a, b\}$.

The Hamiltonian in Equation (5.3) describes two harmonic oscillator coupled via an xx interaction with coupling constant g and can be exactly diagonalized. Considering the position and momentum operators for the two modes, $x_k = (1/\sqrt{2\omega_k})(k^\dagger + k)$ and $y_k = i\sqrt{(\omega_k/2)}(k^\dagger - k)$, Equation (5.3) can be rewritten as

$$H_0 = \frac{1}{2} \sum_{k=a,b} (\omega_k^2 x_k^2 + y_k^2) + 4g\sqrt{\omega_a \omega_b} x_a x_b. \tag{5.4}$$

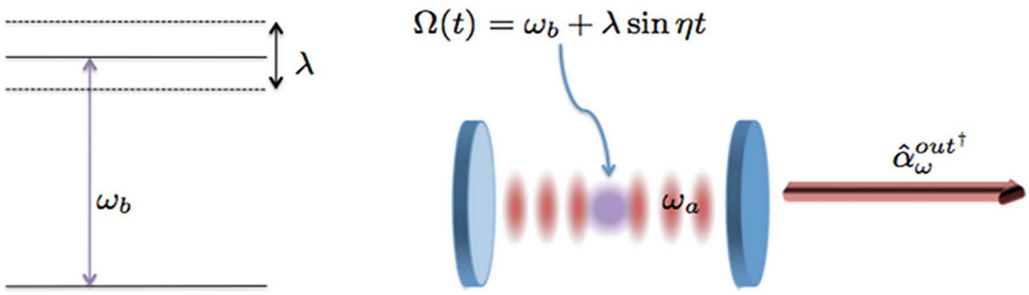

Figure 5.1: Sketch of the system. An atomic cloud consisting of N two level atoms is placed inside a cavity with fundamental frequency ω_a. The static splitting between the ground and the excited state of each atom is ω_b and is modulated in time with amplitude λ and frequency η. The whole atomic cloud is then treated as an harmonic oscillator with time dependent frequency $\Omega(t)$.

The diagonal form is obtained by rotating the coordinate system following the transformations $x_a = q_1 \cos\gamma + q_2 \sin\gamma$ and $x_b = -q_1 \sin\gamma + q_2 \cos\gamma$, where the angle γ is given by

$$\tan 2\gamma = \frac{4g\sqrt{\omega_a \omega_b}}{\omega_b^2 - \omega_a^2}. \tag{5.5}$$

The rotated Hamiltonian (up to an overall shifting) reads as

$$H_0 = \frac{1}{2} \sum_{k=1,2} (\epsilon_k^2 q_k^2 + p_k^2), \tag{5.6}$$

where

$$\begin{aligned} \epsilon_1^2 &= \frac{1}{2}\left(\omega_a^2 + \omega_b^2 - \sqrt{(\omega_b^2 - \omega_a^2)^2 + 16 g^2 \omega_a \omega_b}\right), \\ \epsilon_2^2 &= \frac{1}{2}\left(\omega_a^2 + \omega_b^2 + \sqrt{(\omega_b^2 - \omega_a^2)^2 + 16 g^2 \omega_a \omega_b}\right). \end{aligned} \tag{5.7}$$

Equation (5.6) describes two uncoupled harmonic oscillators with frequencies ϵ_1 and ϵ_2. Introducing the bosonic operators c_k and $c_k^\dagger$ associated with the trans-

formed position and momentum operators q_k and p_k, the Hamiltonian can be also written as

$$H_0 = \epsilon_1 c_1^\dagger c_1 + \epsilon_2 c_2^\dagger c_2. \tag{5.8}$$

The new operators $\{c_1, c_2\}$ are connected with $\{a, b\}$ via Bogoliubov transformations which are given in [141] and reported in Appendix C.1.

It can be noticed from Equation (5.7) that the value of ϵ_1 becomes imaginary when g exceeds the critical value $g_c = \sqrt{\omega_a \omega_b}/2$. That means that the system undergoes different behaviors depending on being in the "normal phase" ($g < g_c$) or in the so called "superraddiant phase" ($g > g_c$), as explained in [141]. Indeed, the existence of this critical value is crucial for the argument we put forth. Since at this stage we are only interested in the normal phase regime, we will not go into the details of the phase transition process. Nevertheless, it is important to point out that the model described above is valid only for $g < g_c$ and that the critical nature of the system plays an important role.

5.1.2 Atomic frequency modulation

We are now ready to address the case in which the atomic splitting is sinusoidally modulated with frequency η and amplitude λ. This is in some sense a generalization of the scheme proposed in [49, 50], where a system consisting of a single two-level atom placed inside a cavity is studied. Let us consider the Hamiltonian given in Equation (5.3) and let us assume that the atomic frequency is no longer ω_b but a time-dependent function on the form $\Omega(t) = \omega_b + \lambda \sin \eta t$ instead. Substituting this expression in Equation (5.3), the time-dependent Hamiltonian of the

system becomes

$$H = \omega_a a^\dagger a + \Omega(t) b^\dagger b + g(a^\dagger + a)(b^\dagger + b). \tag{5.9}$$

The diagonalized Hamiltonian has the same form of the one given in Equation (5.6), with time dependent frequencies $\epsilon_k(t)$ which are obtained simply by substituting ω_b with $\Omega(t)$ in Equation (5.7).

The unitary dynamics of the system can be solved using two different methods. In both cases, we assume that the system is initialized in its ground state, i.e. with all the atoms in the lower energy level and the field in the vacuum state at $t = 0$. The first method consists of solving the Heisenberg equations of motion for the field operators a and $a^\dagger$ and for the atomic cloud bosonic operators b and $b^\dagger$ using the Hamiltonian in Equation (5.9). The Heisenberg equations are given by $\dot{k} = -i[k, H]$ with $k = a, b$. The equations can be recast into an equation for the covariance matrix, which is solved numerically. Alternatively, the problem can be treated in the Schrödinger picture using Lewis-Riesenfeld method [145, 146]. This method gives us a strategy for solving any time dependent problem using the so called dynamical invariants, and it is particularly useful in the case of quadratic Hamiltonians. In this second case, we will make use of the diagonal form of the Hamiltonian in order to make some approximations. In the limit in which the modulation frequency η and the time dependent frequencies $\epsilon_k(t)$ satisfies the conditions

$$\epsilon_2(t) \gg \eta, \qquad \epsilon_2(t) \gg \epsilon_1(t), \tag{5.10}$$

the non-critical mode q_2 will not contribute to the photon production. In the adiabatic approximation we can get rid of the second mode and describe the system

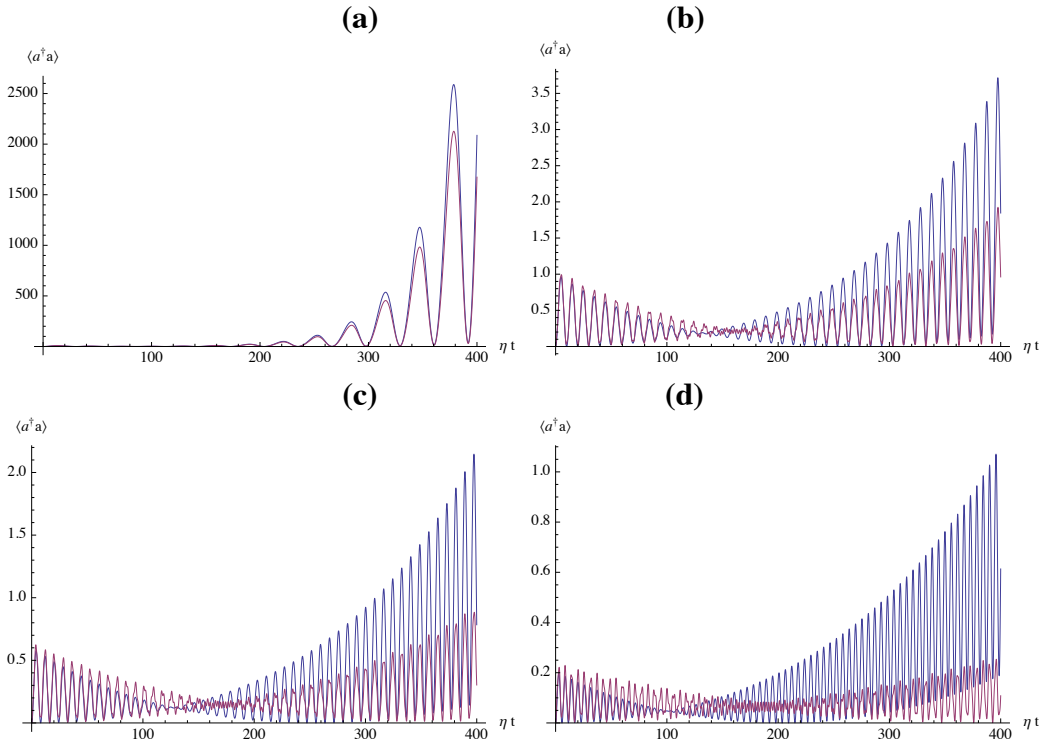

Figure 5.2: Mean number of photons inside a non-leaking cavity against time calculated using the L-R method in the one mode approximation (blue line) and solving the Heisemberg equations of motions for exact the two modes Hamiltonian (red line). The parameters are $\omega_a = \omega_b = 1$, $\eta = 2\epsilon_1$, $\lambda = 0.01$. The values of g are: (a) $g = 0.99g_c = 0.495$, (b) $g = 0.9g_c = 0.45$, (c) $g = 0.85g_c = 0.425$, (d) $g = 0.7g_c = 0.35$.

as a single harmonic oscillator with a time-dependent frequency:

$$H \approx \frac{1}{2}[\epsilon_1^2(t)q^2 + p^2]. \tag{5.11}$$

Comparing the results obtained in the two cases, we can test the validity of the one mode approximation.

The quantity of interest in the DCE context is the mean number of photons $\langle a^\dagger a\rangle$ generated inside the cavity. Figure 5.2 shows the number of photons $\langle a^\dagger a\rangle$

as a function of time for various values of the coupling constant g, calculated using Lewis-Riesenfeld method in the single mode approximation and using the Heisenberg equations for the exact two mode Hamiltonian. It is evident from the plots that a modulation at frequency $\eta = 2\epsilon_1$ results in a generation of photons from vacuum inside the cavity. Moreover, the number of photons generated increases when the coupling constant g approaches its critical value g_c. It can also be noticed from the figure that the two results are very similar when the coupling constant is close to its critical value, e. g. $g = 0.99g_c$, as expected. With the decreasing of g the discrepancy between the two quantity increases. This is due to the fact that the conditions in Equation (5.10) are not fulfilled anymore when g is far away from the critical value g_c and the single mode approximation is not valid any longer. This behavior is conditioned to the choice of the system's parameters. Indeed, g_c is now a time dependent quantity and the system would go through a phase transition if $g_c < g$ at some time t, in which case the model used would fail and the results would not make sense anymore. It is thus important to choose the system's parameters in such a way that the condition $g_c > g$ holds for all t.

Within the single mode approximation and when the modulation amplitude λ is small, a qualitative explanation of the photons' generation mechanism can be given in terms of time-dependent perturbation theory on an unperturbed harmonic oscillator with frequency ϵ_1. Indeed, when $\eta = 2\epsilon_1$, the sinusoidal perturbation produces a resonant coupling between levels that differ in energy by $2\epsilon_1$. This coupling is responsible for the creation of photons inside the cavity. In analogy with usual dynamical Casimir effect and with the single atom schemes proposed in [49, 50], the photons are created in pairs. On the other hand, while in these schemes the modulation frequency is required to be on the order of the photonic

frequency, in our proposal η can be in principle as small as we want, due to the fact that $\epsilon_1 \to 0$ at the phase transition.

The model treated here resembles the many-body Landau-Zener problem studied in References [138, 139], with the crucial difference of the inclusion of the counter-rotating terms in our analysis, which lead *both* to the super-radiant transition and the production of photons. It is also worth to mention that in Reference [137] a model similar to ours but based on a semi-classical approach has been addressed to relate DCE-like effects to Dicke super-radiance. Here we perform a full quantum treatment of both the atom-light interaction and the effects on the photon statistics induced by the driving of the atomic subsystem. Moreover, as discussed in Section 5.3, we will unveil the connection between the DCE-like effects and the Kibble-Zurek mechanism.

5.2 Dissipative Dynamics: Langevin Equations Approach

In the previous Section we have studied the case of a cavity with perfect mirrors and we have shown how is possible to generate photons by modulating the parameters of the system. In this Section, we consider a leaking cavity in which the internal mode experiences photons' losses due to the coupling with the environment. Since we are neglecting atomic decays, the equation of motion for the bosonic operator b describing the atomic cloud is still the Heisemberg equation of motion $\dot{b} = -i[b, H]$. On the other hand, the cavity mode operator a is subjected to dissipative processes , and its open dynamics can be obtained solving the

Langevin equations of the system and making use of the input-output formalism for optical cavities [72]. In this Section we will treat this problem extensively.

5.2.1 Langevin Equations

Solving the dissipative dynamics of the system in presence of counter-rotating terms is a non trivial task and some preliminary remarks are due. To treat the problem, one might be tempted to naively use the Langevin equation for a Markovian process in its common form. This is given by

$$\dot{a} = -i[a, H] - (\gamma/2)a(t) + f(t), \tag{5.12}$$

where γ is the damping rate of the cavity and $f(t)$ is the Langevin force operator which correspond to the stochastic noise function in classical Langevin equation [72]. However, Equation (5.12) gives an appropriate description of the system's evolution only when the rotating wave approximation (RWA) is considered, in which case the dynamics is solved in a rotating frame of reference. When the counter-rotating terms are included, as in the case here at hand, the rotating wave approximation is not valid any longer and it becomes crucial to derive a Langevin equation which describe the correct dissipative dynamics of the system in a non-rotating frame. In order to further clarify this point, let us briefly analyze the derivation of Equation (5.12). To include the interaction with the environment, it is usually assumed that the internal mode of the cavity a is coupled with a bath consisting of a collection of harmonic oscillators with frequencies ν and operators

α_ν. The system-bath coupling Hamiltonian is [72]

$$V = i \int_0^\infty d\nu k_\nu (\alpha_\nu a^\dagger - a\alpha_\nu^\dagger). \tag{5.13}$$

This main assumption is valid regardless of whether the RWA is considered or not. Notice that the negative frequencies of the bath are excluded from the integration, since in any real bath the density of states $\rho(\omega)$ vanishes for $\omega < 0$ and only positive frequencies have a physical meaning [142]. However, when the RWA is considered and the system is studied in a frame of reference rotating at frequency ω_a, the integration limits in Equation (5.13) are shifted by $-\omega_a$ and the integral can be extended to $-\infty$ if ω_a is large. The inclusion of negative frequencies is crucial in the derivation of Equation (5.12). On the other hand, when the counter-rotating terms are included in the Hamiltonian, the system is studied in a non-rotating frame and negative frequencies cannot be included in the integral.

To derive the Langevin equation describing the evolution of the system in the non-rotating frame, we start by assuming a cavity-bath interaction on the form of Equation (5.13). The total Hamiltonian of the system and the bath is then $H_{\mathrm{s+b}} = H + H_{\mathrm{bath}} + V$, where H_{bath} is the free Hamiltonian of the bath given by $H_{\mathrm{bath}} = \sum_\nu \nu \alpha_\nu^\dagger \alpha_\nu$. After some simple steps, the equation of motion for the internal mode of the cavity is written as [72]

$$\dot{a} = -i[a, H] - \int_{-\infty}^{\infty} dt' \gamma(t - t') a(t') + f(t), \tag{5.14}$$

where the damping memory kernel $\gamma(\tau)$ (with $\tau = t - t'$) and the Langevin force

$f(t)$ are given by

$$\begin{aligned}\gamma(\tau) &= \Theta(\tau)\int_0^\infty d\nu |k_\nu|^2 e^{-i\nu\tau},\\ f(t) &= \int_0^\infty d\nu k_\nu e^{-i\nu t}\alpha_\nu^{in}.\end{aligned} \tag{5.15}$$

Here the input and the output field operators are defined in the standard form as $\alpha_\nu^{in} = \lim_{t_0\to-\infty}\alpha_\nu(t_0)e^{-i\nu t_0}$ and $\alpha_\nu^{out} = \lim_{t_1\to\infty}\alpha_\nu(t_1)e^{-i\nu t_1}$, respectively. These operators are linked with the internal mode of the cavity by the relation

$$\alpha_\nu^{out} = \alpha_\nu^{in} - k_\nu^*\tilde{a}(\nu), \tag{5.16}$$

where $\tilde{a}(\omega)$ is the Fourier transform of $a(t)$. The input-output relations in Equation (5.16) link also the power spectrum outside the cavity $\mathcal{S}(\nu)$ with the power spectrum inside $\mathcal{P}(\nu)$. Assuming the input field in the vacuum state we find

$$\mathcal{S}(\nu) = |k_\nu|^2\mathcal{P}(\nu). \tag{5.17}$$

For a generic quadratic two modes Hamiltonian, the equations of motion can be written in a compact matrix notation. Taking into account that the mode b does not experience any dissipation, we define the bosonic operators vector as $u(t) = (a(t), b(t), a^\dagger(t), b^\dagger(t))^T$ and the Langevin forces vector as $F(t) = (f(t), 0, f^\dagger(t), 0)^T$. Within this notation, the equations for the two modes in the domain of time can by rewritten in the form

$$\dot{u}(t) = -iM(t)\cdot u(t) - \int dt'\Gamma(t-t')\cdot u(t') + F(t), \tag{5.18}$$

where $M(t)$ is a time-dependent 4×4 matrix taking into account the unitary evolution and $\Gamma(t-t')$ is the 4×4 matrix of the damping kernels given by $\Gamma(t-t') = \text{diag}[\gamma(t-t'), 0, \gamma(t-t'), 0]$. It is worth to mention that, when $M(t)$ is a periodic function of t with period T, it can be expanded as a Fourier series which in general is given by

$$M(t) = M(t+T) = \sum_{m=-\infty}^{\infty} M_m e^{i\frac{2\pi}{T}mt}. \tag{5.19}$$

Solving Equation (5.18) might be a very hard task due to the presence of a non-trivial convolution integral. The problem can be avoided by moving in the domain of frequencies. Since the Matrix $M(t)$ explicitly depends on time, by moving to the frequencies domain we need to consider all the sidebands contributions coming from the decomposition given in Equation (5.19). Defining $\tilde{u}(\omega) = (\tilde{a}(\omega), \tilde{b}(\omega), \tilde{a}^\dagger(-\omega), \tilde{b}^\dagger(-\omega))^T$ and $\tilde{F}(\omega) = (\tilde{f}(\omega), 0, \tilde{f}^\dagger(-\omega), 0)^T$ as the Fourier transform of the vectors $u(t)$ and $F(t)$ introduced above, the Langevin equations in the domain of frequencies read as [143]

$$i\mathcal{M}(\omega) \cdot \begin{pmatrix} \tilde{u}(\omega - m\eta) \\ \vdots \\ \tilde{u}(\omega) \\ \vdots \\ \tilde{u}(\omega + m\eta) \end{pmatrix} = \begin{pmatrix} \tilde{F}(\omega - m\eta) \\ \vdots \\ \tilde{F}(\omega) \\ \vdots \\ \tilde{F}(\omega + m\eta) \end{pmatrix}, \tag{5.20}$$

where the matrix $\mathcal{M}(\omega)$ is given by

$$\mathcal{M}(\omega) = \begin{pmatrix} B_{-m} & M_1 & M_2 & \dots & M_{2m} \\ M_{-1} & B_{-(m-1)} & M_1 & & \vdots \\ M_{-2} & M_{-1} & B_{-(m-2)} & & \\ \vdots & & & & M_1 \\ M_{-2m} & \dots & & M_{-1} & B_m \end{pmatrix}, \tag{5.21}$$

and where $B_j = M_0 - (\omega + j\eta) - i\tilde{\Gamma}(\omega + j\eta)$. Here $\tilde{\Gamma}(\omega) = \text{diag}[\tilde{\gamma}(\omega), 0, \tilde{\gamma}(-\omega), 0]$ is the Fourier transform of the damping memory kernel and $\eta = 2\pi/T$. The Langevin force operators $\tilde{f}(\omega)$ in the domain of frequencies are linked to the input operators of the cavity by [142]

$$\tilde{f}(\omega) = 2\pi k_\omega \rho(\omega) \alpha_\omega^{in}, \tag{5.22}$$

where $\rho(\omega)$ represents the photonic density of states of the bath. On the other hand, following [142] again, the dacay rates can be written in the domain of frequencies as $\tilde{\gamma}(\omega) = \text{Re}[\tilde{\gamma}(\omega)] + i\text{Im}[\tilde{\gamma}(\omega)]$, where

$$\begin{aligned} \text{Re}[\tilde{\gamma}(\omega)] &= \pi |k_\omega|^2 \rho(\omega), \\ \text{Im}[\tilde{\gamma}(\omega)] &= -\frac{1}{\pi} \text{P} \int_{-\infty}^{\infty} d\omega' \frac{\text{Re}[\tilde{\gamma}(\omega')]}{\omega' - \omega}, \end{aligned} \tag{5.23}$$

and where P denotes the principal value of the integral.

While the imaginary part of $\tilde{\gamma}(\omega)$ is just a fixed Lamb shift, the real part $\text{Re}[\tilde{\gamma}(\omega)]$ is responsible for the frequency-depending damping of the cavity mode. As mentioned above, when the counterrotating terms are taken into account it be-

comes crucial to consider that the density of photonic state in the bath $\rho(\omega)$ is zero for negative frequencies. It follows immediately from Equations (5.22) and (5.23) that $\tilde{\gamma}(\omega) = 0$ and $\tilde{f}(\omega) = 0$ for $\omega < 0$. In the following, we will also suppose that the damping rate assumes the same value for every positive frequency. This is equivalent to assuming that $k_\omega = k \ \forall\omega$ and $\rho(\omega) = 1$ for $\omega > 0$. Within this assumption, we define $\gamma_0 \equiv \pi|k|^2$ and we can write Re$[\tilde{\gamma}(\omega)] = \gamma_0$ for $\omega > 0$ and Re$[\tilde{\gamma}(\omega)] = 0$ for $\omega < 0$.

5.2.2 Solution of Langevin Equations and Photons Generation

For the Hamiltonian considered here, the matrix $M(t)$ includes a sinusoidal modulation with period $T = (2\pi)/\eta$. Recalling Equation (5.19), its Fourier expansion is thus given by $M(t) = M_0 + M_1(e^{i\eta t} - e^{-i\eta t})$, where

$$M_0 = \begin{pmatrix} \omega_a & g & 0 & g \\ g & \omega_b & g & 0 \\ 0 & -g & -\omega_a & -g \\ -g & 0 & -g & -\omega_b \end{pmatrix}; \quad M_1 = \begin{pmatrix} 0 & 0 & 0 & 0 \\ 0 & \lambda & 0 & 0 \\ 0 & 0 & 0 & 0 \\ 0 & 0 & 0 & \lambda \end{pmatrix}. \tag{5.24}$$

So the Fourier expansion of $M(t)$ counts just the three components M_0, M_1 and $M_{-1} = -M_1$. Substituting M_0 and $M_{\pm 1}$, Equation (5.20) can be solved to the m-th order simply by inverting the Matrix $i\mathcal{M}$. We are interested on the solution of Equation (5.20) for the cavity operator $\tilde{a}(\omega)$. Calling $\mathcal{G}(\omega) = [i\mathcal{M}(\omega)]^{-1}$, this

is given by

$$\begin{aligned}\tilde{a}_{(m)}(\omega) = \sum_{j=-m}^{m} & \mathcal{G}_{4m+1,4(m+j)+1}(\omega)\tilde{f}(\omega + j\eta) \\ & + \mathcal{G}_{4m+1,4(m+j)+3}(\omega)\tilde{f}^{\dagger}(-\omega - j\eta),\end{aligned} \tag{5.25}$$

where the index (m) indicates the number of sidebands taken into account and $\mathcal{G}_{i,j}(\omega)$ are the matrix elements of $\mathcal{G}(\omega)$.

We start our analysis by calculating the mean number of photons inside the cavity at the stationary state $\langle a^{\dagger}a\rangle$, which is given by $\langle a^{\dagger}a\rangle = \lim_{t\to\infty}\langle a^{\dagger}(t)a(t)\rangle$. After Fourier Transformation, the limit gives

$$\langle a^{\dagger}a\rangle = \frac{1}{(2\pi)^2}\int_{-\infty}^{\infty} d\omega\langle\tilde{a}^{\dagger}(\omega)\tilde{a}(\omega)\rangle. \tag{5.26}$$

Substituting Equation (5.25) into Equation (5.26) and using the expression linking $\tilde{f}(\omega)$ and α_{ω}^{in} given in Equation (5.22), the mean number of photons inside the cavity at the steady state is given by

$$\begin{aligned}\langle a^{\dagger}a\rangle_{(m)} = & \frac{\gamma_0}{\pi}\sum_{j=-m}^{m}\int_{-\infty}^{\infty} d\omega\rho(-\omega - j\eta)] \\ & \times|\mathcal{G}_{4m+1,4(m+j)+3}(\omega)|^2.\end{aligned} \tag{5.27}$$

Here we have assumed that the input field is in the vacuum state, so the operators α_{ω}^{in} fulfill the condition $\langle\alpha_{\omega}^{in}\alpha_{\omega'}^{in^{\dagger}}\rangle = \delta(\omega - \omega')$. Assuming the damping rate to be the same for every positive frequency, i.e. $\gamma_0 = \pi|k|^2$, and making use of the fact that the state's density function is given by $\rho(\omega) = 1$ for $\omega > 0$ and $\rho(\omega) = 0$ for

$\omega < 0$, Equation (5.27) can be rewritten as

$$\langle a^\dagger a \rangle_{(m)} = \frac{\gamma_0}{\pi} \sum_{j=-m}^{m} \int_{j\eta}^{\infty} d\omega |\mathcal{G}_{4m+1,4(m+j)+3}(-\omega)|^2. \tag{5.28}$$

Let us now consider the explicit calculation of the mean number of photons inside the cavity in two simple cases. The first example is the case in which $m = 0$, i.e. no time-dependent modulation is applied to the system (see [142] for more details). In this case Equation (5.27) simply reduces to

$$\langle a^\dagger a \rangle_{(0)} = \frac{\gamma_0}{\pi} \int_{0}^{\infty} d\omega |\mathcal{G}_{1,3}(-\omega)|^2. \tag{5.29}$$

The behavior of the number of photons $\langle a^\dagger a \rangle_{(0)}$ against the interaction constant g for various values of the decay rate γ is shown in the main panel of Figure 5.3. It is important to point out that the non-vanishing mean number of photons is related to the presence of virtual photons which are trapped inside the cavity and can not be observed. Indeed, due to energy conservation law, it is impossible for the photons to leave the cavity and be detected when the Hamiltonian of the system is time-independent and the input field is in the vacuum state. We will see shortly that the number of photons leaking out of the cavity is identically zero when no-modulation is applied.

Another simple example is given by considering a weak modulation, in which case we can assume that only the first two sidebands give a significant contribution and we truncate the summation in Equation (5.27) at $m = 1$. The number of

photons is then given by

$$\begin{aligned}\langle a^\dagger a\rangle_{(1)} =&\frac{\gamma_0}{\pi}\int_{-\eta}^{\infty} d\omega|\mathcal{G}_{5,3}(-\omega)|^2+\frac{\gamma}{\pi}\int_{0}^{\infty} d\omega|\mathcal{G}_{5,7}(-\omega)|^2+\\ &+\frac{\gamma}{\pi}\int_{\eta}^{\infty} d\omega|\mathcal{G}_{5,11}(-\omega)|^2].\end{aligned} \tag{5.30}$$

The quantity $\langle a^\dagger a\rangle_{(1)}$ is shown in the inner panel of Figure 5.3 as a function of the modulating frequency η. The plot shows a sharp resonance peak at $\eta = 2\epsilon_1$, as expected from the previous analysis in the unitary regime, with the difference that in a leaking cavity the system reaches a stationary state when the photons' creation rate equals the cavity damping rate. However, the number of photons inside the cavity can not be observed, since only the flux of photons leaking out of the cavity is a measurable quantity. We now pass to the explicit calculation of this quantity for the two cases treated above.

To obtain the output operator of the cavity α_ω^{out}, we substitute the solution for the internal operator $\tilde{a}(\omega)$ given by Equation (5.25) into the input-output relation in Equation (5.16). Doing so and using Equation (5.22), the output operator reads as

$$\begin{aligned}\alpha_\omega^{out} =&\alpha_\omega^{in}-2\gamma_0\sum_{j=-m}^{m}\mathcal{G}_{4m+1,4(m+j)+1}(\omega)\rho(\omega+j\eta)\alpha_{\omega+j\eta}^{in}+\\ &+2\gamma_0\sum_{j=-m}^{m}\mathcal{G}_{4m+1,4(m+j)+3}(\omega)\rho(-\omega-j\eta)\alpha_{-\omega-j\eta}^{in^\dagger}.\end{aligned} \tag{5.31}$$

In analogy with Equation (5.26), the photonic flux outside the cavity is given by $\langle\alpha^\dagger\alpha\rangle = \int_0^\infty d\omega\langle\alpha_\omega^{out^\dagger}\alpha_\omega^{out}\rangle$, with the crucial difference that only positive frequencies of the bath are included in the integration. Substituting Equation (5.31) and

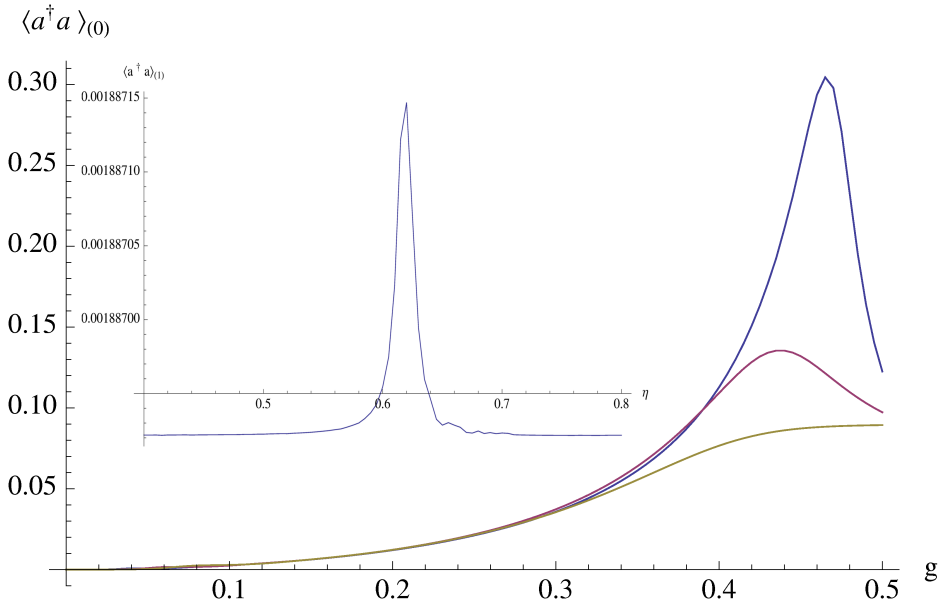

Figure 5.3: (Main panel) mean number of photons inside a leaking cavity against the interaction constant g in the case of no-modulation for $\gamma_0 = 0.1$ (blue line), $\gamma_0 = 0.2$ (red line) and $\gamma_0 = 0.3$ (yellow line). (Inner panel) mean number of photons inside a leaking cavity against the modulation frequency η for $\lambda = 0.00005$ and $\gamma_0 = 0.005$ and $g = 0.45 = 0.9 g_c$.

assuming a vanishing input field such that $\langle \alpha^{in}_{\omega} \alpha^{in^\dagger}_{\omega'} \rangle = \delta(\omega - \omega')$, $\langle \alpha^\dagger \alpha \rangle$ reads as

$$\langle \alpha^\dagger \alpha \rangle_{(m)} = 4\gamma_0^2 \sum_{j=-m}^{m} \int_0^\infty d\omega \Big(|\mathcal{G}_{4m+1,4(m+j)+3}(\omega)|^2 \times \times \rho(-\omega - j\eta) \Big). \tag{5.32}$$

Under the assumptions $\rho(\omega) = 0$ for $\omega < 0$ and $\rho(\omega) = \gamma_0$ for $\omega > 0$, Equation (5.32) can be rewritten as

$$\langle \alpha^\dagger \alpha \rangle_{(m)} = 4\gamma_0^2 \sum_{j=0}^{m} \int_0^{j\eta} d\omega |\mathcal{G}_{4m+1,4(m-j)+3}(\omega)|^2. \tag{5.33}$$

Notice that, having the matrix elements of $\mathcal{G}$ the dimension of time, the quantity

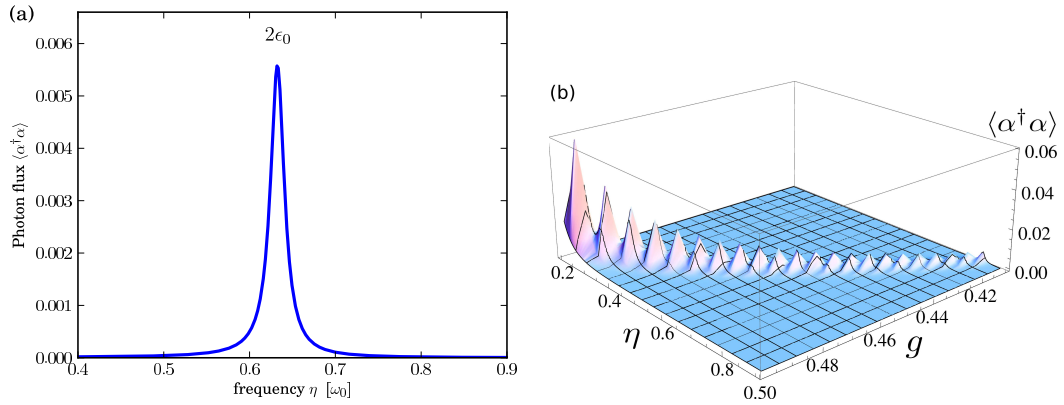

Figure 5.4: Radiation flux outside the cavity. (a) Flux of photons outside the cavity against η for $\omega_a = \omega_b = 1$, $g = 0.9g_c = 0.45$, $\gamma/\omega_a = 0.005$, and $\lambda/\omega_a = 0.005$. For these parameters, $\epsilon_0/\omega_a \approx 0.315$. (b) Flux of photons outside the cavity against η and g for $\omega_b/\omega_a = 1, \gamma/\omega_a = 0.005$ and $\lambda/\omega_a = 0.005$.

$\langle\alpha^\dagger\alpha\rangle$ has the correct dimension of $1/t$ for a flux of photons.

It can be seen immediately from Equation (5.33) that, as expected and according to energy conservation law, no photons' flux outside the cavity is observed when $m = 0$, i.e. when no modulation is applied and the Hamiltonian is time-independent. On the contrary, any time-dependent modulation generates a constant flux of photons. Considering again a small modulation and truncating the sum at $m = 1$, Equation (5.33) counts just one term given by

$$\langle\alpha^\dagger\alpha\rangle_{(1)} = 2\gamma_0^2 \int_0^\eta d\omega |\mathcal{G}_{5,3}(\omega)|^2. \tag{5.34}$$

The flux of photons $\langle\alpha^\dagger\alpha\rangle_{(1)}$ is plotted against the modulation frequency η and the coupling constant g in Figure 5.4. In panel (a) a resonance peak is clearly visible at $\eta \approx 0.63$ when $g = 0.9g_c = 0.45$. For this value of g, the value of smallest eigenvalue ϵ_1 given in Equation (5.7) is $\epsilon_1 \approx 0.315$. So, as expected, the resonance occurs at $\eta \approx 2\epsilon_1$. This profile is the same as the one relative to

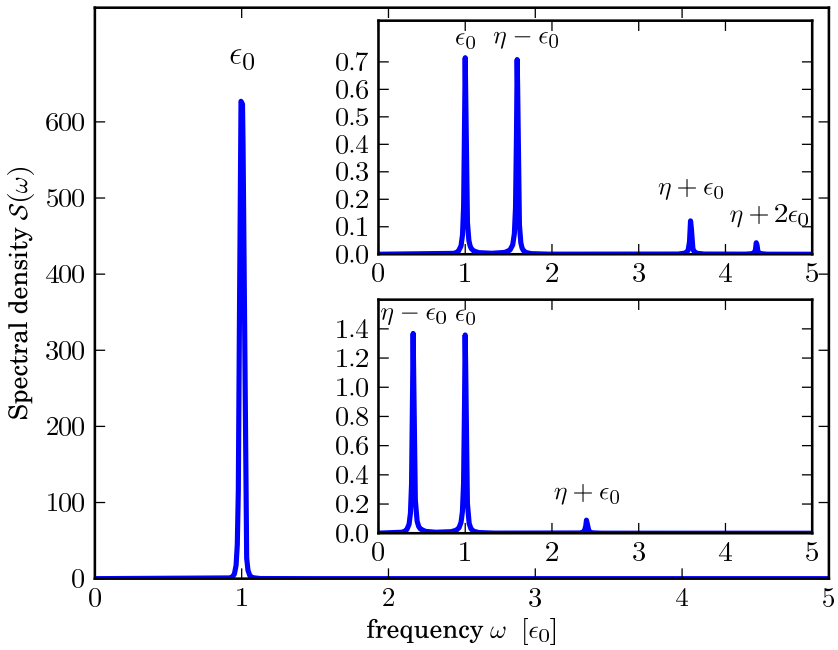

Figure 5.5: Spectral density of the output photons. Taking $\omega_a = \omega_b = 1$, $\lambda = 0.005$, $\gamma = 0.005$, $g = 0.9g_c = 0.45$, we find $\epsilon_0 = 0.315$. We have taken $\eta/2\epsilon_0 = 1$ (corresponding to resonance conditions, main panel), $\eta/2\epsilon_0 = 0.7$ (upper inset), $\eta/2\epsilon_0 = 1.3$ (lower inset).

the photons' flux inside the cavity shown in Figure 5.3. In panel (b), the flux of photons is plotted against g and η. It can be seen that the resonance occurs at $\eta \approx 2\epsilon_1$ regardless the value of ϵ_1. Moreover, the photons' flux at the resonance increases when g approaches its critical value g_c. It is thus evident that bringing the system close to its critical point presents the double advantage of reducing the frequency at which the DCE is observable and increasing the number of photons generated in the process.

In the last part of this Section, we analyze the spectral density $\mathcal{S}(\omega)$ of the output flux of photons, which is linked to the spectral density inside the cavity $\mathcal{P}(\omega)$ via Equation (5.17). To find $\mathcal{P}(\omega)$, we consider the autocorrelation function for the number of photons inside the cavity at the stationary state (i.e. for $t \to \infty$),

which is defined as $F(\tau) = \lim_{t\to\infty}\langle a^\dagger(t+\tau)a(t)\rangle$ [148]. Substituting the Fourier transform of $a(t)$ and $a^\dagger(t)$, the equation above becomes

$$F(\tau) = \int_{-\infty}^{\infty} d\omega \langle a^\dagger(\omega)a(\omega)\rangle e^{-i\omega\tau}. \tag{5.35}$$

Being the spectral density $\mathcal{P}(\omega)$ defined as the Fourier transform of the auto-correlation function, it follows immediately from Equation (5.35) that $\mathcal{P}(\omega) = \langle a^\dagger(\omega)a(\omega)\rangle$. After substituting Equation (5.25), $\mathcal{P}(\omega)$ reads as

$$\mathcal{P}(\omega) = 4\pi\gamma_0 \sum_{j=-m}^{m} |\mathcal{G}_{4m+1,4(m+j)+3}(-\omega - j\eta)|^2 \rho(-\omega - j\eta). \tag{5.36}$$

Using now Equation (5.17) and considering that $\pi|k_\omega|^2 = \gamma_0$, the spectral density of the output flux of photons can be immediately written as $\mathcal{S}(\omega) = (\gamma_0/\pi)\mathcal{P}(\omega)$. In the case of a weak modulation where only the first two sidebands are taken into account and $m = 1$, $\mathcal{S}(\omega)$ is non-vanishing only for $0 < \omega < \eta$ and it can be written as

$$\mathcal{S}(\omega) = 4\gamma_0^2 |\mathcal{G}_{5,3}(-\omega + \eta)|^2. \tag{5.37}$$

The spectral density outside the cavity $\mathcal{S}(\omega)$ for a weak modulation is plotted in Figure 5.5 for various values of the modulation frequency η. When $\eta = \eta_{\rm res} = 2\epsilon_1$, the spectrum reveals a single sharp peak at $\omega \approx \epsilon_1$ (main panel). In the non resonant regime, the emission at $\omega \approx \epsilon_1$ is drastically reduced and others sidebands emission lines appear (inner panels).

5.3 Connection with KZM

Finally, we address the crucial connection between our DCE-like mechanism and the Kibble-Zurek one [44,45]. In this Section, we only consider the single mode approximation, and we thus drop the index and set $\epsilon_1(t) \equiv \epsilon(t)$ to simplify the notation. On approaching the critical point of the model in Equation (5.1), regardless of the value of η, there will always be a regime where the perturbation is non-adiabatic and photons are produced. A first estimate of the unavoidable departure from adiabaticity, with a consequent photon-flux, is obtained by calculating the probability of the system to go into an excited state. For simplicity, we consider one period in the absence of damping. The probability of leaving the ground state at the final time t_f (t_i being the initial time) is

$$P{=}1{-}|\langle\Psi(t_f)|\varphi_0(t_f)\rangle|^2, \tag{5.38}$$

with $|\varphi_n(t)\rangle$ the instantaneous eigenstates of the harmonic oscillator and $|\Psi(t_f)\rangle$ the final state of the system.

The KZM relies on the assumption that the state of a system brought close enough to the critical point *freezes* when the system is not able to adiabatically follow the changes in the control parameter (see Chapter 2). For the driving here at hand, the freeze-out times is found by solving the equation

$$\mathcal{T}(t)/\dot{\mathcal{T}}(t) = \tau(t), \tag{5.39}$$

where $\mathcal{T}(t) = g_c(t)/g - 1$ plays the role of the relative temperature of the system

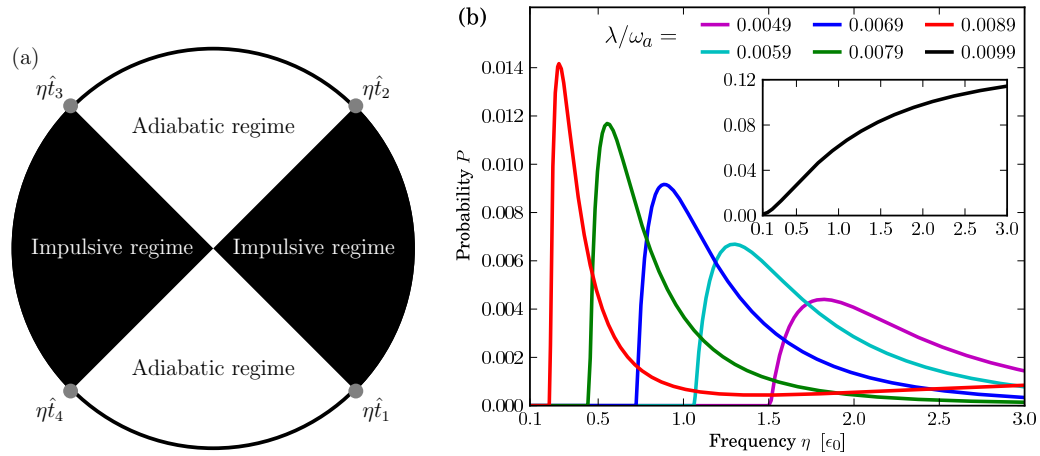

Figure 5.6: (a) Schematic representation of the four freeze-out points in the trigonometric circle. (b) Probability of leaving the ground state against η/ϵ_0 for $g = 0.49/\omega_a$ and various values of λ.

and $\tau = \tau_0/\epsilon(t)$ is its relaxation time ($\tau_0 = 1/\omega$)[1]. For a sinusoidal modulation of $\mathcal{T}(t)$ and if the oscillating terms brings the system sufficiently close to the critical point, one finds four solutions, each embodying a freeze-out time. Figure 5.6 (a) shows their representations in the unit circle. As the system is initialized in its ground state, i.e. $|\Psi(t_i)\rangle = |\varphi_0(t_i)\rangle$, the adiabatic condition $\mathcal{T}(t)/\dot{\mathcal{T}}(t) > \tau$ is satisfied until $t = \hat{t}_1$, where $\hat{t}_1$ is the freeze-out time at which the system enters the so-called impulsive regime. During this period, the state of the system is frozen until $t = \hat{t}_2$, when the adiabatic condition is fulfilled again and the state of the system becomes

$$|\Psi(\hat{t}_2)\rangle = |\varphi_0(\hat{t}_1)\rangle = \sum_n c_{n,0}(\hat{t}_2, \hat{t}_1)|\varphi_n(\hat{t}_2)\rangle, \tag{5.40}$$

where $c_{n,m}(t, t') = \langle\varphi_n(t)|\varphi_m(t')\rangle$. The same argument applies to the second part of the cycle, where the system evolves adiabatically for $t \in [\hat{t}_2, \hat{t}_3]$ and is frozen

[1] Notice that $\mathcal{T}(t)$ is defined as $\mathcal{T}(t) = 1 - g(t)/g_c$ if the time-dependent parameter is g instead of ω.

for $t \in [\hat{t}_3, \hat{t}_4]$. The state at $\hat{t}_4$ is then

$$|\Psi(\hat{t}_4)\rangle = \sum_{k,n} c_{k,n}(\hat{t}_4, \hat{t}_3) c_{n,0}(\hat{t}_2, \hat{t}_1) e^{-i\theta_n} |\varphi_k(\hat{t}_4)\rangle, \tag{5.41}$$

where $\theta_n = \int_{\hat{t}_2}^{\hat{t}_3} dt E_n(t)$. Finally, the last part of the evolution ($t \in [\hat{t}_4, t_f]$) will not affect the probability P, which is thus given by

$$P = 1 - |\langle \Psi(\hat{t}_4) | \varphi_0(\hat{t}_4) \rangle|^2. \tag{5.42}$$

The behavior of the probability P against η is shown in Figure 5.6 (b) for different values of λ. Clearly, the closer the system to the quantum phase transition, the more it is susceptible to a low-frequency driving. A more detailed analysis requires the study of the transient dynamics. The scheme of Figure 5.6 (a) is still valid, the probablity of excitations being calculated by composing four different dissipative maps in the same spirit of Reference [144]. We only expect quantitative changes.

To corroborate the connection between DCE and KZM, we have further analyzed the photon production in the adiabatic and non-adiabatic regimes (cf. Figure 5.7). For $\eta > \epsilon_{\min}$ (being $\epsilon_{\min}$ the minimum value of $\epsilon(t)$ over a cycle), the dynamics is non-adiabatic and photons can be created. Close to criticality, the minimum of the gap vanishes, the system is always in the non-adiabatic regime and the photon-flux increases linearly with η until the maximum value at resonance is reached. Far from the transition, the photon production decreases from the resonance with a Lorentzian behavior: when $\eta < \epsilon_{\min}$, the photon-flux is sharply reduced and a linear behavior is recovered but with a much smaller value. This

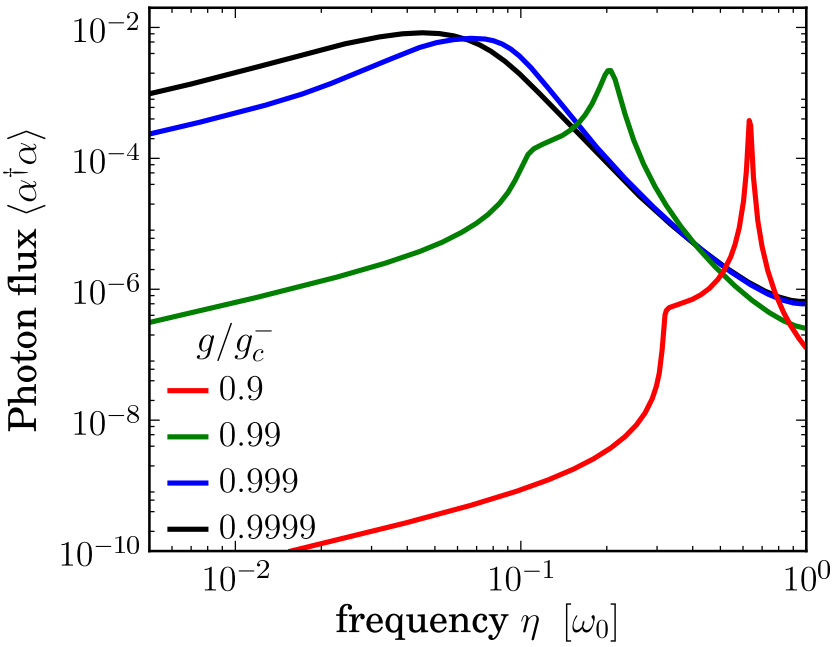

Figure 5.7: Output photon-flux as a function of η for different values of g. The transition between adiabatic and non-adiabatic regime (sharp step) is located at the minimum of the gap and is shifted to lower frequency when the coupling gets closer to the critical coupling. At the critical point the dynamics is purely non-adiabatic.

abrupt transition between the adiabatic and non-adiabatic regimes demonstrates that the breakdown of adiabaticity due to critical slowing-down is at the origin of photon creation in the DCE, a situation totally analogous to what is described by the KZM.

5.4 Conclusive remarks

Some comments are due regarding the observation of the photons' flux outside the cavity. Due to the small frequency of the photons generated when g approaches the critical value (the emission frequency is at $\omega \approx \epsilon_1$), the thermal noise in the output signal may be significant and the detection process may become a very de-

manding task. This problem can be avoided by considering a cavity in which the two mirrors are both semi-transparent and photons are allowed to come in and leak out of the cavity from both sides. Being the thermal baths in the two output fields completely uncorrelated, the noise signal can be virtually eliminated by measuring the correlations between the two output modes. Indeed, the study of such correlations can be regarded as a more general subject for further investigations.

Conclusions

In this thesis, we have explored different aspects of quantum mechanics in the context of mesoscopic open systems and critical systems subjected to time-dependent external driving. We have shown that such systems display highly non-trivial behaviours, which make them perfect candidates for the investigation of the quantum-to-classical transition. In particular, we have proven that genuine quantum features such as non-locality, negative values of the Wigner function and geometric phases can survive to adverse environmental condition such as strong dissipation and high temperatures; surprisingly, our study also demonstrates that, under some particular circumstances, the interaction with the environment itself can generate quantum phenomena otherwise absent. Moreover, we have also proposed a novel strategy for the experimental verification of dynamical Casimir effect in the optical range, revealing the connection of this phenomenon with the Kibble-Zurek mechanism.

In the first part of this thesis, a mediated coupling mechanism between a microscopic and a mesoscopic system in two different setups involving optical cavities with movable mirrors interacting with a three level atom is treated. The resulting dynamics drives the system into states which exhibit strong quantum features in both cases considered. The study of the first setup, involving a single me-

chanical oscillator, reveals strong non-local correlations between the atom and the movable mirror. Considerable violations of Bell-CHSH inequality are observed even when the thermal nature of the mirror's initial state is taken into account. Moreover, projective measurements over the atomic system probabilistically create nonclassical mixed states of the mirror. Such non-classicality, quantified by the negativity of the Wigner function, is robust against mechanical damping, while the dynamical mechanism we used ensures a good protection from other sources of noise. Moreover, a cavity where both mirrors oscillate around their equilibrium positions is considered. The conditional dynamics obtain by a post-selection process on the microscopic part of the system induces truly mesoscopic quantum correlations between the two mirrors which lead again to a violation of CHSH inequality at finite temperature. In analogy with the one-mirror setup, negative values of the Wigner function are found in the dissipative regime.

On the other hand, we also have shown how the qubit-oscillator coupling mechanism can be exploited to generate and detect a geometric phase of the harmonic oscillator. Such model can indeed be seen as an "inverse" Von Neumann measurement scheme, where the qubit is used as a interferometer to measure the phase attached to the oscillator. We show that the conditional displacement in phase space induced by the qubit-oscillator interaction is indeed responsible for the generation of a geometric phase, which is robust against dissipation and temperature. Moreover, the dissipative term arising from the interaction of the system with the environment can itself induce a geometric phase in particular conditions.

Our analysis demonstrates the broad validity of our arguments, both at the single and two-mirror level. We stress the full generality of our method. Although we have illustrated our model in the context of opto-mechanical setups, the same

sort of quantum-correlated state can be engineered in settings consisting of two nano-mechanical resonators capacitively coupled to a Cooper-pair box or two planar superconducting resonators mutually connected via an off-resonant phase or transmon qubit [130–132].

In the second part of the thesis, we consider a scheme to realize the DCE by exploiting the dragging of a driven quantum Dicke model across its critical point. By modeling the atom-field interaction as a linear coupling between two harmonic oscillators, we have made use of the peculiar features of a critical system close to a quantum phase transition to simplify the observation of DCE in the optical frequencies range. In particular, the reduction of the energy gap between the ground and the first excited state has been exploited in order to bring the modulation frequency at which the DCE is observable to the level of experimental feasibility. Moreover, by investigating the transition between the adiabatic and the non-adiabatic regime we have been able to link the photons production arising from the DCE to another fundamental phenomenon in condensed matter systems, the KZM. Indeed, the connection between DCE and KZM, which is supported by qualitative and quantitative evidences in this work, emphasizes how both phenomena can be seen as a consequence of the inability of the system to adiabatically follow the parameters' changes.

We would like to emphasize the novelty and generality of our proposal. Differently from previous works, we address the problems involved in the experimental observation of DCE in the optical regime by exploiting the peculiarities of a critical system, using a full quantum approach and including dissipative processes in our model. Moreover, at the best of our knowledge, no connection have been previously established between three fundamental phenomena like quantum phase

transitions, DCE and KZM. Such a connection represents a crucial result of this work. Although we have explicitly considered a system formed by atoms trapped inside a cavity where the atomic energy splitting is modulated in time, our scheme can be applied to any system in which the Dicke model can be implemented and some parameter can be modulated in time. This last remark suggests a prompt realization of our proposal on the light of the recent experimental achievement of the Dicke phase transition [56] in intra-cavity condensates coupled with the cavity field.

The exploration of the limits of quantum mechanics carried on in this thesis has the potential to trigger novel challenges from the experimental and technological prospective and gives rise to intriguing theoretical questions. Our study of open mesoscopic systems suggests that the rules of quantum mechanics can be extended to parameters regions that are commonly depicted as part of the classical world. In this sense, our results represent a step forward to the frontiers of quantum mechanics and to the understanding of the necessary conditions for the observation of quantum behaviours. Alongside with the fundamental question raised above, our work might have a major impact in the developing of new technologies as well. Indeed, a better understanding of physical phenomena occurring at the transition between the quantum and classical world may improve considerably our ability of design, construct and control miniaturized devices, potentially leading to new exciting discoveries in different scientific fields.

We hope that the results of our study will stimulate new ideas and debates in the physics community, and that it will trigger experimental endeavors directed towards the achievement of the working conditions discussed here.

Appendices

Appendix A

A.1 From sums to integrals

In this appendix, we describe the details of the calculation employed in the derivation of Equation (3.13) in Chapter 3. We want to obtain the state at time $t = N\delta t$. We calculate the density matrix after the first step δt, $\rho(\delta t) = \hat{\mathcal{D}}_{\delta t}\hat{\mathcal{U}}_{\delta t}\rho_0$. We first calculate

$$\begin{aligned}\hat{\mathcal{U}}_{\delta t}\rho_0 =&\frac{1}{2}\Big(|1,\alpha\rangle\langle 1,\alpha| + e^{-i\theta_1}|0,\alpha - i\eta\delta t\rangle\langle 1,\alpha| + \\ &+e^{i\theta_1}|1,\alpha\rangle\langle 0,\alpha - i\eta\delta t| + |0,\alpha - i\eta\delta t\rangle\langle 0,\alpha - i\eta\delta t|\Big).\end{aligned} \tag{A.1}$$

Applying $\hat{\mathcal{D}}_t$ to expression (A.1) and using equation (3.12) we obtain

$$\begin{aligned}\rho(\delta t) =&\frac{1}{2}\Big(|1,\alpha e^{-\gamma\delta t}\rangle\langle 1,\alpha e^{-\gamma\delta t}| + \\ &+e^{-i(\theta_1+\theta_1')}e^{\Gamma_1}|0,\alpha e^{-\gamma\delta t} - i\eta\delta t e^{-\gamma\delta t}\rangle\langle 1,\alpha e^{-\gamma\delta t}| + \\ &+e^{i(\theta_1+\theta_1')}e^{\Gamma_1}|1,\alpha e^{-\gamma\delta t}\rangle\langle 0,\alpha e^{-\gamma\delta t} - i\eta\delta t e^{-\gamma\delta t}| + \\ &+|0,\alpha e^{-\gamma\delta t} - i\eta\delta t e^{-\gamma\delta t}\rangle\langle 0,\alpha e^{-\gamma\delta t} - i\eta\delta t e^{-\gamma\delta t}|\Big),\end{aligned} \tag{A.2}$$

where $\theta_1 = \eta\alpha\delta t$, $\theta'_1 = -\eta\alpha\gamma\delta t^2$ and $\Gamma_1 = -(1/2)\eta^2\gamma\delta t^3$. After N steps, we have

$$\begin{aligned}\rho(N\delta t) =& \frac{1}{2}\Big(\Big|1, \alpha e^{-\gamma N\delta t}\Big\rangle\Big\langle 1, \alpha e^{-\gamma N\delta t}\Big| + \\ &+ e^{-i(\theta_N+\theta'_N)}e^{\Gamma_N}\Big|0, \alpha e^{-\gamma N\delta t} - i\eta\sum_{k=1}^{N}\delta t e^{-\gamma k\delta t}\Big\rangle\Big\langle 1, \alpha e^{-\gamma N\delta t}\Big| + \\ &+ e^{i(\theta_N+\theta'_N)}e^{\Gamma_N}\Big|1, \alpha e^{-\gamma N\delta t}\Big\rangle\Big\langle 0, \alpha e^{-\gamma N\delta t} - i\eta\sum_{k=1}^{N}\delta t e^{-\gamma k\delta t}\Big| + \\ &+ \Big|0, \alpha e^{-\gamma N\delta t} - i\eta\sum_{k=1}^{N}\delta t e^{-\gamma k\delta t}\Big\rangle\Big\langle 0, \alpha e^{-\gamma N\delta t} - i\eta\sum_{k=1}^{N}\delta t e^{-\gamma k\delta t}\Big|\Big),\end{aligned} \tag{A.3}$$

where

$$\begin{aligned}\theta_N &= \eta\alpha\sum_{k=0}^{N}\delta t e^{-\gamma k\delta t}, \\ \theta'_N &= -\eta\alpha\gamma\sum_{k=0}^{N}\delta t e^{-\gamma k\delta t}\sum_{j=0}^{k}\delta t e^{-\gamma j\delta t}, \\ \Gamma_N &= -\frac{1}{2}\eta^2\gamma\sum_{k=0}^{N}\delta t\Big(\sum_{j=0}^{k}\delta t e^{-\gamma j\delta t}\Big)^2.\end{aligned} \tag{A.4}$$

We now go to limit $\delta t \to 0$. In this situation, we can go back to a continuous time and substitute the sums with integrals. So, we are going to make the transformations $\sum_{k=0}^{N}\delta t \to \int_0^t dt'$, where $N\delta t \to t$ and $k\delta t \to t'$. For the double sums in the expressions for Γ and θ' we have to be careful. Indeed, in order to transform the second sum into an integral, it is necessary that $k \gg 1$. The correct transformation

would be

$$\sum_{k=k_0}^{N} \delta t \sum_{j=0}^{k} \delta t \to \int_{t_0}^{t} dt' \int_{0}^{t'} dt'',$$

where $j\delta t \to t''$. However, since $\delta t \to 0$ and $N \to \infty$, we can always choose $k_0 \gg 1$ such that $\sum_{k=k_0}^{N} \delta t \approx \sum_{k=0}^{N} \delta t$ and $\int_{t_0}^{t} dt' \approx \int_{0}^{t} dt'$. Substituting we get

$$\begin{aligned}
\rho(t) =& \frac{1}{2}\Big(\Big|1, \alpha e^{-\gamma t}\Big\rangle\Big\langle 1, \alpha e^{-\gamma t}\Big| + \\
&+ e^{-i(\theta(t)+\theta'(t))} e^{\Gamma(t)} \Big|0, \alpha e^{-\gamma t} - i\eta \int_0^t dt' e^{-\gamma t'}\Big\rangle\Big\langle 1, \alpha e^{-\gamma t}\Big| + \\
&+ e^{i(\theta(t)+\theta'(t))} e^{\Gamma(t)} \Big|1, \alpha e^{-\gamma t}\Big\rangle\Big\langle 0, \alpha e^{-\gamma t} - i\eta \int_0^t dt' e^{-\gamma t'}\Big| + \\
&+ \Big|0, \alpha e^{-\gamma t} - i\eta \int_0^t dt' e^{-\gamma t'}\Big\rangle\Big\langle 0, \alpha e^{-\gamma t} - i\eta \int_0^t dt' e^{-\gamma t'}\Big|\Big),
\end{aligned} \tag{A.5}$$

where

$$\begin{aligned}
\theta(t) &= \eta\alpha \int_0^t dt' e^{-\gamma t'}, \\
\theta'(t) &= -\eta\alpha\gamma \int_0^t dt' e^{-\gamma t'} \int_0^{t'} dt'' e^{-\gamma t''},. \\
\Gamma(t) &= -\frac{1}{2}\eta^2\gamma \int_0^t dt' \Big(\int_0^{t'} dt'' e^{-\gamma t''}\Big)^2.
\end{aligned} \tag{A.6}$$

After the integration, the final expression for $\rho(t)$ turns out to be the one given in Equation (3.13).

Appendix B

B.1 Adiabatic Elimination

We start from Equation (4.2) in Chapter 4 and we adiabatically eliminate the excited state of the atom $|e\rangle$ and the electromagnetic field inside the cavity. In order to do so, we assume $\Delta >> \Omega, g$ and $\delta >> \Omega, g$. We notice that the only terms in the Hamiltonian involving the atomic degrees of freedom are H_a and H_R. Hence, we perform first the adiabatic elimination of the exited level $|e\rangle$ of the atom. The Hamiltonian $H_a + H_R$ can be formally written as a 3×3 matrix with respect of the basis $\{|0\rangle, |1\rangle, |e\rangle\}$:

$$H_a + H_R = \begin{pmatrix} 0 & 0 & \Omega \\ 0 & 0 & ge^{i\Delta t}\hat{a}^\dagger \\ \Omega & ge^{-i\Delta t}\hat{a} & \delta \end{pmatrix}. \tag{B.1}$$

By writing a generic state of the atom as $|\lambda\rangle = c_0|0\rangle + c_1|1\rangle + c_e|e\rangle$ and by setting to zero $\dot{c}_e$ in the corresponding Schrödinger equation $i\partial_t|\lambda\rangle = (H_a + H_R)|\lambda\rangle$, we

find the effective Hamiltonian

$$\begin{aligned} H_{eff} = &- \frac{\Omega^2}{\delta}|0\rangle\langle 0| - \frac{\Omega g e^{-i\Delta t}}{\delta}\hat{a}|0\rangle\langle 1| \\ &- \frac{\Omega g e^{i\Delta t}}{\delta}\hat{a}^\dagger|1\rangle\langle 0| - \frac{g^2}{\delta}\hat{a}^\dagger\hat{a}|1\rangle\langle 1|. \end{aligned} \tag{B.2}$$

After the adiabatic elimination we substitute the terms $H_a + H_R$ with the expression above and the total Hamiltonian of the system reads now $H_{sys} = H_{eff} + H_c + H_m + H_{mc} + H_{cp}$.

The next step is the elimination of the cavity field operators $\hat{a}$ and $\hat{a}^\dagger$. In order to do so, we consider the equations describing the time evolution of those operators $\dot{\hat{a}} = -i[H_{sys}, \hat{a}]$ and $\dot{\hat{a}}^\dagger = -i[H_{sys}, \hat{a}^\dagger]$ and we set to zero the time derivative. Considering that $[H_{sys}, \hat{a}] = [H_c, \hat{a}] + [H_{mc}, \hat{a}] + [H_{eff}, \hat{a}]$, we find that

$$\begin{aligned} [H_{sys}, \hat{a}] = &- \hat{a}\big(\Delta + \chi_1(\hat{b}_1^\dagger + \hat{b}_1) + \chi_2(\hat{b}_2^\dagger + \hat{b}_2) - \frac{g^2}{\delta}|1\rangle\langle 1|\big) \\ &+ \frac{\Omega g}{\delta}e^{i\Delta t}|1\rangle\langle 0|. \end{aligned} \tag{B.3}$$

Setting this quantity to zero and considering that $\Delta \gg \chi, g^2/\delta$, we find

$$\hat{a} = \frac{\Omega g}{\delta\Delta}e^{i\Delta t}|1\rangle\langle 0|. \tag{B.4}$$

In a similar way we find that

$$\hat{a}^\dagger = \frac{\Omega g}{\delta\Delta}e^{-i\Delta t}|0\rangle\langle 1|. \tag{B.5}$$

By substituting these equation in the expression for H_{mc} we find the effective

atom-mirrors interaction which reads as

$$H_{am}^{eff} = \frac{\Omega^2 g^2}{\delta^2 \Delta^2} \chi |0\rangle\langle 0| (\hat{b}^\dagger e^{-i\phi} + \hat{b} e^{-i\phi}), \tag{B.6}$$

with $\eta = \frac{\Omega^2 g^2}{\delta^2 \Delta^2} \chi$ we recover the expression in Equation (4.3)

Appendix C

C.1 Bogoliubov transformations

We first report the Bogoliubov relations between $\{b, b^\dagger, a, a^\dagger\}$ and $\{c_j, c_j^\dagger\}$ ($j = \{1, 2\}$) given in [141]:

.

$$
\begin{aligned}
a^\dagger = \frac{1}{2}\Bigg\{ & \frac{-\cos\gamma}{\sqrt{\omega_a \epsilon_1}}[(\omega_a + \epsilon_1)c_1^\dagger + (\omega_a - \epsilon_1)c_1] + \\
& + \frac{\sin\gamma}{\sqrt{\omega_a \epsilon_2}}[(\omega_a + \epsilon_2)c_2^\dagger + (\omega_a - \epsilon_2)c_2]\Bigg\}, \\
a = \frac{1}{2}\Bigg\{ & \frac{-\cos\gamma}{\sqrt{\omega_a \epsilon_1}}[(\omega_a - \epsilon_1)c_1^\dagger + (\omega_a + \epsilon_1)c_1] + \\
& + \frac{\sin\gamma}{\sqrt{\omega_a \epsilon_2}}[(\omega_a - \epsilon_2)c_2^\dagger + (\omega_a + \epsilon_2)c_2]\Bigg\},
\end{aligned}
\tag{C.1}
$$

$$
\begin{aligned}
b^\dagger &= \frac{1}{2}\Bigg\{ \frac{-\sin\gamma}{\sqrt{\omega_b\epsilon_1}}[(\omega_b+\epsilon_1)c_1^\dagger + (\omega_b-\epsilon_1)c_1] + \\
&\qquad + \frac{\cos\gamma}{\sqrt{\omega_b\epsilon_2}}[(\omega_b+\epsilon_2)c_2^\dagger + (\omega_b-\epsilon_2)c_2]\Bigg\}, \\
b &= \frac{1}{2}\Bigg\{ \frac{-\sin\gamma}{\sqrt{\omega_b\epsilon_1}}[(\omega_b-\epsilon_1)c_1^\dagger + (\omega_b+\epsilon_1)c_1] + \\
&\qquad + \frac{\cos\gamma}{\sqrt{\omega_b\epsilon_2}}[(\omega_b-\epsilon_2)c_2^\dagger + (\omega_b+\epsilon_2)c_2]\Bigg\},
\end{aligned}
\tag{C.2}
$$

Using these relation, it is straightforward to find $b^\dagger b$ as

$$
\begin{aligned}
b^\dagger b = \frac{1}{4}\Bigg\{ & \frac{\sin^2\gamma}{\omega_b\epsilon_1}\Big[(\omega_b+\epsilon_1)(\omega_b-\epsilon_1)c_1^\dagger c_1^\dagger + (\omega_b+\epsilon_1)(\omega_b+\epsilon_1)c_1^\dagger c_1 + \\
& + (\omega_b-\epsilon_1)(\omega_b-\epsilon_1)c_1 c_1^\dagger + (\omega_b-\epsilon_1)(\omega_b+\epsilon_1)c_1 c_1\Big] - \\
& - \frac{\sin\gamma\cos\gamma}{\omega_b\sqrt{\epsilon_1\epsilon_2}}\Big[(\omega_b+\epsilon_1)(\omega_b-\epsilon_2)c_1^\dagger c_2^\dagger + (\omega_b+\epsilon_1)(\omega_b+\epsilon_2)c_1^\dagger c_2 + \\
& + (\omega_b-\epsilon_1)(\omega_b-\epsilon_2)c_1 c_2^\dagger + (\omega_b-\epsilon_1)(\omega_b+\epsilon_2)c_1 c_1 + \\
& + (\omega_b+\epsilon_2)(\omega_b-\epsilon_1)c_2^\dagger c_1^\dagger + (\omega_b+\epsilon_2)(\omega_b+\epsilon_1)c_2^\dagger c_1 + \\
& + (\omega_b-\epsilon_2)(\omega_b-\epsilon_1)c_2 c_1^\dagger + (\omega_b-\epsilon_2)(\omega_b+\epsilon_1)c_2 c_1\Big] + \\
& + \frac{\cos^2\gamma}{\omega_b\epsilon_2}\Big[(\omega_b+\epsilon_2)(\omega_b-\epsilon_2)c_2^\dagger c_2^\dagger + (\omega_b+\epsilon_2)(\omega_b+\epsilon_2)c_2^\dagger c_2 + \\
& + (\omega_b-\epsilon_2)(\omega_b-\epsilon_2)c_2 c_2^\dagger + (\omega_b-\epsilon_2)(\omega_b+\epsilon_2)c_2 c_2\Big]\Bigg\}.
\end{aligned}
\tag{C.3}
$$

Assuming $\omega_a \sim \omega_b$, it can be seen from Equation (5.7) that $\epsilon_2 \sim \omega_b$ and $\epsilon_1 \ll \omega_b$ when g approach g_c. For that reason, we have that $(\omega_b \pm \epsilon_j) \sim \omega_b, \forall j = \{1, 2\}$, and the order of magnitude of the various terms is only given by the factors in front of the square brackets. This means that as long as the condition $\epsilon_1 \ll \epsilon_2$ is fulfilled,

the first line in Equation (C.3) dominates over the other two. Rearranging the first line and considering that $c_1 c_1^\dagger = 1 + c_1^\dagger c_1$, is straightforward to find Equation (C.3). From Equations (C.1) and (C.2) is clear that the same calculation can be done for $a^\dagger a$ just by making the substitutions $\sin \to \cos$ and $\omega_b \to \omega_a$.

C.2 Lewis-Riesenfeld method

The expression in Equation (5.11) represents a quadratic Hamiltonian with time-dependent coefficients and it can be solve exactly using the Lewis-Riesenfeld method [145, 146]. Indeed, this method gives us a strategy for finding the solutions of the Schrodinger equation for any time-dependent Hamiltonian using the so called dynamical invariants of the system. As we will see below, it is particularly useful in case of quadratic hamiltonians.

Let us consider a generic time-dependent Hamiltonian $\hat{H}(t)$. A time-dependent observable $\hat{\mathcal{O}}(t)$ is a dynamical invariant of the system if

$$\frac{d}{dt}\hat{\mathcal{O}}(t) = \frac{\partial}{\partial t}\hat{\mathcal{O}}(t) + i[\hat{\mathcal{O}}(t), \hat{H}(t)] = 0. \tag{C.4}$$

In [145], the authors proved that the eigenvectors $|\varphi_n, t\rangle$ of any dynamical invariant $\hat{\mathcal{O}}(t)$ are linked to the solutions of the Schrödinger equation $i\partial_t|\psi, t\rangle = \hat{H}(t)|\psi, t\rangle$. In particular, any solution of the Schrödinger equation can be write as a linear combination of the eigenvectors $\{|\varphi_n, t\rangle\}$ in the form

$$|\psi, t\rangle = \sum_n c_n \exp\left[i\theta_n(t)\right]|\varphi_n, t\rangle,$$

where the phases $\theta_n(t)$ are given by $\theta_n(t) = \int_0^t dt\langle\varphi_n, t|i\partial_t - \hat{H}(t)|\varphi_n, t\rangle$. This method is particularly useful when we are dealing with quadratic Hamiltonian. Indeed, in this case is possible to find a simple explicit form for the dynamical invariant $\hat{\mathcal{O}}(t)$. The problem is then reduced to the solution of a second order differential equation with time-dependent coefficients [146].

Let us consider a generic quadratic Hamiltonian on the form

$$H(t) = \frac{1}{2}[u(t)\hat{q}^2 + v(t)\hat{p}^2]. \tag{C.5}$$

Notice that the Hamiltonian given in Equation (5.11) is a particular case of the one above with $u(t) = \epsilon_1^2(t)$ and $v(t) = 1$. We choose the time-dependent observable $\hat{n}_t = \hat{d}_t^\dagger \hat{d}_t$, with operators $\hat{d}_t$ and $\hat{d}_t^\dagger$ given by

$$\begin{aligned} \hat{d}_t &= A(t)\hat{q} + B(t)\hat{p}, \\ \hat{d}_t^\dagger &= A^*(t)\hat{q} + B^*(t)\hat{p}. \end{aligned} \tag{C.6}$$

Using Equation (C.4), it can be proven [146] that $\hat{n}_t$ is a dynamical invariant with respect to $\hat{H}(t)$ if the coefficients $A(t)$ and $B(t)$ fulfill the equations

$$\begin{aligned} \ddot{B}(t) &= \frac{\dot{u}(t)}{u(t)}\dot{B}(t) - u(t)v(t)B(t), \\ A(t) &= -\frac{\dot{B}(t)}{u(t)}, \\ A(t)B^*(t) &- A^*(t)B(t) = -i. \end{aligned} \tag{C.7}$$

The last Equation is the Wronskian condition which ensure the correct commutation rules ($[\hat{d}_t^\dagger, \hat{d}_t] = -1$) for the time-dependent bosonic operators. If these equations are fulfilled, the observable $\hat{n}_t$ is a dynamical invariant of the system.

We can easily write its eigenvectors as time-dependent Fock states in the form

$$|n,t\rangle = \frac{(\hat{d}_t^\dagger)^n}{\sqrt{n}}|0,t\rangle. \tag{C.8}$$

We still need to find the ground state $|0,t\rangle$. In order to do so, we explore the proprieties of the bosonic annihilation operator $\hat{d}_t$. Indeed, the action of this operator on $|0,t\rangle$ gives zero. This means that the ground state has to fulfill the equation $\hat{d}_t|0,t\rangle = 0$. If we write this equation in term of wave-function, we substitute the operators $\hat{q}$ and $\hat{p}$ with q and $(1/i)\partial_q$, and the ket $|0,t\rangle$ with the corresponding wave-function $\Phi_0(q,t)$. Doing so and using Equation (C.6), the equation defining the ground state becomes

$$A(t)q\Phi_0(q,t) + \frac{1}{i}B(t)\partial_q\Phi_0(q,t) = 0 \tag{C.9}$$

and its solution can be easily found to be

$$\Phi_0(q,t) = \left(\frac{1}{2\pi|B(t)|^2}\right)^{\frac{1}{4}} e^{i\frac{A(t)}{2B(t)}q^2}. \tag{C.10}$$

At this point the states $|n,t\rangle$ are completely defined, and we can write the solution of the Sch odinger equation as linear combinations of these states.

Modulating the atomic splitting results on Bogoliubov bosons generation from vacuum. In order to show this effect, we calculate the mean number of excitations $\langle\hat{c}^\dagger\hat{c}\rangle$ in the system. Inverting equations (C.6), we can write the time-independent

operators $\{\hat{c}^\dagger\hat{c}\}$ in terms of the time-dependent ones $\{\hat{d}_t^\dagger, \hat{d}_t\}$ as

$$\begin{aligned}\hat{c} &= f_1(t)\hat{d}_t + f_2(t)\hat{d}_t^\dagger, \\ \hat{c}^\dagger &= f_2^*(t)\hat{d}_t + f_1^*(t)\hat{d}_t^\dagger.\end{aligned} \tag{C.11}$$

where $f_1(t)$ and $f_2(t)$ can be simplified to

$$\begin{aligned}f_1(t) &= \frac{1}{2}(A^*(t) + iB^*(t)), \\ f_2(t) &= -\frac{1}{2}(A(t) + iB(t)).\end{aligned} \tag{C.12}$$

We used the Wronskian condition (third equation in (C.7)) in order to obtain this expressions.

We can easily calculate the mean number of excitations $\langle\hat{c}^\dagger\hat{c}\rangle$ from Equation (C.11) as

$$\begin{aligned}\langle\hat{c}^\dagger\hat{c}\rangle =& f_1(t)f_2^*(t)\langle\hat{d}_t\hat{d}_t\rangle + |f_2(t)|^2(1 + \langle\hat{d}_t^\dagger\hat{d}_t)\rangle + \\ &+|f_1(t)|^2\langle\hat{d}_t^\dagger\hat{d}_t\rangle + f_1^*(t)f_2(t)\langle\hat{d}_t^\dagger\hat{d}_t^\dagger\rangle.\end{aligned} \tag{C.13}$$

We assume the initial state of the system at $t = 0$ is the ground state of the $\hat{c}$ mode. The state at time t is the time-dependent "ground" state of the $\hat{d}_t$ mode $|0, t\rangle$. Considering the mean values over this state, the expression above becomes

$$\langle\hat{c}^\dagger\hat{c}\rangle = |f_2(t)|^2. \tag{C.14}$$

In order to obtain the function $f_2(t)$ is sufficient to solve the differential equations given in (C.7).

C.3 Langevin equations in time domain

In order to address the case of a leaking cavity, we will use the quantum Langevin equations formalism. The dissipative dynamics of a generic system can be described using Langevin equation $\partial_t \mathcal{O} = -i[\mathcal{O}, H] + \mathcal{N}$ where H is the Hamiltonian, $\mathcal{O}$ is a generic observable of the system and $\mathcal{N}$ is the noise operator associated with $\mathcal{O}$. In the case we are considering, we neglect all the atomic decays, so we have to take into account only the cavity's photon loosing rate. Following [147], the noise operator is then $\mathcal{N} = -[\mathcal{O}, a^\dagger](\frac{\gamma}{2}a + \sqrt{\gamma}a_{\rm in}) + (\frac{\gamma}{2}a^\dagger + \sqrt{\gamma}a_{\rm in}^\dagger)[\mathcal{O}, a]$. We consider the two modes Hamiltonian instead of the approximated one mode Hamiltonian in Equation (5.11). That means that the following description is valid also when the coupling constant g is far away from its critical value. The Langevin equations for the two modes read as

$$\begin{aligned}
\dot{\hat{q}}_a &= \omega \hat{p}_a - \gamma \hat{q}_a + \sqrt{2\gamma}\hat{\xi}_q, \\
\dot{\hat{p}}_a &= -\omega \hat{q}_a - g\hat{q}_b - \gamma \hat{p}_a + \sqrt{2\gamma}\hat{\xi}_p, \\
\dot{\hat{q}}_b &= \lambda \sin(\eta t)\hat{p}_b, \\
\dot{\hat{p}}_b &= -\lambda \sin(\eta t)\hat{q}_b - g\hat{q}_a,
\end{aligned} \tag{C.15}$$

where γ is the decay rate of the cavity and $\hat{\xi}_q$ ($\hat{\xi}_p$) is a white noise operator associated with q (p). These operators are defined as $\hat{\xi}_q = (1/\sqrt{2})(\hat{a}_{in}^\dagger + \hat{a}_{in})$ and $\hat{\xi}_p = (i/\sqrt{2})(\hat{a}_{in}^\dagger - \hat{a}_{in})$.

Equations in (C.15) can be formally written in a more elegant and convenient way. By defining the quadratures vector as $\mu = (\hat{q}_a, \hat{p}_a, \hat{q}_b, \hat{p}_b)^T$ and the noise

vector as $n = (\sqrt{2\gamma}\hat{\xi}_q, \sqrt{2\gamma}\hat{\xi}_p, 0, 0)^T$, the Langevin equations assume the form

$$\dot{\mu}(t) = A(t)\mu(t) + n(t), \tag{C.16}$$

where $A(t)$ is a time-dependent 4×4 matrix given by

$$A(t) = \begin{pmatrix} -\gamma & \omega & 0 & 0 \\ -\omega & -\gamma & -g & 0 \\ 0 & 0 & 0 & \lambda \sin(\eta t) \\ -g & 0 & -\lambda \sin(\eta t) & 0 \end{pmatrix}.$$

Starting from the Langevin equations, we can reconstruct the dynamics of the system looking at the time dependent covariance matrix $V(t)$ for the two modes. The covariance matrix is a 4×4 matrix collecting the second moments of the two quadratures and is defined as $V_{i,j} = \langle \mu_i \mu_j + \mu_j \mu_i \rangle / 2$. For Gaussian states, the covariance matrix represent a complete description of the state of system. The differential equation for $V(t)$ corresponding to Equation (C.16) reads as [75,143]:

$$\dot{V}(t) = A(t)V(t) + V(t)A^T(t) + \mathcal{N}, \tag{C.17}$$

where $\mathcal{N}$ is a 4×4 matrix collecting the auto-correlation function for the noise. For white noise $\mathcal{N} = \text{diag}[\gamma, \gamma, 0, 0]$. From the definition of the quadrature operators given by $\hat{q}_a = (1/\sqrt{2})(\hat{a}^\dagger + \hat{a})$ and $\hat{p}_a = (i/\sqrt{2})(\hat{a}^\dagger - \hat{a})$, the mean number of photons in the cavity is given by $\langle \hat{a}^\dagger \hat{a} \rangle = (1/2)(\langle \hat{q}_a^2 \rangle + \langle \hat{p}_a^2 \rangle - 1) = (1/2)(V_{11} + V_{22} - 1)$.

Bibliography

[1] A. Einstein, B. Podolsky and N. Rosen, *Physical Review* **47**, 777 (1935).

[2] E. Schrödinger, *Naturweissenschaften* **23**, 807; 823; 844 (1935); English translation: *Proceedings of American Philosophical Society* **124**, 323 (1980).

[3] R. Feynman, *The character of physical law*, The M.I.T. press (1965).

[4] F. Brennecke, T. Donner, S. Ritter, T. Bourdel, M. Köhl and T. Esslinger, *Nature* **450**, 268 (2007).

[5] Y. Colombe, T. Steinmetz, G. Dubois, F. Linke, D. Hunger and J. Reichel, *Nature* **450**, 272 (2007).

[6] A. Wallraff, D. I. Schuster, A. Blais, L. Frunzio, R.- S. Huang, J. Majer, S. Kumar, S. M. Girvin and R. J. Schoelkopf, *Nature* **431**, 161 (2004).

[7] J. Majer, J. M. Chow, J. M. Gambetta, Jens Koch, B. R. Johnson, J. A. Schreier, L. Frunzio, D. I. Schuster, A. A. Houck, A. Wallraff, A. Blais, M. H. Devoret, S. M. Girvin and R. J. Schoelkopf, *Nature* **449**, 443 (2007).

[8] A. Wallraff, D. I. Schuster, A. Blais, J. M. Gambetta, J. Schreier, L. Frunzio, M. H. Devoret, S. M. Girvin, and R. J. Schoelkopf, *Physical Review Letters* **99**, 050501 (2007).

[9] A. Naik, O. Buu, M. D. LaHaye, A. D. Armour, A. A. Clerk, M. P. Blencowe and K. C. Schwab, *Nature* **443**, 193 (2006).

[10] S. Gigan, H. R. Böhm, M. Paternostro, F. Blaser, G. Langer, J. B. Hertzberg, K. C. Schwab, D. Bäuerle, M. Aspelmeyer and A. Zeilinger, *Nature* **444**, 67 (2006).

[11] O. Arcizet, P.-F. Cohadon, T. Briant, M. Pinard and A. Heidmann, *Nature* **444**, 71 (2006).

[12] D. Kleckner and D. Bouwmeester, *Nature* **444**, 75 (2006).

[13] A. Schliesser, P. DelHaye, N. Nooshi, K. J. Vahala, and T. J. Kippenberg, *Physical Review Letters* **97**, 243905 (2006).

[14] A. Schliesser, R. Riviere, G. Anetsberger, O. Arcizet and T. J. Kippenberg, *Nature Physics* **4**, 415 (2008).

[15] S. Gröblacher, J. B. Hertzberg, M. R. Vanner, G. D. Cole, S. Gigan, K. C. Schwab and M. Aspelmeyer, *Nature Physics* **5**, 485 (2009).

[16] A. Schliesser, O. Arcizet, R. Riviere, G. Anetsberger and T. J. Kippenberg, *Nature Physics* **5**, 509 (2009).

[17] A. D. O' Connell, M. Hofheinz, M. Ansmann, R. C. Bialczak, M. Lenander, E. Lucero, M. Neeley, D. Sank, H. Wang, M. Weides, J. Wenner, J. M. Martinis and A. N. Cleland, *Nature* **464**, 697 (2010).

[18] Jasper Chan, T. P. Mayer Alegre, Amir H. Safavi-Naeini, Jeff T. Hill, Alex Krause, Simon Gröblacher, Markus Aspelmeyer and Oskar Painter, *Nature* **478**, 89 (2011).

[19] J. D. Thompson, B. M. Zwickl, A. M. Jayich, Florian Marquardt, S. M. Girvin and J. G. E. Harris, *Nature* **452**, 72 (2008).

[20] O. Arcizet, P.-F. Cohadon, T. Briant, M. Pinard, and A. Heidmann , *Physical Review Letters* **97**, 133601 (2006).

[21] T. Corbitt, Y. Chen, E. Innerhofer, H. Müller-Ebhardt, D. Ottaway, H. Rehbein, D. Sigg, S. Whitcomb, C. Wipf and N. Mavalvala, *Physical Review Letters* **98**, 150802 (2007).

[22] S. Gröblacher, K. Hammerer, M. R. Vanner and M. Aspelmeyer, *Nature* **460**, 724 (2009).

[23] F. De Martini, F. Sciarrino, and C. Vitelli, *Physical Review Letters* **100**, 253601 (2008).

[24] P. Sekatski, N. Brunner, C. Branciard, N. Gisin and C. Simon, *Physical Review Letters* **103**, 113601 (2009).

[25] W. Marshall, C. Simon, R. Penrose, and D. Bouwmeester, *Physical Review Letters* **91**, 130401 (2003).

[26] A. Ferreira, A. Guerreiro, V. Vedral, *Physical Review Letters* **96**, 060407 (2006).

[27] S. Mancini, V. Giovannetti, D. Vitali, P. Tombesi, *Physical Review Letters* **88**, 120401 (2006).

[28] D. Vitali, S. Gigan, A. Ferreira, H. R. Böhm, P. Tombesi, A. Guerreiro, V. Vedral, A. Zeilinger, M. Aspelmeyer, *Physical Review Letters* **98**, 030405 (2007).

[29] S. Pirandola, D. Vitali, P. Tombesi, S. Lloyd, *Physical Review Letters* **97**, 150403 (2006).

[30] G. Vacanti, M. Paternostro, G. M. Palma and V. Vedral, *New Journal of Physics* **10**, 095014, (2008).

[31] G. Vacanti, R. Fazio, M. S. Kim, G. M. Palma, M. Paternostro and V. Vedral, *Physical Review A* **85**, 022129 (2012).

[32] G. Vacanti, M. Paternostro, G. M. Palma, M. S. Kim and V. Vedral, (under review).

[33] S. Pugnetti, Y.M. Blanter, and R. Fazio, *Europhysics Letters* **90**, 48007 (2010).

[34] S. Pugnetti, Y. M. Blanter, F. Dolcini, and R. Fazio, *Physical Review B* **79**, 174516 (2009).

[35] D. Leibfried, B. DeMarco, V. Meyer, D. Lucas, M. Barrett, J. Britton, W. M. Itano, B. Jelenković, C. Langer, T. Rosenband and D. J. Wineland, *Nature* **422**, 412 (2003).

[36] P. Rabl, A. Shnirman and P. Zoller, *Physical Review B* **70**, 205304 (2004).

[37] I. Wilson-Rae, P. Zoller, and A. Imamoglu, *Physical Review Letters* **92**, 075507 (2004).

[38] M. D. LaHaye, O. Buu, B. Camarota, and K. C. Schwab, *Science* **304**, 74 (2004).

[39] G. T. Moore, *Journal of Mathematical Physics* **11**, 2679 (1970).

[40] S. A. Fulling, P. C. W. Davies, *Proceedings of the Royal Society A* **348**, 393-414 (1976).

[41] P. C. W. Davies, S. A. Fulling, *Proceedings of the Royal Society A* **356**, 237-257 (1977).

[42] E. Yablonovitch, *Physical Review Letters* **62**, 1742 (1989).

[43] J. Schwinger, *Proceedings of the National Academy of Sciences USA* **89**, 4091 (1992).

[44] T. W. B. Kibble, *Journal of Physics A* **9**, 1387 (1976).

[45] W. H. Zurek, *Nature (London)* **317**, 505 (1985).

[46] J. Dziarmaga, *Advances in Physics* **59**, 1063 (2010).

[47] V. V. Dodonov, *Physica Scripta* **82**, 038105 (2010).

[48] J. R. Johansson, G. Johansson, C. M. Wilson, and F. Nori, *Physical Review Letters* **103**, 147003 (2009).

[49] A. V. Dodonov, L. C. Celeri, F. Pascoal, M. D. Lukin and S. F. Yelin, *arXiv:0806.4035v3* (2008).

[50] S. De Liberato, D. Gerace, I. Carusotto, and C. Ciuti, *Physical Review A* **80**, 053810 (2009).

[51] C. M. Wilson, G. Johansson, A. Pourkabirian, M. Simoen, J. R. Johansson, T. Duty, F. Nori, and P. Delsing, *Nature (London)* **479**, 376 (2011).

[52] B. Damski, *Physical Review Letters* **95**, 035701 (2005).

[53] G. Vacanti, S. Pugnetti, N. Didier, M. Paternostro, G. M. Palma, R. Fazio, and V. Vedral, *Physical Review Letters* **108**, 093603 (2012).

[54] G. Vacanti, S. Pugnetti, N. Didier, M. Paternostro, G. M. Palma, R. Fazio, and V. Vedral, *Physica Scripta* **T 151**, 014071 (2012).

[55] R. H. Dicke, *Physical Review* **93**, 99 (1954).

[56] K. Baumann, C. Guerlin, F, Brennecke and T. Esslinger, *Nature* **464**, 1301 (2010).

[57] S. M. Barnett, and P. M. Radmore, *Methods in Theoretical Quantum Optics* (Oxford University Press, Oxford, 2003).

[58] M. V. Berry, *Proceedings of the Royal Society A* **329**, 45 (1984).

[59] Y. Aharonov, J. Anandan, *Physical Review Letters* **58**, 1593 (1987).

[60] N. Mukunda and R. Simon, *Annals of Physics* **228**, 205 (1993).

[61] Angelo Carollo, *Geometric phase in composite quantum systems*, Phd thesis (Imperial College London, 2003).

[62] E. Sjoqvist, A. K. Pati, A. Ekert, J. S. Anandan, M. Ericsson, D. K. L. Oi, V. Vedral, *Physical Review Letters* **85**, 2845 (2000).

[63] C. Cohen-Tannoudji, B. Diu, F. Laloë, *Quantum Mechanics* (Wiley 1977).

[64] R. P. Feynman, R. B. Leighton, M. L. Sands, M. A. Gottlieb, *The Faynman lectures on physics, Vol. 3* (Pearson/Addison-Wesley 1963).

[65] S. Pancharatnam, Proceedings of the Indian Academy of Science A **44**, 247 (1956).

[66] V. Bargmann, *Journal of Mathematical Physics* **5**, 862 (1964).

[67] E. M. Rabei, Arvind, N. Mukunda and R. Simon, *Physical Review A* **60**, 3397 (1999).

[68] P. Lebedev, *Untersuchungen ber die Druckkräfte des Lichtes*, Annalen der Physik, (1901).

[69] E. F. Nichols and G. F. Hull, *The Astrophysical Journal* **17**, 315-351 (1903)

[70] C. K. Law, *Physical Review A* **49**, 433 (1994).

[71] S. Bose, K. Jacobs and P. L. Knight *Physical Review A* **56**, 4175 (1997).

[72] D. F. Walls and G. J. Milburn, *Quantum Optics* (Springer, Heidelberg, 1994).

[73] S. Mancini, D. Vitali, and P. Tombesi, *Physical Review Letters* **90**, 137901 (2003)

[74] M. Paternostro, S. Gigan, M. S. Kim, F. Blaser, H. R. Böhm and M. Aspelmeyer, *New Journal of Physics* **8**, 107 (2006).

[75] M. Paternostro, D. Vitali, s. Gigan, M. S. Kim, C. Brukner, J. Eisert, M. Aspelmeyer, *Physical Review Letters* **99**, 250401 (2007).

[76] A. Peres, *Physical Review Letters* **77**, 1413 (1996).

[77] M. Horodecki, P. Horodecki and R. Horodecki, *Physics Letters A* **223**, 1 (1996).

[78] M. B. Plenio, *Physical Review Letters* **95**, 090503 (2005).

[79] R. Simon, *Physical Review Letters* **84**, 2726 (2000).

[80] G. Adesso and F. Illuminati, *Journal of Physics A* **40**, 7821(2007).

[81] J. Bell, *Physics* **1**, 195 (1964).

[82] J. Bell, *Speakable And Unspeakable In Quantum Mechanics*, Cambridge University Press (1987).

[83] J. F. Clauser, M. A. Horne, A. Shimony and R. A. Holt, *Physical Review Letters* **23**, 880 (1969).

[84] R. F. Werner, *Physical Review A* **40**, 4277 (1989).

[85] E. Wigner, *Physical Review* **40**, 749 (1932).

[86] H. B. G. Casimir and D. Polder, *Physical Review* **73**, 360 (1948).

[87] I. Segal, *Lectures at the 1960 Boulder Summer Seminar*, AMS, Providence, RI (1963).

[88] L. Landau, *Physics of the Soviet Union* **2**, 46 (1932).

[89] C. Zener, *Proceedings of the Royal Society of London A* **137**, 696 (1932).

[90] F. Pellegrini, *Dynamics of a Quantum Phase Transition in the XXZ Model*, Master thesis, (Scuola Normale Superiore di Pisa, 2007).

[91] A. Carollo, I. Fuentes-Guridi, M. Franca Santos, V. Vedral, *Physical Review Letters* **90**, 160402 (2003).

[92] A. Carollo, I. Fuentes-Guridi, M. Franca Santos, V. Vedral, *Physical Review Letters* **92**, 020402 (2004).

[93] G. J. Milburn, S. Scheneider, and D. F. V. James, *Fortschritte der Physik* **48**, 801 (2000).

[94] H. F. Trotter, *Proceedings of the American Mathematical Society* **10**, 545 (1959).

[95] M. Suzuki, *Communications in Mathematical Physics* **51**, 183 (1976).

[96] H. Jeong, *Physical Review A* **72**, 034305 (2005).

[97] D. F. Walls and G. J. Milburn, *Physical Review A* **31**, 2403 (1985).

[98] S. J. D. Phoenix, *Physical Review A* **41**, 5132 (1989).

[99] L. M. Arévalo-Aguilar and H. Moya-Cessa, *Quantum and Semiclassical Optics* **10**, 671 (1998).

[100] K. C. Schwab and M. L. Roukes, *Physics Today* **58**, 36 (2005).

[101] M. Wallquist, K. Hammerer and P. Zoller, *Physical Review A* **81**, 023816 (2010).

[102] K. Hammerer, M. Wallquist, C. Genes, M. Ludwig, F. Marquardt, P. Treutlein, P. Zoller, J. Ye and H. J. Kimble, *Physical Review Letters* **103**, 063005 (2009).

[103] D. E. Chang, C. A. Regal, S. B. Papp, D. J. Wilson, J. Ye, O. Painter, H. J. Kimble, and P. Zoller, *Proceedings of the National Academy of Science USA* **107**, 1005 (2010).

[104] Oriol Romero-Isart, Mathieu L. Juan, Romain Quidant, and J Ignacio Cirac, *New Journal of Physics* **12**, 033015 (2010).

[105] M. Paternostro, G. De Chiara, and G. M. Palma, *Physical Review Letters* **104**, 243602 (2010).

[106] C. Genes, D. Vitali, and P. Tombesi, *Physical Review A* **77**, 050307(R) (2008).

[107] G. De Chiara, M. Paternostro, and G. M. Palma, *Physical Review A* **83**, 052324 (2011).

[108] P. Verlot, A. Tavernarakis, T. Briant, P.-F. Cohadon, and A. Heidmann, *Physical Review Letters* **104**, 133602 (2010).

[109] M. Pechal, S. Berger, A. A. Abdumalikov Jr., J. M. Fink, J. A. Mlynek, L. Steffen, A. Wallraff and S. Filipp, *arXiv:1109.1157* (2011).

[110] M. Aspelmeyer, S. Groeblacher, K. Hammerer, and N. Kiesel, *Journal of the Optical Society of America B* **27**, A189 (2010).

[111] T. J. Kippenberg and K. J. Vahala, *Science* **321**, 1172 (2008).

[112] F. Marquardt and S. M. Girvin, *Physics* **2**, 40 (1993).

[113] K. C. Schwab and M. L. Roukes, *Physics Today* **58**, 36 (2005).

[114] M. Poot, H. S. J. van der Zant, *Physics Reports* **511**, 273-335 (2012).

[115] A. D. Armour, M. P. Blencowe, and K. C. Schwab, *Physical Review Letters* **88**, 148301 (2002).

[116] P. Rabl, A. Shnirman, and P. Zoller, *Physical Review B* **70**, 205304 (2004).

[117] L. Tian, *Physical Review B* **72**, 195411 (2005).

[118] D. A. Rodrigues, J. Imbers, and A. D. Armour, *Physical Review Letters* **98**, 067204 (2007).

[119] L. Davidovich, A. Maali, M. Brune, J. M. Raimond and S. Haroche, *Physical Review Letters* **71**, 2360 (1993).

[120] H. Jeong and T. C. Ralph, *Physical Review Letters* **97**, 100401 (2006).

[121] H. Jeong, M. Paternostro, and T. C. Ralph, *Physical Review Letters* **102**, 060403 (2009).

[122] K. Banaszek and K. Wódkiewicz, *Physical Review A* **58**, 4345 (1998).

[123] K. Wódkiewicz, *New Journal of Physics* **2**, 21 (2000).

[124] S. Bose, I. Fuentes-Guridi, P. L. Knight and V. Vedral, *Physical Review Letters* **87**, 050401 (2001).

[125] J. Lee, M. S. Kim, Y. J. Park and S. Lee, *Journal of Modern Optics* **47**, 2151 (2000).

[126] B. C. Sanders, *Physical Review A* **45**, 6811 (1992).

[127] H. Jeong and M. S. Kim, *Physical Review A* **65**, 042305 (2002).

[128] M. Paternostro (unpublished).

[129] S. Gröblacher, (Private communication).

[130] M. Paternostro, G. De Chiara, and G. M. Palma, *Physical Review Letters* **104**, 243602 (2010).

[131] J. M. Martinis, S. Nam and J. Aumentado, *Physical Review Letters* **89**, 117901 (2002).

[132] J. Koch, T. M. Yu, J. Gambetta, A. A. Houck, D. I. Schuster, J. Majer, Alexandre Blais, M. H. Devoret, S. M. Girvin and R. J. Schoelkopf, *Physical Review A* **76**, 042319 (2007).

[133] W. H. Zurek, U. Dorner, and P. Zoller, *Physical Review Letters* **95**, 105701 (2005).

[134] A. Polkovnikov, *Physical Review B* **72**, 161201(R) (2005).

[135] E. Farhi, J. Goldstone, S. Gutmann, J. Lapan, A. Lundgren and D. Preda, *Science* **292**, 472 (2001).

[136] G. E. Santoro, R. Martonak, E. Tosatti and R. Car, *Science* **295**, 2427 (2002).

[137] I. L. Kirilyuk, *Optics and Spectroscopy* **92**, 719 (2002).

[138] A. Altland, V. Gurarie, T. Kriecherbauer, and A. Polkovnikov, *Physical Review A* **79**, 042703 (2009).

[139] A. Altland and V. Gurarie, *Physical Review Letters* **100**, 063602 (2008).

[140] T. Holstein and H. Primakoff, *Physical Review* **58**, 1098 (1940).

[141] C. Emary and T. Brandes, *Physical Review E* **67**, 066203 (2003).

[142] C. Ciuti and I. Carusotto, *Physical Review A* **74**, 033811 (2006).

[143] A. Mari and J. Eisert, *Physical Review Letters* **103**, 213603 (2009).

[144] A. V. Shytov, D. A. Ivanov and M. V. Feigel'man, *European Physical Journal B* **36**, 263 (2003).

[145] H. R. Lewis and W. B. Riesenfeld, *Journal of Mathematical Physics* **10** 1458 (1968).

[146] V. M. Bastidas, J. H. Reina, C. Emary and T. Brandes, *arXiv:0910.1600v1* (2010).

[147] C. Gardiner and P. Zoller, *Quantum Noise* (Springer 2004).

[148] H. J. Carmichael, *Statistical Methods in Quantum Optics 1, 2nd edition* (Springer 2002).